Western Washington University
Western CEDAR

WWU Graduate School Collection | WWU Graduate and Undergraduate Scholarship

Summer 1988

The Geology and Petrology of the Fifes Peak Formation in the Cliffdell Area, Central Cascades, Washington

Brad A. (Bradley Allen) Carkin
Western Washington University

Follow this and additional works at: https://cedar.wwu.edu/wwuet

 Part of the Geology Commons

Recommended Citation

Carkin, Brad A. (Bradley Allen), "The Geology and Petrology of the Fifes Peak Formation in the Cliffdell Area, Central Cascades, Washington" (1988). *WWU Graduate School Collection*. 844.
https://cedar.wwu.edu/wwuet/844

This Masters Thesis is brought to you for free and open access by the WWU Graduate and Undergraduate Scholarship at Western CEDAR. It has been accepted for inclusion in WWU Graduate School Collection by an authorized administrator of Western CEDAR. For more information, please contact westerncedar@wwu.edu.

MASTER'S THESIS

In presenting this thesis in partial fulfillment of the requirements for a master's degree at Western Washington University, I agree that the Library shall make its copies freely available for inspection. I further agree that extensive copying of this thesis is allowable only for scholarly purposes. It is understood, however, that any copying or publication of this thesis for commercial purposes, or for financial gain, shall not be allowed without my written permission.

Signature _____

Date 9-16-88

The Geology and Petrology of the Fifes Peak Formation in the Cliffdell Area, Central Cascades, Washington

A Thesis

Presented to

The Faculty of

Western Washington University

In Partial Fulfillment

of the Requirements for the Degree

Master of Science

by

Brad A. Carkin

September, 1988

The Geology and Petrology of the Fifes Peak Formation in the Cliffdell Area, Central Cascades, Washington

by

Brad A. Carkin

Accepted in Partial Completion

of the Requirements for the Degree

Master of Science

September, 1988

_____

Dean of Graduate School

Advisory Committee

_____

Chairman

_____

_____

MASTER'S THESIS

In presenting this thesis in partial fulfillment of the requirements for a master's degree at Western Washington University, I grant to Western Washington University the non-exclusive royalty-free right to archive, reproduce, distribute, and display the thesis in any and all forms, including electronic format, via any digital library mechanisms maintained by WWU.

I represent and warrant this is my original work and does not infringe or violate any rights of others. I warrant that I have obtained written permissions from the owner of any third party copyrighted material included in these files.

I acknowledge that I retain ownership rights to the copyright of this work, including but not limited to the right to use all or part of this work in future works, such as articles or books.

Library users are granted permission for individual, research and non-commercial reproduction of this work for educational purposes only. Any further digital posting of this document requires specific permission from the author.

Any copying or publication of this thesis for commercial purposes, or for financial gain, is not allowed without my written permission.

Name: Brad Carkin

Signature: _____

Date: 7-23-18

ABSTRACT

The Fifes Peak Formation in the Cliffdell area is comprised of two structurally, lithologically and geochemically distinct members separated by a pronounced unconformity. The older member (Edgar Rock member) is comprised of highly brecciated lava flows, coarse laharic breccia and lesser volcaniclastic sediments and tuffs. A thickness of at least 1,800 m is exposed near Edgar Rock. K-Ar ages indicate a latest Oligocene age of about 24 to 27 Ma. Lava compositions range from basalt to dacite, but are mostly basaltic andesite. These lavas are typically highly porphyritic and contain an anhydrous phenocryst assemblage of plagioclase, olivine, minor clinopyroxene and magnetite. Gabbroic inclusions, various pyroxene clots and green spinel are present in some basaltic andesite flows. The most common type of laharic breccia contains clasts and matrix constituents petrographically similar to the abundant basaltic andesite lavas. A less common type of lahar-like breccia contains abundant silicic lapilli and variable amounts of basaltic andesite. Clasts of non-Fifes Peak Fm. lithologies, including gabbroic plutonic rocks, sandstone and altered volcanic rocks, are most commonly associated with these units.

Beds in the Edgar Rock member define the circular Edgar Rock dome. An extensive system of radial dikes, truncated at the top of the member, has a focal area near the structural center of the dome. Dike compositions range from basaltic andesite to dacite and are petrographically diverse, indicating a history of multiple intrusions. Mafic dikes broadly resemble the mafic flows in the Edgar Rock member, but andesite and dacite dikes are petrographically distinct from flows of similar composition.

The Edgar Rock dome is probably the site of a major volcanic center in

the Fifes Peak Fm. Present steep dips are a combination of primary depositional attitudes and syn- and post-depositional uplift, perhaps partly related to the intrusion of the radial dike system. Volcaniclastic interbeds and laharic breccias constrain primary attitudes in the dome from nearly horizontal up to about 15 degrees. The Edgar Rock member on the flanks of the dome represents the proximal apron facies of a cone, mostly removed by erosion, located near the focus of the dike system.

The younger member of the Fifes Peak Fm. (Nile Creek Member) unconformably overlies the Edgar Rock dome. The Nile Creek member is comprised mostly of andesite flows and coarse laharic breccias. Lavas are petrographically uniform, highly porphyritic and contain phenocrysts of plagioclase, clinopyroxene, orthopyroxene, magnetite and olivine. K-Ar ages indicate an early Miocene age of about 24 to 19.5 Ma. An ash-flow tuff has a fission-track age of 23.3 Ma. The source of the Nile Creek lavas was not identified in this study.

The principal structure of the study area, the Edgar Rock dome, formed during Fifes Peak time (pre-24 Ma). A NW-trending monocline offsets the Edgar Rock member and is coeval with the adjacent Little Naches Syncline.

The Cliffdell area lavas and dikes have geochemical features common to continental margin, subduction-related lavas. Enrichments in K and related LIL and light-REE are characteristic of calc-alkaline lavas, but high FeO/MgO ratios, especially of the Edgar Rock suite, are typical of tholeiitic lavas. High Al_2O_3 and low MgO, Ni and Cr of mafic Edgar Rock lavas are characteristic of orogenic high-alumina basalts. Edgar Rock lavas and dikes are enriched in LIL, REE and HFS elements relative to the Nile Creek lavas. The Cliffdell suites, especially the Edgar Rock, are Fe-enriched relative to the coeval Cascade batholiths. Separate source regions or magmatic differentiation processes, or both, are indicated.

ACKNOWLEDGMENTS

Thesis committee members Drs. R. Scott Babcock and Robert A. Christman of Western Washington University and Dr. Robert D. Bentley of Central Washington University are thanked for their guidance and critical reading reading of this thesis.

Discussions in the field with Dr. Newell Campbell of Yakima Valley Community College and Dr. Paul Hammond of Portland State University were helpful. Discussions with Julie Schultz (thesis in press) were helpful and provided insights into adjacent areas of the Fifes Peak Formation.

Dr. Roman A. Schmitt, Mike Conrady and Steve Carter and others at the Radiation Center at Oregon State University are thanked for their efforts carrying out neutron activation analysis for trace elements on rocks from the study area.

Dr. Joseph A. Vance at the University of Washington is gratefully acknowledged for allowing inspection of a pre-publication manuscript and performing a fission-track date on a tuff sample.

Tim Walsh and others of the Division of Geology and Earth Resources in Lacey are thanked for providing funds for field work, information and for performing tasks critical to the preparation of the map for this thesis.

Steve Reidel of Rockwell International, Richland, is thanked for making possible the acquisition of K-Ar dates.

I would also like to thank George Jefferson of the former Gold Run Store and Cafe for providing comfortable living accomodations, some free beer and tall tales during many of my visits to the study area.

TABLE OF CONTENTS

LIST OF FIGURES

LIST OF TABLES

Table

LIST OF APPENDICES

Appendix

LIST OF PLATES

Plate

INTRODUCTION

The Fifes Peak Formation is a voluminous, regionally extensive volcanic assemblage of late Oligocene through early Miocene age exposed in the Mt. Rainier area of the central Cascade Range. It is a part of the volcanic basement upon which the more imposing Cascade stratovolcanoes have been formed. The Fifes Peak Formation and rocks of equivalent age, together with the Oligocene Ohanapecosh Formation, form the bulk of the volcanic Cascade arc in Washington.

The subject of this thesis ia a part of the Fifes Peak Formation located along the Naches River at Cliffdell (Fig. 1). The study area is situated along the eastern margin of the outcrop belt where the Fifes Peak Formation and older rocks disappear beneath the extensive cover of the Columbia River Basalt Group. The study area encompasses about 116 km^2 (45 $miles^2$) situated NE and SW of the Naches River at Cliffdell within the Cliffdell and Manastash Lake 7.5 minute quadrangles.

The study area is located within the transition zone between the heavily forested Cascades and the sagebrush country typical of the eastern part of the state. Access through much of the area is excellent, as are exposures in many places. Elevations vary from 695 m in the Naches River valley to above 1800 m in the Bald Mountain area.

Purpose of Study

The principal objectives of this study are to:

1) map or refine the outcrop margin of the Fifes Peak Formation;
2) describe the stratigraphy and structure of the Cliffdell area, with emphasis on the Fifes Peak Formation;
3) classify and characterize the lavas of the Fifes Peak Formation

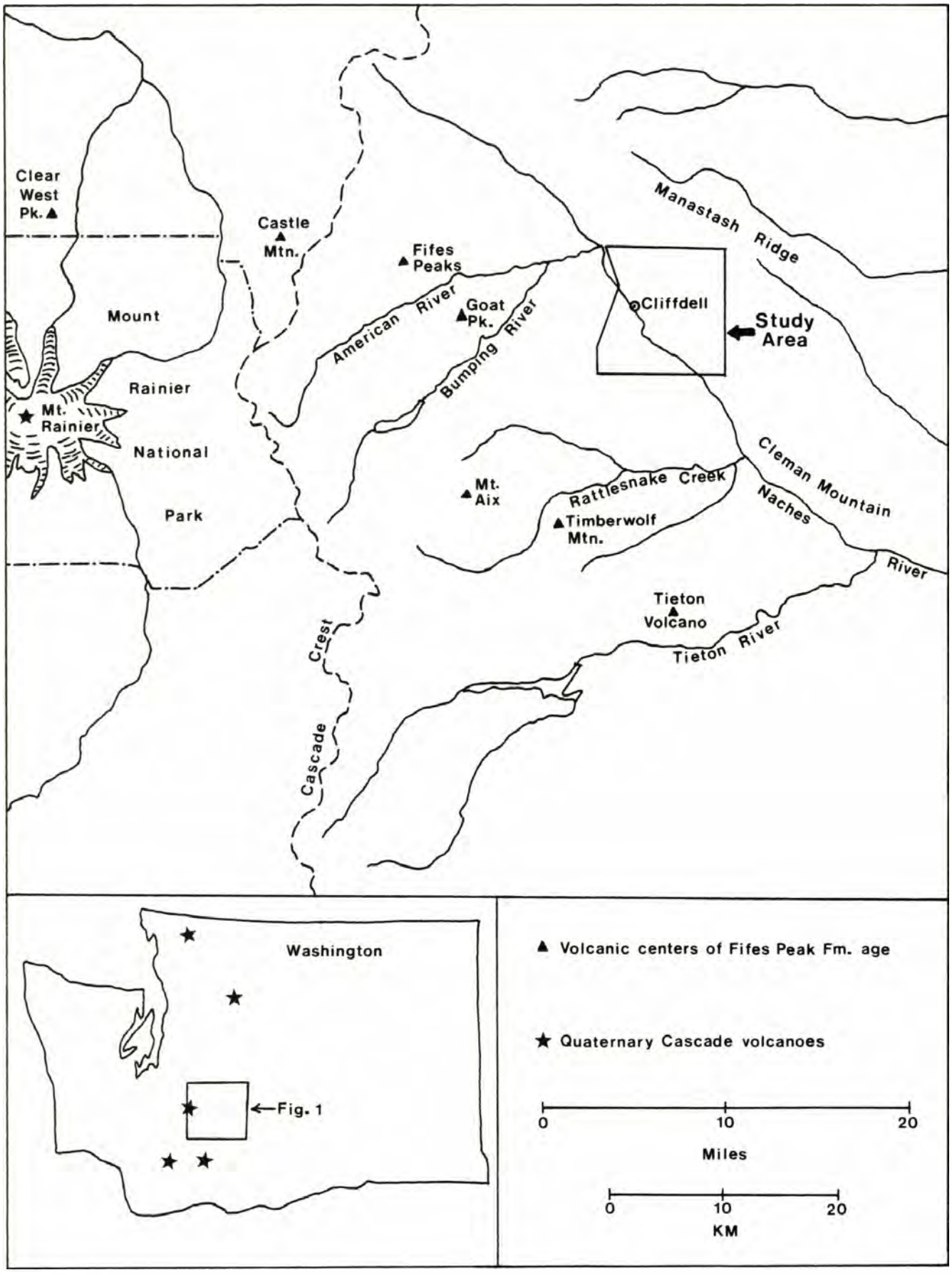

Figure 1. Location map of the study area in the central Cascades Range of Washington.

petrographically and geochemically;

4) evaluate the Cliffdell area as a volcanic center in the Fifes Peak Formation; and to

5) discuss the Cliffdell area in relation to the Fifes Peak Formation elsewhere and in the context of Tertiary volcanism in the Cascades Range.

The Fifes Peak Formation provides an excellent opportunity to examine the stratigraphy and structure of a deeply eroded volcanic terrain. The Fifes Peak Formation has received relatively little attention geochemically and should be a part of any comprehensive interpretation of the volcanic evolution of the Cascade Range. This study will contribute to our understanding of the stratigraphy, structure and geochemistry of the middle Tertiary volcanic basement of this region.

Tectonic and Regional Setting of the Study Area

The Cascade Range is a continental margin volcanic arc. The present N-S-oriented range was initiated at about 37 m.y. (Vance et al., 1987) following accretion of the Coast Range and Olympic Mountains. The Cascade Range is comprised of thick and varied volcanic assemblages intruded by epizonal batholiths along its length. The oldest rocks exposed in the vicinity of the study area are the pre-Tertiary crystalline rocks of the Tieton inlier (Clayton, 1983) and those exposed north of the study area along Manastash Ridge (Stout, 1964).

A three-fold stratigraphic sequence had long been recognized in the Mt. Rainier vicinity (Waters, 1961; Fiske et al., 1963) consisting, in ascending order, of: the Ohanapecosh Formation, the Stevens Ridge Formation and the Fifes Peak Formation. Acquisition of new dates, however, have shown that the type section of the Fifes Peak Formation is

older than the type section of the Stevens Ridge Formation (Vance et al., 1987). Vance et al. (1987) have proposed redefining the Fifes Peak Formation to include the Stevens Ridge Formation as a member.

Volcanic rocks coeval with the Fifes Peak Formation in Washington extend as far south as the Columbia River (Phillips et al., 1986; Evarts et al., 1987; Walsh et al., 1987), but are far less extensive than the Ohanapecosh Formation, having probably been removed by erosion over much of the area. These rocks are only locally exposed north of Snoqualmie Pass (Frizzell et al., 1984).

The Fifes Peak episode of volcanism, from 27 to about 20 Ma (Vance et al., 1987), was initiated following uplift and erosion of the Ohanapecosh Formation at 28 to 27 Ma (Vance et al., 1987). Fifes Peak volcanism was characterized by the eruption of dominantly andesitic lava sequences with interbedded silicic ignimbrites. The eruption of lavas occurred at scattered shield and stratovolcanoes (Fig. 1), including the Tieton Volcano (Swanson, 1964) and the type section at Fifes Peaks. Eruptive products coalesced to form a volcanic field that, in the Mt. Rainier area, was at least 75 km wide (Walsh et al., 1987).

Previous Work

Smith (1903) and Smith and Calkins (1906) carried out the earliest work in the central Cascades and were the first to begin subdivision of the vast quantities of volcanic materials exposed there. Warren (1941) was the first to distinguish a heterogeneous assemblage of lava flows, mudflows and volcaniclastic sediments, which he named the Fifes Peak Andesite. The type section is at Fifes Peaks, located about 34 km northeast of Mt. Rainier. Warren mapped a narrow strip of the Fifes Peak

andesite southward into the Tieton River area, and recognized that these rocks were older than the widespread Columbia River Basalt. Abbott (1953) mapped and described the petrography of the andesitic breccias and lava flows at the type section at Fifes Peaks.

Waters (1961) and Fiske et al. (1963) significantly revised and clarified the stratigraphy and nomenclature of the Mt. Rainier area. In Mt. Rainier National Park, a sequence of slightly to moderately altered olivine basalt to basaltic andesite lava flows , subordinate mudflows and minor tuffaceous clastic rocks were correlated with Warren's Fifes Peak andesite and redefined as the Fifes Peak Formation.

Warren (1941) identified several possible sources for the volcanic materials of the Fifes Peak Formation: the type locality at Fifes Peaks; along the Tieton River near Rimrock Lake; and along the Naches River at Cliffdell. Swanson (1964, 1966) confirmed Warren's suggestion and described in detail the structure and petrology of two overlapping cones along the Tieton River east of Rimrock Lake. In the Cliffdell area, Warren (p. 801, 1941) referred to a "low dome of lower Keechelus rocks surrounded by outward-dipping beds of the Fifes Peak andesite." He believed the area to be "the site of a volcano which has since been thoroughly eroded."

Campbell (1975) briefly described the steeply-dipping volcanics of the Cliffdell area as forming part of a high volcanic cone.

Bentley (1977) mapped the Cliffdell area in reconnaissance fashion. The Fifes Peak Formation of the Cliffdell area is shown in part on the map by Hammond (1980) of the central and southern Cascades.

Furlong (1982) included samples from the Fifes Peak Formation in the Cliffdell area in his thesis on the paleomagnetism of the Mt. Rainier area. No specific conclusions regarding the Cliffdell area were reported.

Recent work on the Fifes Peak Formation in the greater Mt. Rainier vicinity by Vance et al. (1987) has provided many new dates and thus contributed greatly to understanding of the complex stratigraphy in the south-central Cascades.

Mapping from this study has been incorporated into the new geologic map of the SW quadrant of Washington (Walsh et al., 1987). A volcanic center in the Fifes Peak Formation at Timberwolf Mtn., located about 15 km south of the study area, has been recently mapped and studied by Shultz (1988).

Analytical Methods

Major elements were determined by x-ray fluorescence at Washington State University with a Philips P.W. 1410 manual spectrometer. Samples were ground and doubly fused with lithium tetraborate at WSU. Analyses were reported on an anhydrous basis normalized to 100%.

For trace element determinations, rock chips from the same samples used above were crushed to centimeter or less sizes in a 315 stainless steel mortar and pestal. Chips were agitated in water and rinsed to remove any possible metallic fragments, then ground in a Bico "pulverizer" using aluminum oxide grinding plates. Enough material was ground to obtain between 70 and 100 grams of powder for each sample.

The elements Ni, Sr, V and Y were determined by x-ray fluorescence at Washington State University. Other trace elements were determined by instrumental neutron activation at Oregon State University. At OSU, (C.V. Smith, personal comm.) approximately 0.8 grams of each sample were activated for 3 hours at 1 MW in the rotating rack of the OSU TRIGA reactor. After a decay period of 5 days, the samples were counted with a

Ge(Li) detector connected to a ND-600 multichannel analyzer to obtain La, Sm, Yb and Lu abundances. After an additional decay period of 40 days, the samples were counted with a Ge(Li) detector connected to a ND-2200 multichannel analyzer to obtain Sc, Cr, Fe, Co, Ni, Sr, Zr, Ba, Ce, Eu, Tb, Hf, Ta and Th. For all trace elements other than REE, the rock standard BHVO (Basalt, Hawaiian Volcanic Observatory) was used. REE were normalized to CRB2, an inhouse OSU standard from the same quarry as BCR-1. Abundances obtained from these standards and estimated errors are listed together with the results in Appendices A through F.

Sample 93 in Appendix E contains low abundances of Cs, Rb, Sr, Sc, Cr, Co, Ta and possibly Zr. These low abundances probably reflect inadequate equipment warm-up time (written comm., A.G. Johnson, 1986). Eu and Tb values for this sample are uncertain also.

Ferrous iron contents were determined by ammonium metavanadate titration (Peters, 1968). Using the total iron given by the XRF analysis, ferric iron was calculated and the analysis subsequently renormalized to 100%.

Modes were determined by point-counting standard thin sections with a 0.5 mm x 0.5 mm grid. Total points counted on each thin section varied between 1,000 and 2,000 points. Modal abundances reported to two decimal places are unrounded data and are not intended to be so precise.

Whole-rock K-Ar dates were performed by Teledyne Isotopes of Westwood, New Jersey, courtesy of Steve Reidel, Rockwell International, Richland.

STRATIGRAPHY

Rocks in the Cliffdell area range in age from late Eocene to late Miocene. The Fifes Peak Formation overlies the late Eocene to Oligocene(?) Naches Formation (Tabor et al., 1984) and other rocks that could be part of the Naches Formation or the Oligocene Ohanapecosh Formation. The middle Miocene Grande Ronde Basalt and the late Miocene Ellensburg Formation both overlie the Fifes Peak Formation. The age of the Fifes Peak Formation in the study area is latest Oligocene to early Miocene and will be discussed in a separate section. In the stratigraphy sections to follow, emphasis will be placed on lithologic description of the Fifes Peak Formation. Rocks pre-dating and post-dating the Fifes Peak Formation will be briefly described. A schematic, composite stratigraphic section which illustrates the interpreted structural relationships and relative thicknesses of the various rock units in the study area is shown in Figure 2.

Pre-Fifes Peak Formation Rocks

Rocks older than the Fifes Peak Formation are exposed in two principal areas: in the Milk Creek valley in the northern part of the map area and as an erosional inlier surrounded by the Fifes Peak Formation in the central part of the map area. Other exposures of rocks possibly pre-dating the Fifes Peak Formation are present at Devils Slide and at the southwest margin of the map area.

Naches Formation

The Naches Formation is exposed unconformably beneath the Fifes Peak Formation in the Milk Creek Valley. Naches rocks were examined in detail only south of Milk Creek and in the vicinity of Milk Pond. The Naches

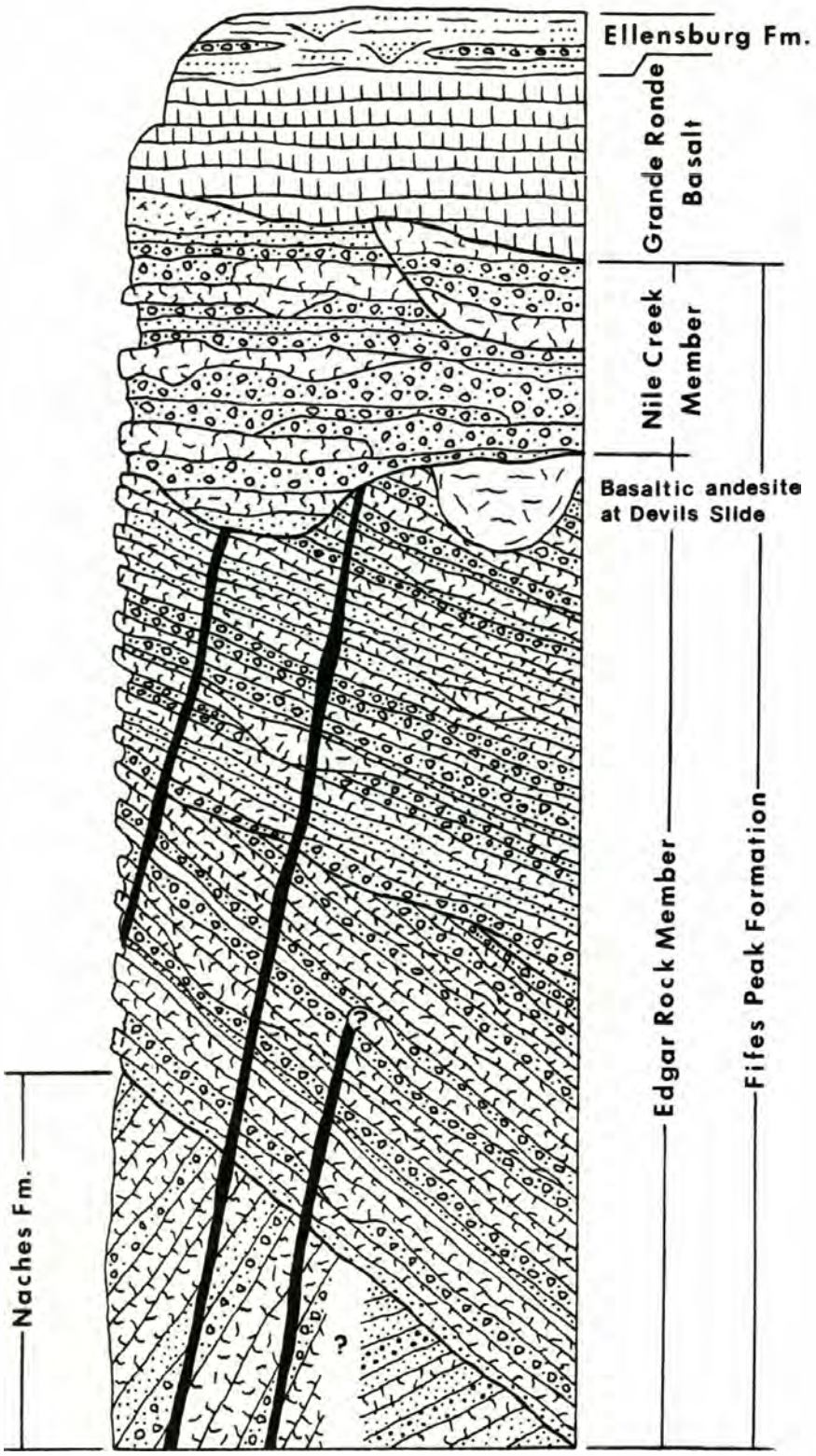

Figure 2. Schematic, composite stratigraphic column of rocks in the Cliffdell area.

Figure 3. Volcanic sandstone, granulestone and coarser conglomerate of the Naches Formation at Milk Pond. Beds are dipping 40 degrees SW.

Formation is well exposed only in road cuts; landslide debris and thick cover obscure much of the area.

Volcaniclastic rocks are the most abundant rock type and comprise medium- to coarse-grained, lithic to feldspathic volcanic sandstones, granulestones and coarser conglomerates (Fig. 3). Most of these rocks are poorly indurated and occur in shades of green, blue-green, purple and brown. Volcanic sandstones and granulestones are composed of angular to rounded clasts of a wide variety of volcanic rocks as well as minor grains of fresh pyroxene and traces of quartz. Feldspathic sandstones contain abundant clouded plagioclase only slightly rounded. Sandstones generally occur in beds less than 1 to 2.5 m in thickness.

Interbedded with sandstones are pebble to boulder conglomerates. These occur in beds 10 cm to 4 m in thickness and are composed of generally well-rounded volcanic clasts reaching 0.5 m across. Some conglomerate is well indurated with a fine-grained, blue matrix.

Volcaniclastic rocks make up only a small portion of the Naches Formation and occur mainly in the upper part of the formation (Stout, 1964; Tabor et al., 1984). The feldspathic to feldspatholithic subquartzose sandstone typical of the Naches Formation (Tabor et al., 1984) was not observed in the Milk Creek valley; and, although some sandstones contain abundant feldspar, quartz is present in only minor amounts. The Naches Formation of the Milk Creek valley may represent a volcanic-rich facies high in the Naches stratigraphic section.

Lava flows (or sills) within the Naches Formation occur south of Milk Creek SE of Milk Pond. These rocks are black when fresh, unbrecciated, and weather to brown, partly spheroidally-weathered surfaces. They contain phenocrysts of plagioclase and minor olivine within intersertal

groundmasses.

In the NE corner of section 11, a N15E-trending, columnar-jointed, basaltic andesite dike (sample 76, Appendix B) about 8 m thick intrudes purple sediments. This dike contains phenocrysts of plagioclase, olivine and minor, stubby, prismatic to equant clinopyroxene and lesser orthopyroxene. The intersertal groundmass contains blocky plagioclase, pyroxene granules, altered olivine, magnetite and altered glass. Coarser, gabbroic inclusions are also present in the dike. The petrography of this dike was examined in detail to evaluate the possibility of it being a feeder for flows in the Fifes Peak Formation. The presence in the dike of euhedral pyroxene phenocrysts and microphenocrysts distinguishes it from most lavas of similar composition in the Fifes Peak Formation. Chemically, however, it is very similar to some of the analyzed dikes related to the Fifes Peak Formation. This dike is very similar to the Naches flows just described, but it has larger and slightly more abundant plagioclase phenocrysts. It is possible that these rocks represent sills that are cogenetic with flows in the Fifes Peak Formation.

Undifferentiated Tertiary Volcanics

Roadcuts along Highway 410 in the central part of the map area expose altered volcanic rocks which are situated unconformably beneath the Fifes Peak Formation. Elsewhere these rocks are poorly exposed. These rocks include lava flows, volcanic breccias and minor volcaniclastic sediments which have undergone partial propylitization. Most fresh exposures are shades of green in color and weather brown.

The most common rock type is lava of andesitic composition. Plagioclase phenocrysts are fresh or partially replaced by carbonate, sericite and chlorite. Ferromagnesian phenocrysts, pyroxenes and

hornblende, are generally completely replaced by carbonate and chlorite. Hornblende phenocrysts retain recognizable opacite rims. Groundmasses are partially replaced by carbonate, chlorite and quartz. Vesicles are filled with carbonate, chlorite and minor zeolites. Nonporphyritic, green and white, altered diabase may represent dikes. Other evidence of hydrothermal alteration throughout the undifferentiated Tertiary volcanics includes carbonate and lesser quartz veining, patchy exposures of highly oxidized, rusty-brown rock and disseminated sulfides.

Volcanic breccias are heterolithologic and contain angular to subrounded volcanic clasts up to 30 cm across.

Exposures are generally massive or highly fractured with little evidence of primary structure or bedding visible. However, at the turnout of the Gold Creek road (Fig. 4), beds are dipping 65 degrees NW. Here also, shear zones and fractures intersect bedding at high angles.

Warren (1941) correlated the undifferentiated Tertiary volcanics with rocks that are now known to be Ohanapecosh Formation. Bentley (1977) assigned these rocks to the Naches Formation and also separated other rocks which he regarded as pre- Tertiary, but all rocks appear sufficiently similar to be regarded as one unit. The abundance of altered andesitic lavas distinguishes these rocks from those in the Milk Creek valley. The rocks are also distinct from the well-bedded rocks of the Wildcat Creek beds exposed west of the study area in the Tieton River area (Swanson, 1964) and in the Nelson Butte area (Schreiber, 1981). As the Wildcat Creek beds are regarded as a distal facies of the Ohanapecosh Formation (Vance et al., 1987), a correlation with the Ohanapecosh Formation is less likely, unless proximity to another volcanic center is indicated. In this regard, the undifferentiated Tertiary volcanics may be part of the Timberwolf Mtn. facies of the Ohanapecosh Formation, mapped by

Figure 4. Undifferentiated Tertiary volcanics exposed at the turnout of the Gold Creek road at Highway 410.

Shultz (1988) at Timberwolf Mtn., about 15 km south of the study area.

Other possible pre-Fifes Peak Formation Rocks

At Devils Slide in the upper part of the Milk Creek valley (Fig. 5), a generally massive unit of pyroclastic(?) breccia and minor lava is exposed beneath typical lithologies of the Fifes Peak Formation. The massive pyroclastic(?) breccias are light brown, yellowish and pink in color. Alteration in the form of patchy, rust-colored areas, traces of sulfide mineralization and carbonate-filled fractures resemble some of the alteration in the undifferentiated Tertiary volcanics. At the east end of Devils Slide, coarse laharic breccias with clasts up to 2 m across are present, striking 35 degrees E and dipping 15 degrees SE.

The massive nature of the unit and the higher degree of alteration distinguishes these rocks from typical rocks of the Fifes Peak Formation. Dips are discordant to Fifes Peak beds at Devils Slide. This unit is distinct from other rocks predating the Fifes Peak Formation at lower elevations in the Milk Creek valley and in the undifferentiated Tertiary volcanics.

At the southern margin of the map area, a roadcut near the section line between sections 14 and 15 along the North Fork of Nile Creek road exposes a light gray unit of massive to finely laminated, silicified tuff or fine-grained sediment. The rock produces a distinctive quartzite-like clink when struck with a hammer. A XRF analysis revealed a SiO_2 content of about 99.5 %, with traces of titanium, sodium and phosphorus. This highly altered rock is also presumed to pre-date the Fifes Peak Formation.

Figure 5. Devils Slide viewed from the north across the upper Milk Creek valley. Well-bedded sediments, lava flows and breccias of the Edgar Rock member of the Fifes Peak Formation (above dashed line) overlie massive, light-colored pyroclastic(?) breccias. Massive lava at right center producing the talus slope is the basaltic andesite at Devils Slide. The slide scarp is about 1.7 km long and 200 m high.

Fifes Peak Formation

Mapping in the Cliffdell area has revealed that undivided rocks belonging to the Fifes Peak Formation mapped by previous workers (Warren, 1941; Bentley, 1977; Hammond, 1980) can be divided into two lithologically and structurally distinct groups of rocks separated by a pronounced angular unconformity. The oldest group is informally named, by the writer, the Edgar Rock member, after the prominent topographic feature composed of these rocks at Cliffdell (Fig. 6). The younger group is informally named the Nile Creek member.

The stratigraphic relations at Cliffdell are similar to those described by Swanson (1964) in the Tieton River area; in both areas an older, more deformed unit is overlain by a younger sequence distinctly different than the older one.

Edgar Rock Member

The Edgar Rock member is a thick sequence of interbedded lava flows, laharic breccias, bedded volcaniclastic sediments and tuffs. These rocks form most of the rugged exposures in the Cliffdell area and define a circular dome of outwardly-dipping beds surrounding the core of undifferentiated Tertiary volcanics previously described. Bentley (1977) referred to this structure as the Edgar Rock dome. This name will be retained for use in this study. A thickness of at least 1,800 m is exposed along Highway 410 at Edgar Rock. The base of the member lies with angular unconformity upon pre-Fifes Peak Formation rocks; the top is overlain with angular unconformity by the Nile Creek member, the Grande Ronde Basalt or the Ellensburg Formation.

The Edgar Rock member is composed predominantly of laharic breccia and

Figure 6. Edgar Rock at Cliffdell. Interbedded lava flows, laharic breccia and sediments dip 45 to 50 degrees to the northwest. Topographic relief is about 400 m.

lava flows; bedded sediments are subordinate and tuffs are very minor. Few of these units are distinctive. The discontinuous nature of individual units, lack of continuous exposure and possible lateral gradations, all hamper tracing beds for any great distance.

Stratigraphic sections Three partial stratigraphic sections within the Edgar Rock member are shown in Figure 7. These sections represent most of the lithologic variation found within the Edgar Rock member and illustrate the typical thickness and character of interbedding of the lithologies of the Edgar Rock member. Section A is from a cliff facing the center of the Edgar Rock dome about 4 km from the center of the dome. Section B is located on a SW-facing cliff along the Lefthand Fork of Rock Creek. Section C is located in the northern part of the map area at sample location 40.

Lava flows and flow breccia The basaltic andesite lava flows of the Edgar Rock member are characteristically highly brecciated. Individual flows range in thickness from 2 m to about 40 m, but most are between 5 and 10 m thick. Where exposure is complete, a three-tiered structure is apparent in many flows. At the base of a flow is a monolithologic breccia (Fig. 8), varying from less than 1 up to 2 m in thickness, which is composed of angular to subrounded clasts within a matrix of granulated rock and crystals. The basal breccia is well indurated and both matrix and clasts are purplish in color. Overlying the basal breccia is an unbrecciated zone of dense or only slightly vesicular, blocky jointed lava. This zone, although absent in some flows, is commonly 0.5 to 1.5 m thick; the maximum thickness observed was about 5 to 6 m. Overlying the unbrecciated zone and commonly making up most of the thickness of a flow

Figure 7. Representative, partial stratigraphic sections within the Edgar Rock member.

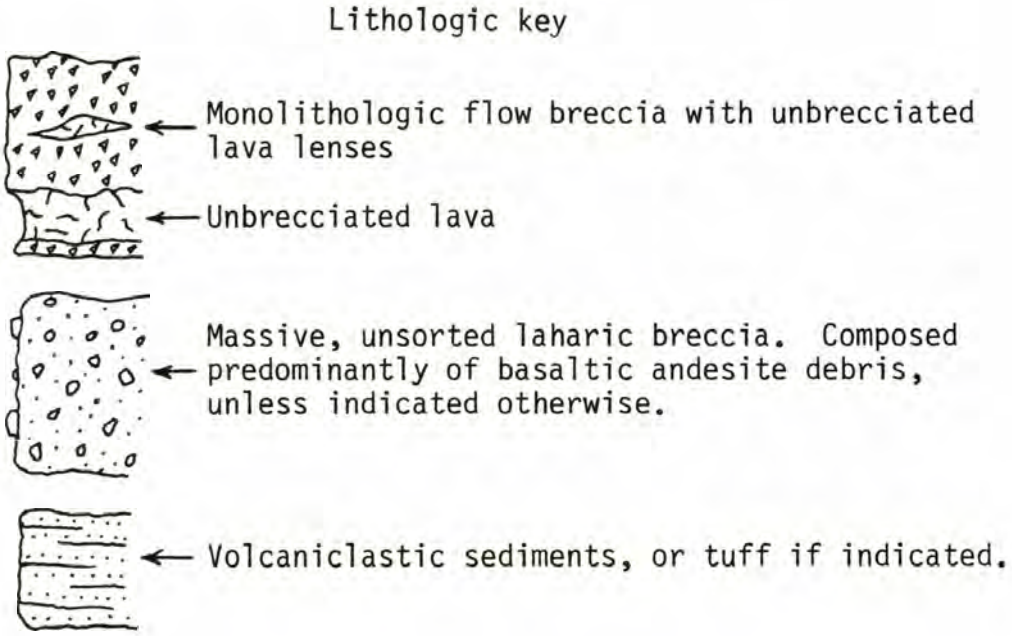

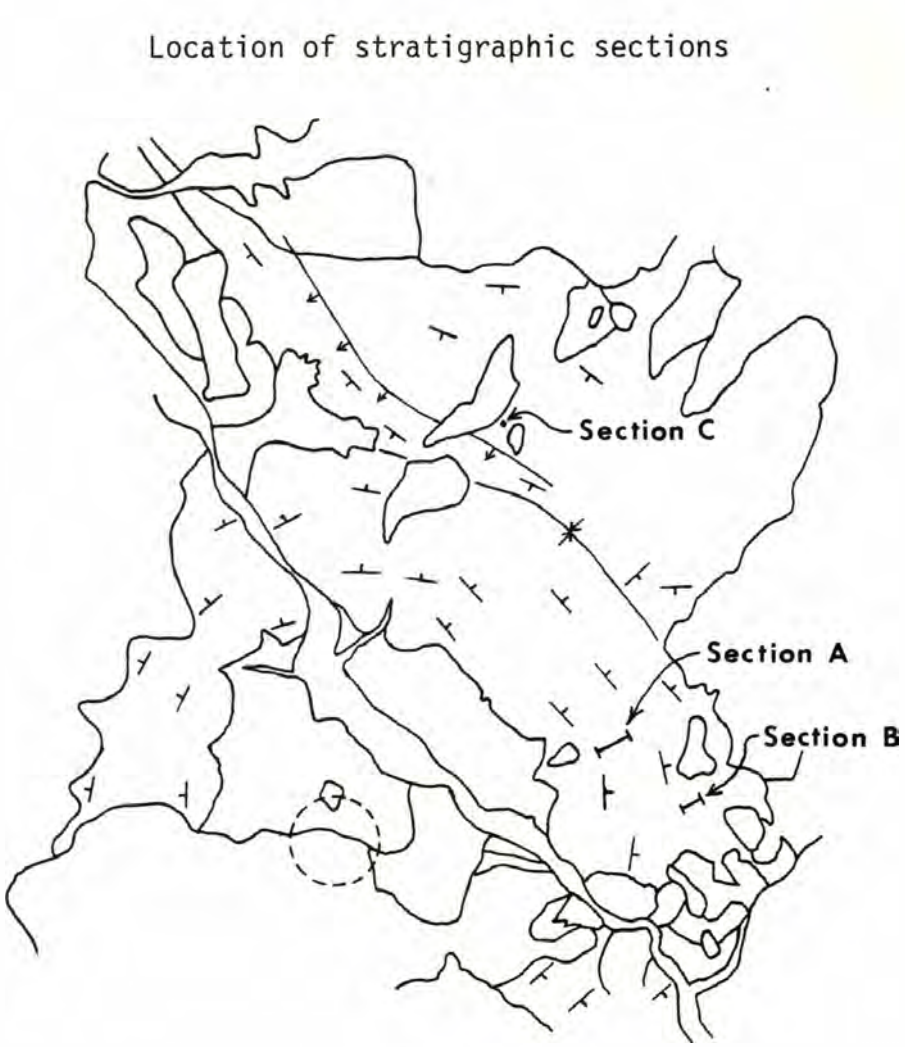

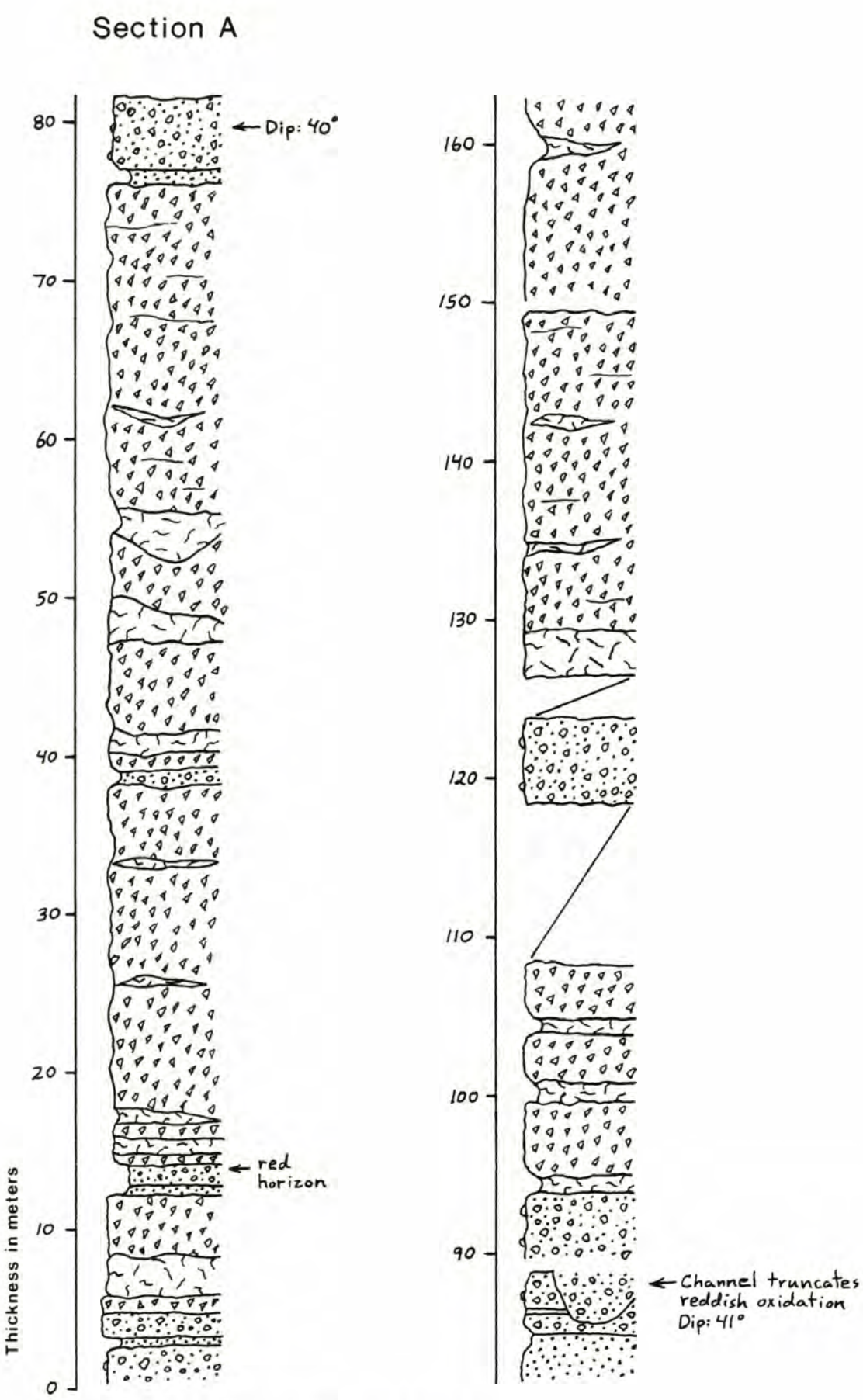

Figure 7, continued

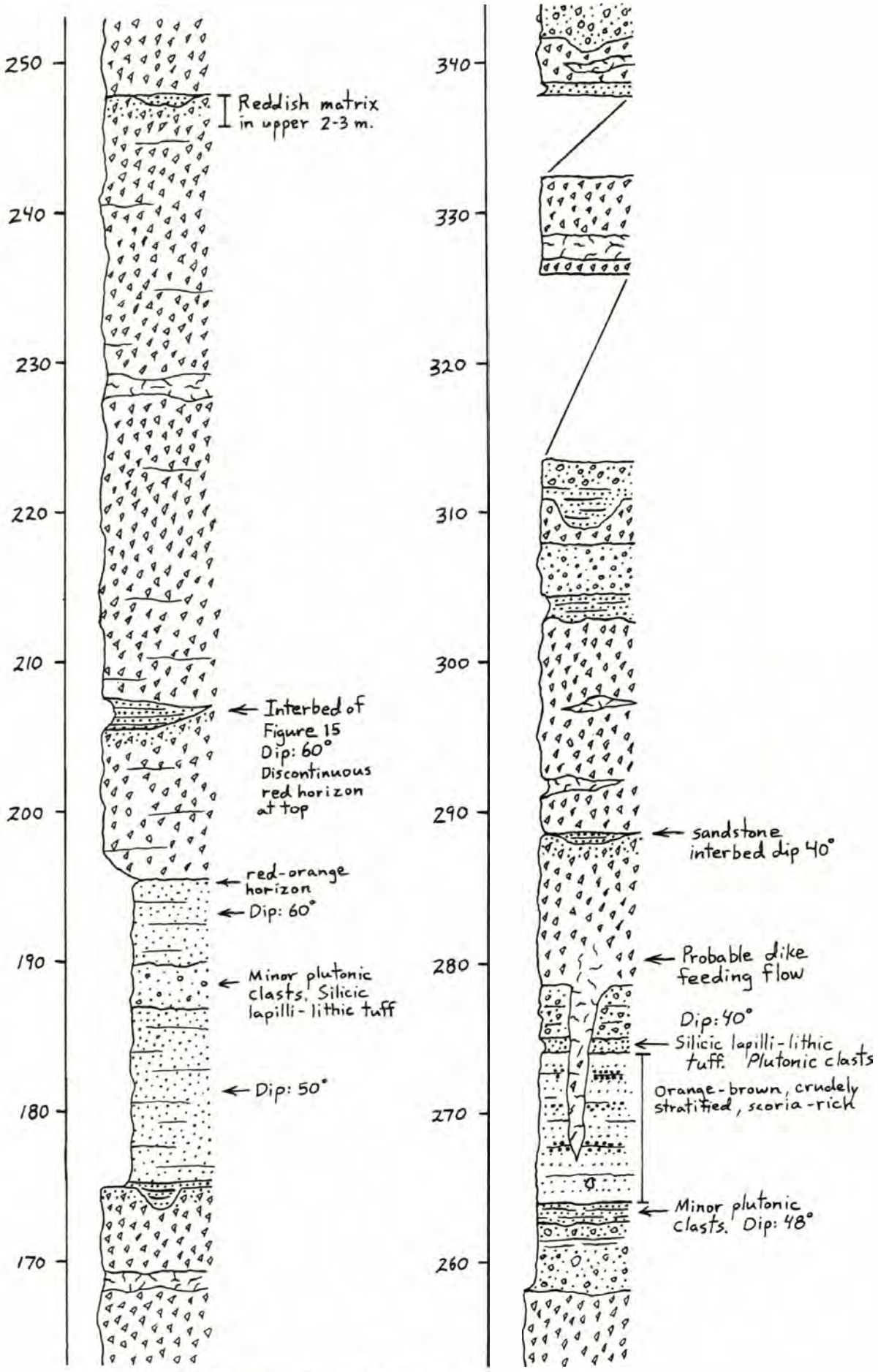

Figure 7, continued

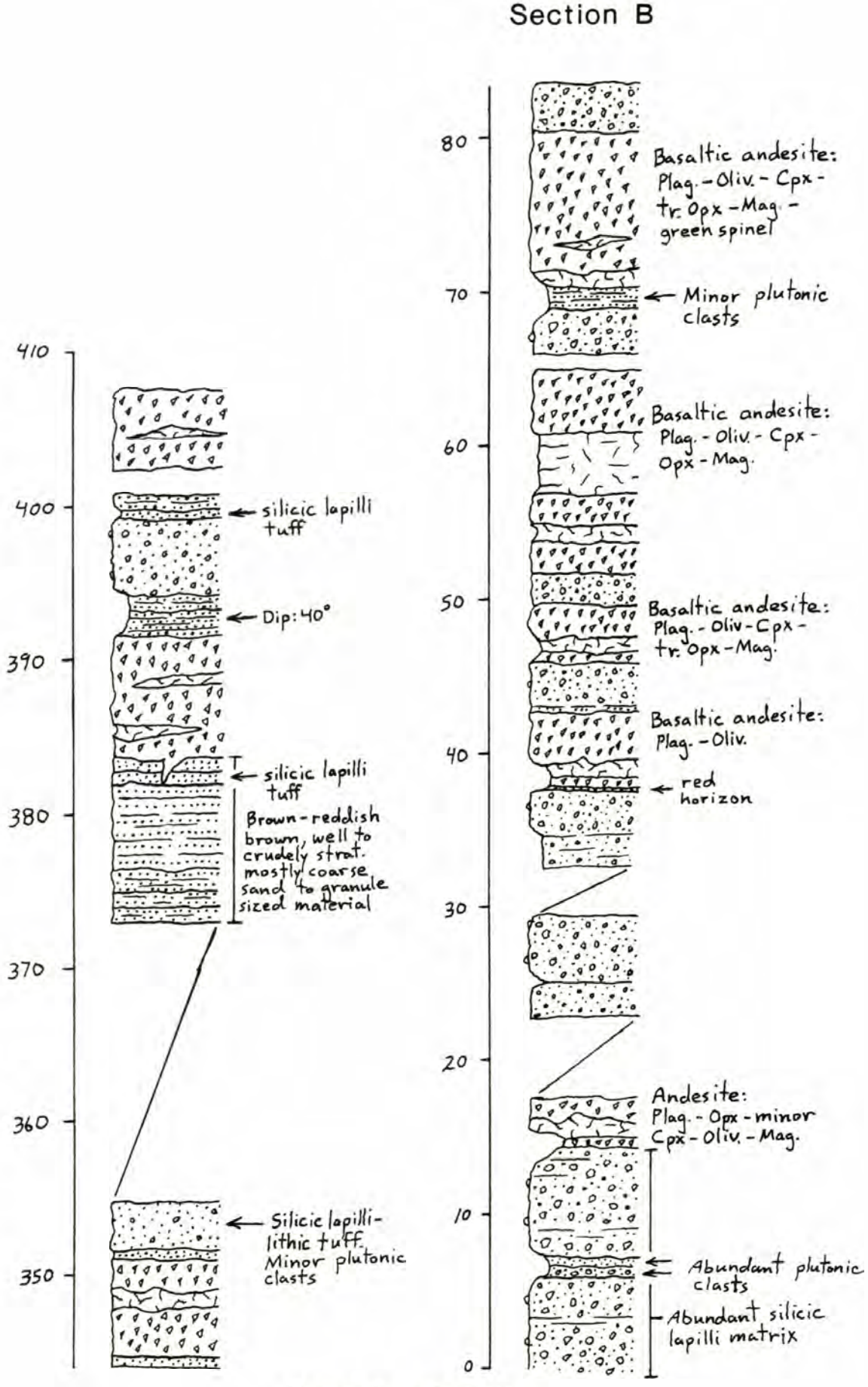

Figure 7, continued

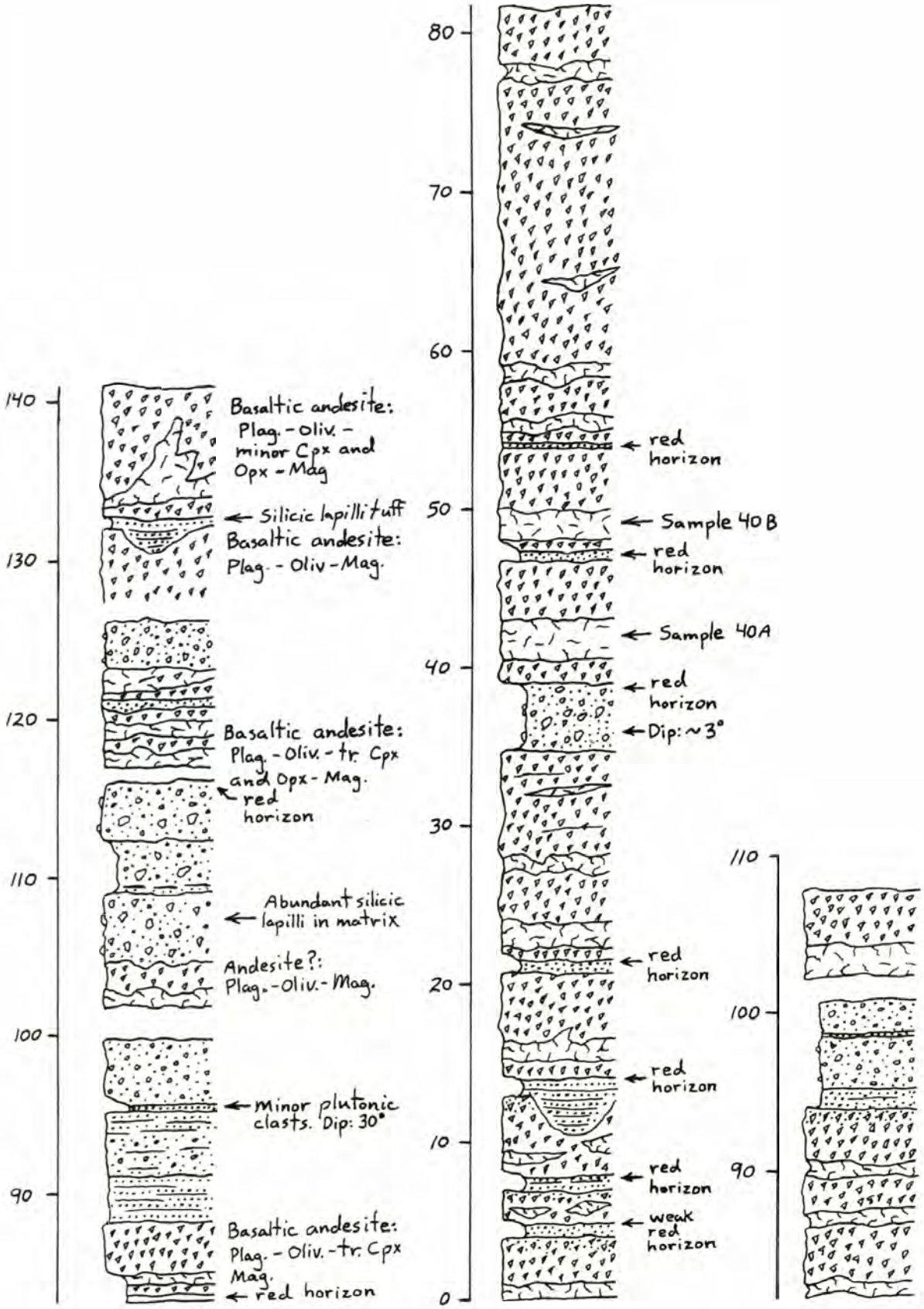

Figure 7, continued

Figure 8. Basal breccia of a basaltic andesite lava flow, Edgar Rock member. The contact with unbrecciated lava is visible at the upper right. Hammer handle is 34 cm long. Located in the canyon of the Lefthand Fork of Rock Creek.

is an upper or flow top breccia. This breccia is monolithologic and comprised of dense to scoriacous, angular to subrounded clasts in a sparser matrix similar in composition to that of the basal breccia. Breccia clasts are commonly very uniform in size and generally range in size from 2 to 5 cm. Like the basal breccia, the flow top breccia is invariably purplish in color. Streaks and lenses of unbrecciated lava are commonly present within the upper breccia. The upper breccia is well indurated and in many places overhangs a recessively-weathering unbrecciated zone (Fig. 9). The contact at the top of the upper breccia is commonly abrupt. In places, however, sediments fill interstices in the upper breccia to a depth of about 1 m.

The overall structure of these autobrecciated basaltic andesite flows is similar to that of block lava (Macdonald, 1953; Curtis, 1954), although the breccia clasts lack the smooth, polyhedral form which generally characterizes block lava (Fisher, 1960).

Some flows consist of interlayered brecciated lava and unbrecciated lava (Fig. 10), possibly representing superposition of successive flow units. Thicker flows (20 to 40 m thick) are nearly completely brecciated from base to top. Vague stratification is defined by streaks or lenses of unbrecciated lava or by slight variations in breccia clast size. Columnar jointing was not observed in any flows of the Edgar Rock member.

A probable connection between a lava flow and a dike is exposed in the SW 1/4 of section 32, T. 17 N, R. 15 E (see stratigraphic section A). A narrow dike 30 to 50 cm thick connects directly with the base of a lava flow. The dike is unbrecciated, but blocky-jointed, and flares in width, to about 2 m, a few meters below the base of the flow. The margins of the dike are undulating and appear to have baked the adjacent sediments. A tongue of unbrecciated lava from the dike extends upward into flow

Figure 9. Interbedded lava flows, laharic breccias and volcaniclastic sediments in a cliff face in the canyon of the Lefthand Fork of Rock Creek. The prominent gray unit in the center of the photo (upper left to lower right) is a highly brecciated basaltic andesite lava flow about 5 m thick. Note the recessively-weathering unbrecciated lava near the base of the flow. The dip here is about 30 degrees east.

Figure 10. Thick basaltic andesite lava flow in the Edgar Rock Member. The flow is 15 to 20 m thick and consists of interlayered brecciated and unbrecciated lava. A narrow red baked(?) horizon immediately underlies the flow. Brilliantly colored red to purple breccias of uncertain origin are situated beneath a tan colored tuff bed containing scoria bombs(?). Located near the radio tower in the SW1/4 of section 24 along the North Fork of Gold Creek.

breccia. This relationship suggests rapid brecciation of the lava upon extrusion to the surface. A "quiet" eruption is suggested by the lack of scoria and spatter.

A brilliant brick red to orange, oxidized layer is situated beneath the basal breccia of some lava flows (Fig. 10). Such layers are particularly well developed in the northcentral part of the map area ("red horizons", Fig. 7, section C; also in sections A and B). These layers are generally less than a meter thick and are developed in tuff, clastic layers or laharic breccia. The top is partially caught up in the basal breccia fragments; the base can be sharp or grade into the underlying material. These layers could be the result of baking by the overlying lava flow or weathering, or both, but the absence of such intensely colored layers where lava flows are not present suggests that baking is the most common cause.

Andesite and dacite flows are brecciated in a fashion similar to flows of more mafic compositions. Andesite flows more commonly exhibit platey jointing or greater vesicularity.

The basaltic andesite at Devils Slide (Plate 1; Fig. 5) has been interpreted as a flow which occupies a deep channel eroded into the Edgar Rock member. The flow is exposed in cross section at Devils Slide and is at least 150 m thick. Rock recognizably part of the flow extends to the SW for only about 1 km.

Laharic breccia Laharic breccias occur in depositional units varying from less than 1 m up to about 10 m in thickness. Most breccias exhibit little vertical size grading, but when grading is visible, it is normal. All laharic breccias are matrix supported (Figures 11 and 12). Matrix colors range from tan through shades of brown to reddish brown. In

general, a darker brown or reddish brown color reflects a monolithologic character of the laharic breccia (Fig. 11). These brownish colors of laharic breccias are in contrast to the almost invariable purple color of monolithologic flow breccia, allowing for positive identification in the field.

Most commonly the largest clasts are 0.5 to 1 m across, but a few were found up to about 2 m across. Clasts are generally angular to subangular. Subrounded to rounded clasts are very rare and only occur as isolated clasts amongst more angular material.

Clast texture varies through a complete range from dense to highly vesicular and scoriaceous. The relative proportion of dense to highly vesicular clasts varies between lahars, reflecting variations in source material or mode of origin of the lahar. All clasts appear to fall within the compositional range of basalt to andesite. Dense and vesicular clasts are most commonly highly porphyritic and occur in a variety of colors: black, gray and brown being most common. Weathering rinds occur on some clasts, but are not common. Scoriaceous clasts are generally less than 10 cm across and are angular to irregular. Forms suggestive of an origin as bombs with either ballistic or breadcrust surfaces are rarely recognizable. Fresh scoria clasts occur most commonly in shades of brown, but are also purple, orange and red. Yellowish, altered scoria lapilli, 1 to 2 cm across, are common in many laharic breccias.

Approximately 30 clasts from 4 laharic breccias were examined in thin section. These clasts are characterized by the phenocryst assemblage of plagioclase and olivine with minor magnetite. Clinopyroxene is absent or present in minor amounts. Groundmass textures are intergranular and tend to be finer grained than the coarsest intergranular texture found in the

Figure 11. Thick basaltic andesite laharic breccia of the Edgar Rock member. This laharic breccia is nearly monolithologic and contains massive to scoriaceous clasts up to 1 m across. The large clast at center is 0.7 m across. Some scoriaceous clasts are concentrated in the "surge" (S) visible near the top of the lahar at the right side of the photo. Plagioclase and olivine are the only phenocryst phases of the clasts and matrix material. The matrix contains crystalline lithic fragments, plagioclase and olivine grains and porphyritic scoriacous material with nearly opaque groundmasses. The top 1.5 m of the lahar (D) is finer grained and shows some reworking, or represents a later, more dilute, phase of the depositional sequence.

Figure 12. Basaltic andesite laharic breccia, Edgar Rock member. The entire unit is about 10 m thick and dips 45 degrees NW. Clast at left center is 0.6 m across. Hammer handle is 34 cm long. Located along the Spring Creek road 0.5 km NW of the junction with Highway 410.

unbrecciated parts of lava flows. Field observation indicates that olivine is also a common phenocryst present.

In thin section, the matrix material (all material less than about 1 cm across) is comprised of angular to rounded, scoriaceous to dense fragments. Scoriaceous fragments are porphyritic and contain plagioclase and olivine phenocrysts set in nearly opaque, glassy and commonly microlitic grandmasses. Some scoria fragments have primary rounded edges. Dense fragments are similar to the larger clasts. Olivine, replaced by iddingsite, and plagioclase grains with adhering groundmass are also present. Yellowish secondary material, and less commonly carbonate, occur with the finest matrix material and may fill vesicles in scoriaceous fragments.

It is possible that some of the mass flowage deposits of the Edgar Rock member may be pyroclastic flows. However, recognition requires a careful study of depositional structures or thermoremnant magnetism which was beyond the scope of this study (cf. Hoblitt and Kellogg [1979]; Fisher and Schmincke [1984]).

Features indicative of heat, such as welding, columnar jointing, fossil fumarole pipes or carbonized wood (wood in any form or indications of it were rarely observed), were not observed in any laharic breccias. However, the abundance of scoriaceous and glassy material in some breccias, especially in the matrix (as in the lahar of Fig. 11) suggest that they could have been deposited either as hot pyroclastic flows or pyroclastic flows which have become variably diluted with water.

Mullineaux and Crandell (1962) describe a "probable lahar" in the upper Kalama River valley about 15 km from the summit of Mt. St. Helens. The deposit is 5 to 7 m thick and is unstratified and ungraded. The coarse-sand fraction of the friable, sandy matrix is comprised of

fragments of crystal-rich devitrified glass and euhedral crystals of plagioclase, hypersthene and clinopyroxene that are found as phenocrysts in the larger clasts. Scoria, pale brown vesicular glass, rounded white pumice and clear glass shards comprise 20 to 30% of the coarse-sand size. The overall color of this deposit is light gray, but the upper 2 m have a faint reddish color (Mullineaux and Crandell, 1962). Paleomagnetic evidence suggests that most of the larger clasts were near or above the Curie point during final emplacement. Carbonized logs are present within the deposit. Beacause the Kalama River lahar was at a high temperature and contains pumice in the matrix, Mullineaux and Crandell believe that the lahar resembles the deposit of a gas-rich glowing avalanche. The predominantly nonvesicular nature of the bulk of the deposit, however, distinguishes the Kalama River deposit from gas-rich glowing avalanches (Mullineaux and Crandell, 1962). Mullineaux and Crandell suggest that the Kalama River deposit began either as an intermediate type of hot avalanche or a gas-poor avalanche that incorporated fresh, vesicular materials.

Some laharic breccias of the Edgar Rock member possess characteristics similar to the Kalama River lahar. Glassy and scoriaceous material (except for light-colored silicic material or shards) are present in amounts similar to that in the Kalama River lahar. Color changes to reds or reddish brown occur in the upper parts of some laharic breccias in the Edgar Rock member. Pyroclastic flow deposits can be oxidized to reddish colors in their upper parts due to the escape of hot gases (Fisher and Schmincke, 1984). Reddish tops of mass flowage deposits in early Mt. St. Helens valley fill assemblages (Crandell and Mullineaux, 1973; Hyde, 1975) have been used by these authors to distinguish pyroclastic flows from lahars. The lahar of Figure 11 is one of the most striking examples of

this type of color change observed in the Edgar Rock member.

In conclusion, some laharic breccias of the Edgar Rock member possess characteristics suggesting that they were emplaced at high temperature and thus may be intermediate between cooler, water mobilized laharic breccias and pyroclastic flows.

Silicic lapilli laharic breccias Laharic breccias consisting almost exclusively of basaltic andesite debris are the most common variety in the Edgar Rock member, but a less common type contains variable amounts of silicic material (Fig. 13). The silicic material is in the form of gray, white to light pink, angular lapilli. These occur in a very restricted size range, averaging about 1 cm across and rarely reaching 4 or 5 cm. Many lapilli are finely banded, either parallel or contorted. Most lapilli are nonvesicular, but some contain very fine vesicles. They are never pumiceous.

In thin section the lapilli are shown to be a sparsely porphyritic, silicic volcanic rock containing phenocrysts of plagioclase, orthopyroxene, magnetite and rare hornblende and quartz in a very fine-grained, devitrified groundmass containing plagioclase microlites.

These lapilli are present in variable proportions in laharic breccias. The lapilli can dominate a deposit (Fig. 13), occur as a dominant matrix constituent to other more typical basaltic andesite clasts, or occur as a minor component scattered throughout basaltic andesite laharic breccias. Similar silicic lapilli also occur in thinner (several cm to 1 m thick), massive, nearly pure beds. These are probably airfall tuffs.

The silicic lapilli laharic breccia of Figure 13 is at least 7 m thick and is the thickest such bed observed in the Edgar Rock member. It is markedly graded with dense to highly vesicular basaltic andesite clasts up

Figure 13. Silicic lapilli laharic breccia of the Edgar Rock member. A: This wide view shows the silicic lapilli as the dominant component of the unit and a concentration of basaltic andesite clasts near the base of the unit. B: Close-up of the unit within the basal clast concentration with greater resolution of the matrix. Hammer handle is 34 cm long.

A

B

to 2 m in length concentrated near the base. These clasts may be concentrated along the axis of a shallow channel. Minor clasts of plutonic rock up to several cm across are scattered through the deposit. Fine-grained matrix material is very sparse and interstices are in part open voids.

A possible origin for this deposit and others similar to it relates to the restricted size range of the silicic lapilli. Mobilization of a large amount of loose, sorted airfall tephra on the slopes of a volcano, perhaps by saturation with water, or by dry collapse on a steep slope, could result in a debris flow which entrained clasts of larger size and different composition as it swept downslope.

The silicic lapilli laharic breccias could have been derived from the same source as the other laharic breccias and lava flows, because they probably flowed down the same aggradational paleoslope and contain typical olivine-bearing basaltic andesite clasts.

Accidental clasts in laharic breccias Accidental clasts of plutonic rock, sandstone and altered volcanic rock are present in some laharic breccias and silicic lapilli laharic breccias. All of these rock types are distinct from typical materials present in the Edgar Rock member and were not observed as inclusions in lava flows.

Plutonic clasts are generally medium-grained rocks of gabbro to diorite composition. Sizes range from small plutonic aggregates visible only in thin section, to clasts about 30 cm across. The clasts are typically angular to subangular. Two varieties of plutonic material are present. One is a black and white, fresh-appearing rock which is composed of abundant calcic plagioclase (An 65), clinopyroxene and hornblende. Hornblende is green to brown and either rims and replaces clinopyroxene or

occurs as extensive ophitic grains up to 20 mm across. Other minerals present in minor amounts are orthopyroxene, olivine, brown biotite, apatite, magnetite, quartz and potassium feldspar. The other plutonic variety is somewhat finer grained and weathers to a pale yellowish color. Some plutonic clasts are partially encased in a rind of light-colored volcanic rock (Fig. 14) which is similar to some of the silicic lapilli observed elsewhere.

Sandstone clasts are generally light-colored, medium-grained quartzo-feldspathic sandstone which generally occurs as friable clasts less than 5 cm across. The largest clast observed was an angular, pebbly block about 25 cm across.

Altered volcanic rocks are green to brownish green, porphyritic lava which has undergone more intense alteration than is typical for most material in the Edgar Rock member. Some of these clasts resemble, but are not necessarily derived from, the altered volcanic rock in the undifferentiated Tertiary volcanic unit below the Edgar Rock member.

Plutonic clasts are very rare in laharic breccias comprised primarily of basaltic andesite debris. They are more abundant, but still a minor component, in silicic lapilli laharic breccias, and are concentrated in certain thin (about 1 m thick) heterolithologic laharic breccias. Sandstone and altered volcanic clasts are usually present with plutonic material, but are much less abundant. Plutonic clasts are present at a number of horizons throughout approximately 600 m of section in the vicinity of the Lefthand Fork of Rock Creek. Horizons where plutonic clasts were found are noted on the stratigraphic columns in Figure 7.

Possible origins for the accidental clasts include: ejection as accidental lithics from a volcanic vent, plucking from outcrops by lahars, or incorporation from streams carrying these rock types. The repeated

Figure 14. Plutonic clast in a heterolithologic laharic breccia. The clast (about 6 cm long) is present in a thin (about 1 m thick) laharic breccia in which plutonic clasts are concentrated. The clast is partially enclosed by a rind of silicic volcanic rock similar to some of the silicic material in the silicic lapilli laharic breccias. This plutonic-bearing horizon is the lowest one depicted on stratigraphic section B, Figure 7. Located in the canyon of the Lefthand Fork of Rock Creek.

occurence of plutonic clast-bearing horizons throughout the considerable stratigraphic thickness suggests a source which was either continuously exposed or that clasts were episodically made available through volcanic eruptions. The accidental clasts show no visible evidence of baking or metamorphism that might be caused by being carried within a volcanic system and, as previously stated, were not observed within lava flows.

Incorporation from streams carrying these materials seems unlikely based on the generally angular form of the clasts and the lack of any other stream-rounded materials that would be expected to be present. Any outcrops between the source area of the laharic breccias and the depositional site would likely become progressively buried by the repeated passage of lahars. The presence of a silicic, volcanic rind on some plutonic clasts suggests that these, and probably the others as well, may have been ejected by explosive eruptions.

Bedded sediments Bedded sediments are generally confined to narrow sequences between some coarser, nonbedded laharic breccias or lava flows. These sediments are composed of: well-sorted, medium- to coarse-grained volcanic sandstone (less than 1 to 2 m thick), angular granule to pebbly sandstone (up to about 4 m thick), poorly sorted cobbley sandstone (1 to 2 m thick), and rarer large cobble- to boulder-bearing sandstones (2 to 3 m thick) containing clasts up to about 0.5 m across.

As observed in thin section, volcanic sandstones are composed of angular, microlitic to porphyritic, dense to vesicular rock fragments, olivine and plagioclase grains with adhering groundmass, subordinate pyroxene, and rare hornblende, quartz and glass shards. Most pore spaces are open voids. The composition of the sandstones is similar to that of the fine-grained material in laharic breccias. The sandstones contain the

phenocryst assemblage (plagioclase and olivine) typical of the most abundant lava flows and laharic breccia clasts.

Bedding in all sediments is parallel. This combined with poor sorting and the rare occurence of boulders in some, suggest that most of these sediments were deposited rapidly as hyperconcentrated flood flows (Smith, 1986). Conspicuously absent in the Edgar Rock member are well rounded, fluvial conglomerates, such as are present in the younger Ellensburg Formation. The lack of such sediments suggests that the Edgar Rock member was not the product of larger, more permanent, through-flowing streams.

Bedded sediments, though minor in volume, are significant because they provide the least ambiguous paleoslope indicators. In this sense, the sediments do not provide a unique dip for a deposit, but only suggest that it was low. Horizontally bedded sandstones or other bedded sediments are present at a number of horizons around the Edgar Rock dome (Fig. 15). Such sediments were probably deposited at rather low initial dip and suggest that the presently observed dips in the Edgar Rock dome cannot be interpreted as representing the steeper flanks of a volcanic cone.

Tuffs Several varieties of primary to reworked, mainly airfall tuffs can be identified in the Edgar Rock member. In general, tuffs are not abundant and are confined to discrete horizons. Coarse-ash tuffs are tan to light gray, generally massive and rarely exceed a meter in thickness. Lapilli tuffs are more common and are composed of both scoriaceous and silicic lapilli. Scoria lapilli tuffs are massive to vaguely bedded and range in thickness from less than one meter to at least 5 meters. Fresh scoria lapilli are shades of brown in color, whereas more altered scoria is yellowish.

Lapilli tuffs composed of angular silicic lapilli and variable

Figure 15. Steeply dipping sedimentary interbed in the Edgar Rock member. The sediments are dipping 60 degrees and are situated between two nearly completely brecciated lava flows. Occurrences like this suggest a large component of deformational dip, rather than primary, dip. Located in the cliffs facing the center of the Edgar Rock dome in the SW 1/4 of section 32, T. 17N, R. 15E. Interbed location noted on stratigraphic column A, Figure 7. Hammer for scale near the center of the photo.

proportions of angular lithic lapilli are the most distinctive type of lapilli tuff observed in the Edgar Rock member (Fig. 16). These tuffs occur in beds up to about 3 m in thickness, but are most commonly less than a meter thick. In some units, the tuffs have an open, porous framework and a fine-grained fraction is very minor or absent. Silicic lapilli occur in colors ranging from white to light gray and average about 1 cm across. The largest are up to about 5 cm across. Prismatic hornblende is an abundant phenocryst of the lapilli in certain tuff beds. Lithic lapilli are porphyritic basaltic andesite. Some are up to 10 to 15 cm across. Plutonic fragments are a minor, but common, constituent in these tuffs. They range in size from less than 1 cm to rare fragments up to about 6 cm across. Silicic lapilli tuffs appear to be most abundant in the eastern half of the map area, as are laharic breccias containing abundant quantities of silicic lapilli. Very little material of this type was observed in the thick section at Edgar Rock.

Figure 16. Silicic lapilli tuff in an Edgar Rock member laharic breccia sequence. An approximately 25 m thick sequence contains laharic breccia units less than 1 m to about 4 m in thickness. The largest clasts present are about 0.6 m across. Tuff bed is 0.3 m thick. Dip is about 11 degrees south. Located 0.5 km west of Devils Slide in the NE 1/4 of section 18, T. 17 N, R. 14 E.

The Radial Dike System

Intruding the Edgar Rock member and the older rocks below it is an extensive system of radial dikes with a projected area of focus SW of the Naches River in sections 2 and 11, T. 16N, R. 14E (Fig. 22). Only the northern half of the radial pattern is exposed. The southern half is probably covered by the Nile Creek member and younger rocks. The area of focus is near the structural center of the Edgar Rock dome, located perhaps 1 to 1.5 km southwest of it. No dikes were observed to intrude the Nile Creek member or the Grande Ronde Basalt.

Dikes are most abundantly exposed in the cliffs of the Edgar Rock member facing the center of the dome. Dikes are present up to the highest elevations in the cliffs, but are more abundant at lower elevations (Fig. 17). Most dikes are located within a distance of about 5 km from the area of focus. One dike on the radial trend was identified about 7 km distant. Due to incomplete exposure and difficult access on the cliffs, most dikes were not traceable for any great distance. Dikes of all compositions appear to conform to the radial pattern.

The dike thicknesses range from a few centimeters up to about 3 m, but average about 1 m. Dikes typically intrude strata along nearly planar contacts, but can also follow sinuous courses or be deflected by resistent units, forming a sill for a short distance. Dips of the dikes range from vertical to about 55 degrees. Columnar jointing and chilled margins are commonly present in the dikes, with columnar jointing developed more prominently in andesitic dikes. Some dikes have weathered-out to form deep, narrow slots, whereas others stand up as vertical walls (Fig. 18). Elongated vesicles in some dikes suggest that flow within the dikes was upward and outward from the area of focus of the dike system. Multiple

Figure 17. Dikes intruding the Edgar Rock member along Highway 410 near Edgar Rock. These dikes are situated near the base of the member.

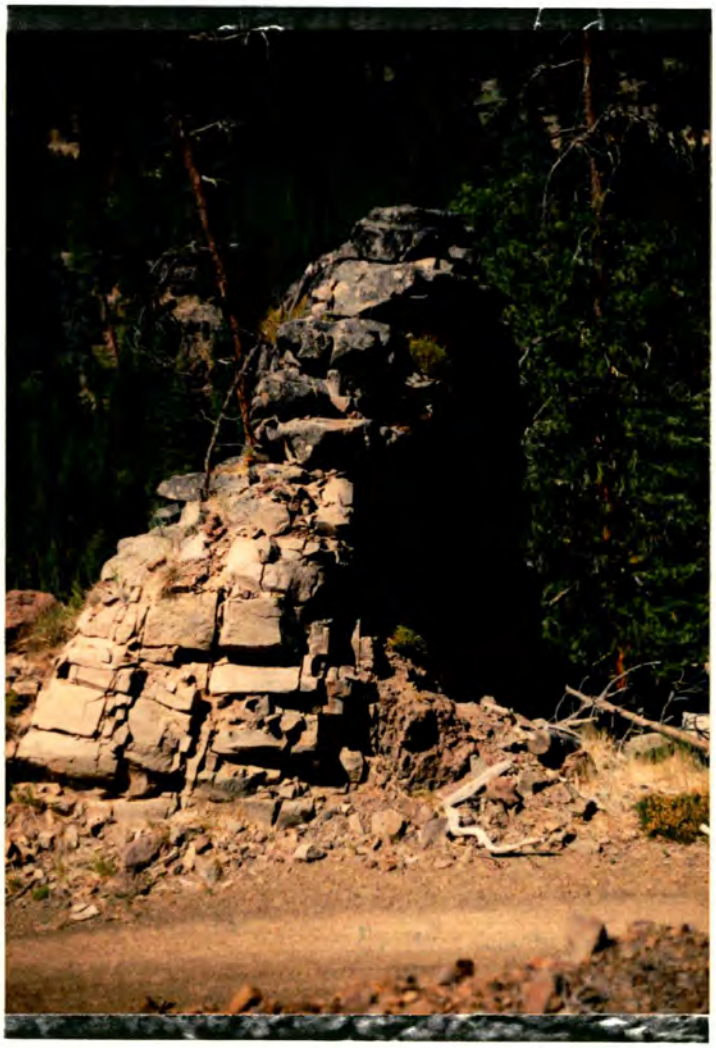

Figure 18. Andesite dike intruding the Edgar Rock member 1.5 km SW of Haystack Rock. The columnar jointed dike is 2 to 3 m thick and contains phenocrysts of plagioclase, orthopyroxene, clinopyroxene, magnetite and a trace of olivine.

dike injections are visible in some places and are up to 4 or 5 m wide. As previously described, one probable feeder dike for a lava flow within the Edgar Rock member was located.

At the area of focus, poor exposure prevents observation of any increase in dike abundance and no intrusive bodies or volcanic neck are apparent. However, such bodies could be small, concealed by dense vegetation or covered in the Naches River valley. The central plug of the Tieton Volcano (Swanson, 1964) produces no topographic expression.

The undifferentiated Tertiary volcanics below the Edgar Rock member, where they are exposed along Highway 410, contain far fewer dikes than would be expected considering their abundance in the cliffs. Generally, dikes which are on trend with good exposures along the highway are not recognizable in the pre-Edgar Rock member rocks.

Nile Creek Member

The younger, informally-named, Nile Creek member of the Fifes Peak Formation unconformably overlies the Edgar Rock member. The Nile Creek member is largely exposed SW of the Naches River, but extends across the Naches River in the SE corner of the map area (Plate 1; Fig. 22). Here, the Nile Creek member covers a rugged erosional surface developed on the southern part of the Edgar Rock dome. A remnant of an E-W trending paleochannel at least 300 m deep is present in sections 12, 7 and 8. The extent of the Nile Creek member beyond the map area is unknown.

The Nile Creek member is comprised largely of coarse laharic breccia and lava flows, but it also contains minor, poorly sorted, volcaniclastic debris and silicic ash flow tuff. Lavas and laharic breccias are interbedded in part, but the distribution of flows is variable across the area of exposure. Lava flows are abundant in sections 12 and 7, whereas 3 km to the west in the NE corner of section 10, no lava flows were observed in over 250 m of strata. The Nile Creek member is thickest in the SE part of the map area, where it is as much as 550 m thick.

The lava flows of the Nile Creek member are almost exclusively andesites and range in thickness from about 10 to 40 m. Flows commonly display platy jointing and flow banding; some are columnar jointed (Fig. 19). The flows are only sparsely vesicular with minor rounded to ellipsoidal vesicles up to 5 cm across.

The basal colonnade of a thick flow (flow 95) is visible along Highway 410 in the eastern half of section 7 in the southern part of the map area. Thick, platey jointed columns up to 15 m high form a vertical cliff for a distance of about 0.3 km. Based on the attitude of the columns, this part of the flow is nearly flat-lying, but 0.3 km to the west it is dipping 25

Figure 19. Andesite flow of the Nile Creek member. The flow is columnar jointed with weakly developed platey jointing and flow banding. The flow is located in the southern part of the map area along Highway 410.

degrees to the SE. The flow does not appear to be deformed. This structure may represent the margin of the flow as it banked against an erosional surface within the Nile Creek member.

Laharic breccias in the Nile Creek Member contain angular to subangular clasts up to 3.5 m across. The clasts are almost exclusively massive, porphyritic andesite very similar in texture and mineralogy to the andesite flows. The laharic breccias are, on average, coarser, more clast-rich and the matrices are lighter in color than the laharic breccias of the Edgar Rock member. A thick laharic breccia is well exposed along Highway 410 (Fig. 20). Along the northeastern margin of the map area in section 28, laharic breccia exposed in a limited area contains andesite clasts similar to those in the Nile Creek member. This breccia is distant from other Nile Creek exposures, but it could be a remnant of the Nile Creek member.

In the extreme SW corner of the map area (section 17, T. 16N, R. 14E) yellowish to nearly white, poorly consolidated, pumice-ash tuff is interbedded with laharic breccia of the Nile Creek member. Minor volcanic clasts and small plutonic fragments are present within the tuff. In the NE corner of section 17, a massive, non-welded, pumice-rich ash-flow tuff is overlain by Grande Ronde Basalt. This tuff yielded an age of 23.3 +/- 2.4 Ma; its significance will be discussed further in a section to follow. This tuff of the Nile Creek member closely resembles a yellowish, poorly consolidated tuff exposed along Highway 410 near the junction of the Bumping Lake road (Campbell, 1975, p. 35, road log mile 27.5).

The source of the volcanic materials of the Nile Creek member was not identified in this study. Similarity of lava and laharic breccia clast petrography suggest derivation from a single source, but no dikes that

Figure 20. Laharic breccia of the Nile Creek member. Note the coarse, clast-rich nature of the unit and the presence of faint, horizontal structure near the center of the photo, which might suggest the presence of at least two flow units, or an intra-flow surge. The large clast at the top is about 3.5 m across. The outcrop is located in the southern part of the map area along Highway 410.

could have fed lava flows or evidence of a cone structure were observed in the map area. The major element chemistry (analysis in Swanson, 1964) and mode of the Westfall Rocks microdiorite at Rimrock Lake closely resemble those of the andesites of the Nile Creek member, although a direct physical connection between the two areas is not being suggested. The andesites of the Nile Creek member are also similar, both in age and petrography, to andesites at Timberwolf Mtn. (Shultz, 1988), located about 15 km south of the study area. More detailed work is necessary to evaluate presently known volcanic centers as potential sources for the Nile Creek member.

Age of the Fifes Peak Formation in the Cliffdell area

Four lava flows and one dike from the Cliffdell area were dated by the whole-rock K-Ar method. These samples and analytical data are listed in Table 1. Sample numbers correspond to chemical analysis sites plotted on Plate 1. In addition, a fission-track age was determined on a tuff in the Nile Creek member by J.A. Vance at the University of Washington.

The two dated flows from the Edgar Rock member are within the upper half of this member and, although separated by about 4.5 km, are believed to represent a broadly similar stratigraphic position.

Sample 100 from the Nile Creek member is from a flow situated near the base of the member in the SW part of the map area. The other Nile Creek sample (sample 95) was taken from a thick columnar-jointed flow located 1 km SE of sample 100. Both flows are at nearly the same elevation (2,600 ft.). The dated dike intrudes the Edgar Rock member about midway through the section near Edgar Rock along Highway 410.

The dated tuff in the Nile Creek member (sample 115 on Plate 1) is located in the extreme SW corner of the map area in the NW quarter of section 17. This tuff yielded an age of 23.3 +/- 2.4 Ma.

The two oldest ages from the Nile Creek member are consistent with their inferred stratigraphic positions and suggest a 23 to 24 Ma age for the Nile Creek member SW of the Naches River. Sample 95 is young considering its elevation and proximity to sample 100. This young age can be reconciled with the others if the flow occupies a channel eroded within the Nile Creek member. The form of the flow, as discussed earlier, also suggests this is the case. Petrographic and geochemical characteristics of this flow are quite similar to other Nile Creek member flows, a

Table 1

K-Ar ages of Fifes Peak Formation volcanic rocks from the Cliffdell area

Sample	Material analyzed	%K	Ar^{40}_{rad} (scc/gm x 10^{-5})	$\%Ar^{40}_{rad}$	Isotopic age (Ma)
Edgar Rock member					
13, lava flow	whole rock	1.11, 1.13	0.102, 0.107	60.1, 68.4	23.8 ± 1.2
35-1, lava flow	whole rock	1.03, 1.03	0.107, 0.108	61.6, 64.3	26.7 ± 1.3
35-2, lava flow same as 35-1	whole rock	1.06, 1.06	0.098, 0.102	58.1, 58.1	24.1 ± 1.2
84, dike	whole rock	0.93, 0.93	0.092, 0.096	29.5, 27.0	25.8 ± 2.2
Nile Creek member					
95, lava flow	whole rock	1.69, 1.70	0.131, 0.127	77.3, 66.8	19.5 ± 1.0
100, lava flow	whole rock	1.14, 1.15	0.108, 0.109	65.5, 63.3	24.2 ± 1.2

situation which would suggest either production of similar magmas through this time interval or that the other sampled andesites are young also.

A minimum age for the Edgar Rock member is set by the age of the base of the Nile Creek member, about 24 Ma. Also, an unknown amount of time elapsed during the erosion of the Edgar Rock dome before the deposition of the Nile Creek member. The older age from flow 35 in the Edgar Rock member (26.7 Ma., sample 35-1) is assumed to be representative of the age of the Edgar Rock member. The 23.8 Ma age for sample 13 is slightly young under this assumption and has probably undergone some Ar loss. A likely age range for the Edgar Rock member is 25 to 27 Ma. The age of the dike is consistent with the observation that no dikes were observed to intrude the Nile Creek member.

Recent dates obtained from the Fifes Peak Formation in the Mt. Rainier vicinity (Vance et al., 1987) indicate an age range of 27 to 20 Ma for the Fifes Peak Formation. Ages from the Cliffdell area suggest that volcanism in the Cliffdell area began at about the same time as volcanism in the American River area and at the Mt. Aix caldera.

A basal ash-flow tuff, present in many Fifes Peak Formation stratigraphic sections in the Mt. Rainier vicinity (Vance et al., 1987), is absent in the Cliffdell area. The ash-flow tuff in the Nile Creek member is the only tuff identified in the Cliffdell area which may correlate with other recognized tuffs in the Mt. Rainier vicinity. Correlation with the Bumping River and Rattlesnake tuffs seems unlikely based on stratigraphic position and the available age dates. The Nile Creek member tuff is closer in age to the Burnt Mtn. tuff in the Tieton River area (Vance et al., 1987).

Grande Ronde Basalt

The Columbia River Basalt overlying the Fifes Peak Formation and surrounding much of the map area is the middle Miocene Grande Ronde Basalt. Its age in the study area is 15 to 16 Ma (Reidel et al., in press). Bentley (1977) mapped the basalt occupying the Little Naches Syncline as magnetically normal, possibly N_2 (the second magnetically normal subdivision upward from the base of the Grande Ronde Basalt), and both R_2 and N_2 are present along the eastern margin of the map area (Bentley, personal communication). The basalt is at least 400 m thick on the east side of Rock Creek, but is considerably thinner on the west and southwest margins of the map area. Basalt lapped onto a rugged erosion surface formed by the dipping beds of the Edgar Rock dome. Palagonite-tachylite breccias are present in many places at the base of the basalts.

Ellensburg Formation

The Ellensburg Formation in the Cliffdell is similar to the middle Ellensburg Formation as described by Bentley (1977) and also resembles the undifferentiated Ellensburg Formation near Nile described by Luker (1985). The age of the Ellensburg Formation is probably late Miocene (Luker, 1985).

Sediments of the Ellensburg Formation are widely exposed southwest of the Naches River. The formation overlies the Grande Ronde Basalt and parts of both members of the Fifes Peak Formation. Ellensburg Formation is also present in the axis of the Little Naches Syncline.

The Ellensburg Formation in the Cliffdell area consists mostly of a variety of silty to pebbly volcaniclastic sediments, bouldery laharic breccias and well-rounded, pebble to boulder conglomerates. The formation

is about 100 m thick along the western periphery of the map area. The sediments, tuffs and laharic breccia matrices are gray to grayish white in color and contrast with the darker or more yellowish hues of the Fifes Peak Formation rocks. Volcaniclastic sediments are commonly poorly sorted. Parallel bedding and the presence of scattered outsized clasts suggest some were deposited as hyperconcentrated flood flows. Matrix-supported bouldery laharic breccia is present, but appears to be less abundant than at the Ellensburg exposures near Nile. Conglomerates are poorly consolidated and consist of well-rounded, pebble- to boulder-sized clasts composed of gray, brown to pink, intermediate to silicic lavas. The Ellensburg Formation can always be distinguished from both members of the Fifes Peak Formation by its presence of well-rounded conglomerate clasts.

Quaternary deposits and landslides

Alluvium occupies the Naches River valley and the lower reaches of larger tributary streams. Near the mouth of Gold Creek, well-rounded, unconsolidated gravels are present up to perhaps 100 m above the present valley of the Naches River. Although mapped as Quaternary terrace alluvium (Qalt), these sediments may be remnants of an older, perhaps Pleistocene, outwash terrace.

A number of landslides are present in the map area. The most spectacular is Devils Slide in the upper part of the Milk Creek valley (Figure 5). The scarp of this slide is a near vertical wall about 1.7 km long and 200 m high. The slide sent a debris flow down the Milk Creek valley probably as far as the Naches River. A hummocky valley-fill is present at Milk Pond, and the pond itself was formed as the debris blocked a tributary valley.

STRUCTURE

Structural Setting and History

The Cliffdell area is located astride the deformed zone of Columbia River Basalt which defines part of the Olympic - Wallowa lineament (OWL). This is a NW-trending zone of faulting and folding originally identified by Raisz (1945) and extends from the Wallowa Mountains in Oregon to the northern Olympic penninsula. The central third of the OWL, the Cle Elum - Wallula lineament, CLEW (Kienle et al., 1977), in which the study area is located (Fig. 21), is the topographically and structurally most expressed part of the OWL (Kienle, et al., 1977).

The N-S-trending Straight Creek Fault merges with the middle part of the OWL about 20 km N-NW of the study area (Fig. 21). The joining of these two structures occurs within an elevated, highly deformed structural zone between the Little Naches and Yakima Rivers and involves both the Cabin Creek and Manastash River blocks of Tabor et al. (1984). Within this zone, the Straight Creek Fault and its splays swing into parallel alignment with the NW-trending structures within the OWL (Tabor et al., 1984; Vance and Miller, 1981). The White River Fault (Frizzell et al., 1984) appears to emanate from the OWL in this area. The backbone of the structural zone along Manastash Ridge exposes pre-Tertiary metamorphic rocks. As mapped by Tabor et al. (1984), the main splay of the Straight Creek Fault passes the study area about 14.5 km NE of Edgar Rock beneath the Columbia River Basalt.

The Straight Creek Fault has been intruded by the Snoqualmie Batholith, showing that strike-slip motion had ceased by 25 Ma (Tabor et al., 1984) and had probably ceased by 37 Ma (Vance, 1985). Subsequent to strike-slip motion, primarily vertical movements within the Cabin Creek

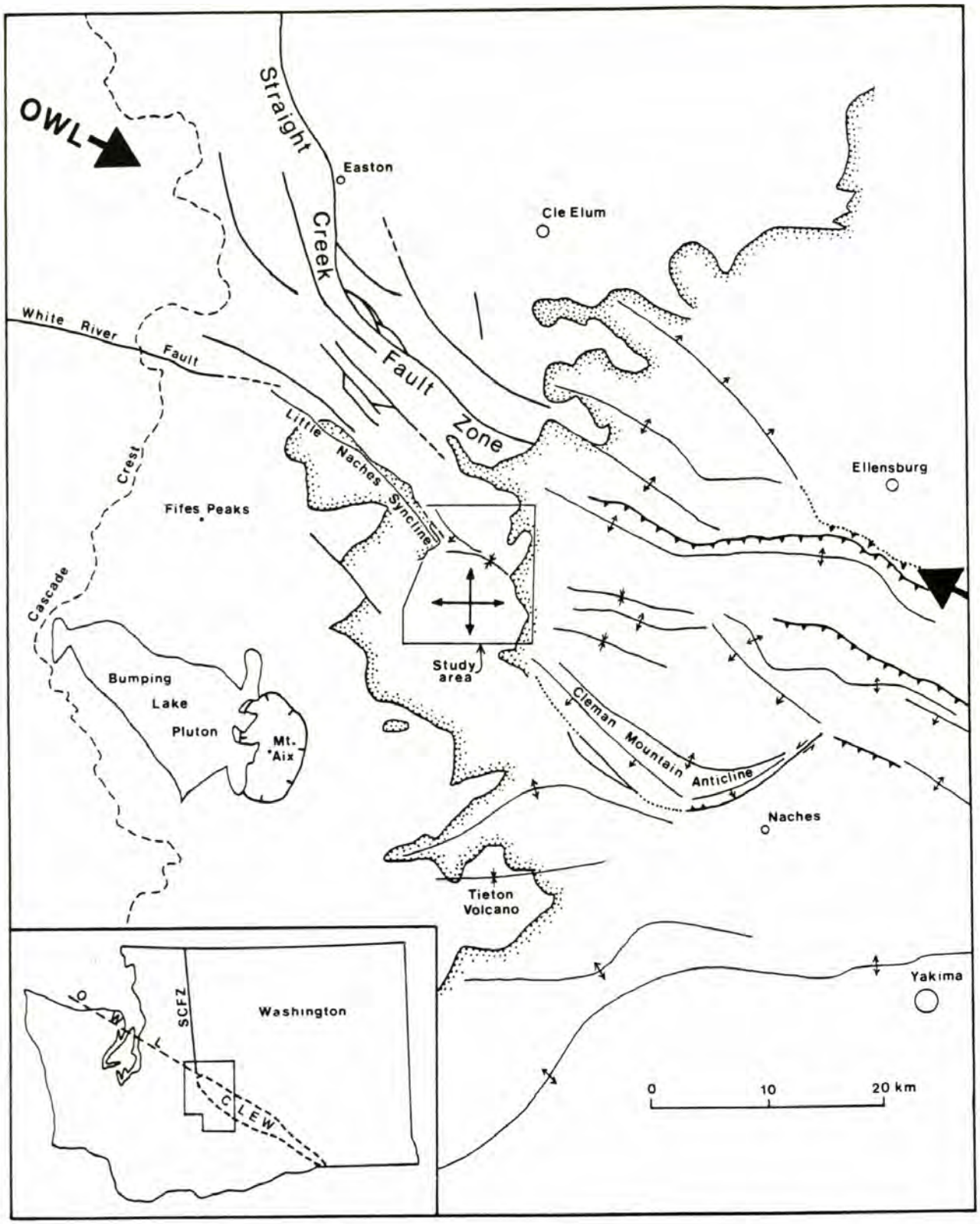

Figure 21. Structural setting of the Cliffdell area relative to the Olympic-Wallowa lineament (OWL) and the Cle Elum-Wallula lineament (CLEW). Stippled boundary is the margin of the Columbia River Basalt. Structures adapted from Bentley (1977), Bentley and Campbell (1983), Frizzell et al. (1984) and Walsh et al. (1987). The Edgar Rock dome is shown by the doubly-plunging cross.

and Manastash River blocks died out during the late Eocene and Oligocene and had ceased by the Miocene (Vance and Miller, 1981; Tabor et al, 1984; Vance, 1985).

Middle Miocene and later deformation has profoundly affected the Columbia River Basalt, giving rise to a system of folded, faulted and monoclinal structures of the CLEW parallel to the older structures within the OWL. Structures within the CLEW typically follow a N60W trend, which is slightly en echelon to the overall trend of the CLEW (Kienle et al., 1977). Although the fundamental nature of the OWL is still unknown (Tabor et al., 1984), the older structures have localized the deformation within the Columbia River Basalt along the OWL.

The Edgar Rock Dome

The most important structural feature of the Cliffdell area is the Edgar Rock dome (Plate 2; Fig. 22). The dome is a roughly circular structure and is defined by outwardly-dipping beds of the Edgar Rock member. The SW quarter of the dome is obscured mostly by the younger Nile Creek member. The dome is bisected by the SE-flowing Naches River, which has entrenched 200 to 300 m into pre-Edgar Rock member rocks.

The dome formed during Fifes Peak time (pre-24 Ma) and had undergone considerable erosion before deposition of the Nile Creek member. Its age is pre-Grande Ronde Basalt as is shown in the SE 1/4 of section 5, T. 16 N, R. 15 E, where the nearly flat-lying Grande Ronde Basalt lapped onto steeply dipping beds of the Edgar Rock member. Beds in the Edgar Rock member generally dip 30 to 50 degrees, but locally are as steep as 60 to 70 degrees (Fig. 15).

The N-NE flank of the dome is bordered by an arcuate syncline (convex to the north, Fig. 22) which separates beds of the dome from more shallow

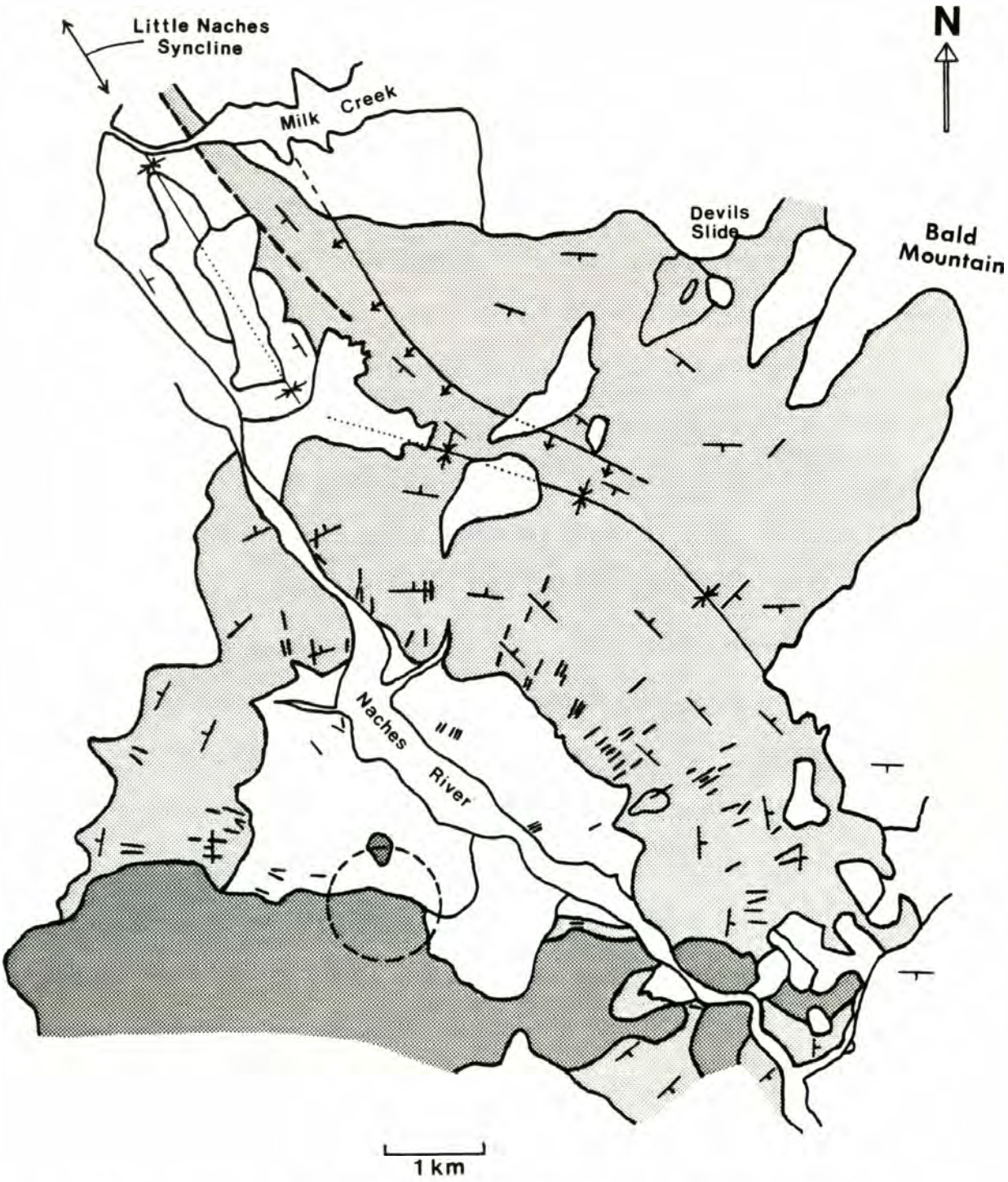

Figure 22. Simplified geologic and structural map of the Fifes Peak Formation in the Cliffdell area. Light stipple is the Edgar Rock member; dark stipple is the Nile Creek member. Short dashes are dikes of the radial dike system. Dashed circle is the focus of the radial dike system.

S- to SE-dipping beds north and east of the syncline. The Grande Ronde Basalt overlaps this structure on the eastern margin of the map area and is not deformed by it. This relationship shows that the syncline formed before the deposition of the Grande Ronde Basalt.

Bedding in the Edgar Rock dome is commonly offset by small normal faults with less than 10 cm up to perhaps 10 m of displacement. These faults are parallel to subparallel to the radial dike trend. A pronounced radial lineation visible on aerial photographs is defined mostly by linear chasms produced, in part, by weathering along faults and fractures , but more commonly by weathering-out of radial dikes.

Syndepositional deformation of the Edgar Rock member is shown by the presence of an angular unconformity within the Edgar Rock member (Fig. 23). Coarse-grained , parallel-bedded, pebbly sandstone (strike and dip: 20W, 40NE) is overlain by coarse , plutonic clast-bearing laharic breccias (strike and dip: 60W, 30NE). Approximately 10 degrees of discordance is present across the unconformity. Dikes in the area cut the unconformity. A discontinuity in dip (perhaps 25 degrees) is present near the NE 1/4 of section 25, t. 17 N, R. 14 E, and suggests another unconformable relationship.

Up-section variations in dip are present in one area of the Edgar Rock member examined in detail (Fig. 7, section A). This section is located 0.6 km from the unconformity of Figure 23. These variations could be due to syndepositional uplift, a continuation of the unconformity, primary depositional attitudes or any combination of the above.

The basal contact of the Edgar Rock member dips outward 20 to 30 degrees from the center of the dome. Near Haystack Rock the basal contact dips about 30 degrees.

Figure 23. Angular unconformity within the Edgar Rock member. Light-colored horizontally-bedded, pebbly sandstone at lower left forms a dip-slope with strike and dip: 20W, 40NE. Overlying coarse laharic breccia has strike and dip: 60W, 30NE. Located in the canyon of the Lefthand Fork of Rock Creek (NE1/4 section 6, T. 16N, R.15E).

The Edgar Rock member north of the structures bordering the dome dips more shallowly. In the NE and northcentral part of the map area, the beds are nearly concordant with the Grande Ronde Basalt along the eastern margin of the study area. This relation shows that beds in this part of the Edgar Rock member were nearly flat-lying before burial by the basalt.

The origin and other structural aspects of the Edgar Rock dome are discussed further in a following section.

Relationship Between the Edgar Rock Dome and Adjacent CLEW Structures

Three structures in and adjacent to the study area form the SW margin of the CLEW. From NW to SE these are: the Little Naches Syncline, the Edgar Rock dome and the Cleman Mountain anticline. The Little Naches Syncline and the Cleman Mountain anticline are structures within the Grande Ronde Basalt.

The Little Naches Syncline is a N60W-trending assymetric syncline with a steep SW-dipping limb. Its axis follows near the course of the Little Naches River for about 19 km NW of the study area (Bentley, 1977). It terminates within the study area on the NW side of the Edgar Rock dome.

Southeast of the study area is the Cleman Mountain anticline. This structure is the most intensely deformed element of the CLEW (Kienle et al., 1977). The structure is assymetrically steep on its SW margin and has over 1000m of structural relief at its culmination near the junction of the Naches and Tieton Rivers (Kienle et al., 1977) about 25 km SE of the study area.

The Grande Ronde Basalt has been displaced (dropped down to the SW), probably through a combination of faulting and folding, nearly 1000 m from a relatively flat-lying position in the vicinity of Bald Mountain east of Devils Slide (Fig. 22) to the trough of the Little Naches Syncline. This

structural displacement continues farther to the NW (Frizzell et al., 1984). Along the immediate eastern margin of the study area, a similar difference in elevation is present, but the basalt traverses this elevation difference through a fairly even, low dip (about 4 degrees) homocline. The basalt in the NW part of the study area has undergone a more complex deformation. Part of the 1,000 m displacement in the basalt is visible in the Fifes Peak Formation as a SW-dipping monocline (Plate 1; Fig. 22). This monocline appears to originate in the Gold Creek valley, as it is not recognizable east along its projected trend. Dips on the monocline generally increase to the NW, becoming parallel to the SW limb of the Little Naches Syncline, showing that the monocline most likely formed together with the syncline. SW-dipping shear surfaces and alteration in the form of carbonate veining and amygdules were observed along part of the trend of the monocline. The monocline merges, in part, with the older syncline which borders the Edgar Rock dome. Thus, the dome is bordered on its northern margin by structures formed during two periods of deformation. A NW-trending fault on the eastern margin of the Little Naches Syncline (Plate 1; Fig. 22) may not be a significant structure, but a trend of smaller offsets parallel to a more fundamental structure producing the monocline. The monocline is on strike with the projected extention of one of the strands of the White River Fault (Frizzell et al., 1984), suggesting a further SW extention of that fault system.

Bentley (1977) states that, like the Cleman Mountain anticline, the Edgar Rock dome is assymetrically steep on its SW margin. No SW assymetry related to CLEW structures was recognized in this study. The SW limb of the Cleman Mountain anticline forms a prominent hogback just south of the map area on the west side of the Naches River. The crestline of the

anticline perhaps swings westward and south of the map area, dies out just SE of the map area or undergoes a structural transition. In any case, a clear pattern of deformation within the Fifes Peak Formation in this area is difficult to recognize. The Little Naches Syncline and a syncline on the SW margin of the Cleman Mountain are of similar form and along strike with one another (Bentley, 1977), but they are not continuous structures.

In conclusion, the Edgar Rock dome retains a form which originated during Fifes Peak time. The influence of post-Grande Ronde Basalt deformation is clearest in the NW part of the study area, but its possible influence is less apparent to the SE.

INTERPRETATION OF STRATIGRAPHIC AND STRUCTURAL RELATIONSHIPS

The Origin of the Edgar Rock Dome

The coincidence of the focus of the radial dike system with the center of the Edgar Rock dome suggests that the dome is a part of a volcanic cone. Warren (1941) was the first to suggest that the Cliffdell area was a vent for the "Fifes Peak andesite." Campbell (1975) also briefly referred to the steeply dipping volcanics at Cliffdell as forming part of a high volcanic cone. Many dips, however are far too steep to represent the primary attitudes of a volcanic cone. This problem is further exacerbated when one considers the laharic breccias and volcaniclastic interbeds that have these high dips. Dips expected on a volcanic cone are generally about 30 degrees (i.e. Fiske et al., 1963. p. 74). Dips in the Edgar Rock dome are commonly greater than 40 degrees and are as high as 65 degrees. Considering these facts together with the outward dip of the basal contact of the Edgar Rock member and the unconformities within it, the dome probably represents a combination of initial dip and combined syn- and post-depositional uplift, most of which occurred during Fifes Peak time.

Evaluation of the Cliffdell Area as a Volcanic Center

Pertinent stratigraphic and structural observations will be considered here to evaluate the Cliffdell area as a volcanic center and attempt to constrain primary structural relations in the study area.

The density of dikes within the radial dike system centered on the Edgar Rock dome is clear evidence that the dome represents the site of an intrusive center and probably the site of a deeply eroded volcanic edifice. Radial dike systems are common at volcanic centers in deeply

eroded volcanic terrains, e.g., the Absaroka volcanics of northwestern Wyoming (Parsons, 1939; Smedes and Prostka, 1972), and are present elsewhere in the Fifes Peak Formation (Swanson, 1963; Hartman, 1973). Mafic dikes in the Cliffdell area are similar to the abundant basaltic andesite flows in many respects. One probable feeder dike for a flow was located. The chemical and petrographic diversity of the dikes require a history of multiple magma intrusions, implying the presence of a long-lived, polygenetic volcanic center.

The lithologies prevailing within the Edgar Rock member - thick flow breccias, coarse laharic breccias and minor reworked or waterlaid sediments - are consistent with a near-source volcanic facies (Parsons, 1969; Fisher and Schmincke, 1984). Repetitive interbedding of lava flows with petrographically similar laharic breccias indicates derivation of these materials from the same source and that the source was probably not far distant.

The maximum slopes upon which laharic breccias can be deposited has significant implications for the primary dips within the Edgar Rock member, as was previously pointed out for the volcaniclastic interbeds. Descriptions (Bloomfield and Valastro, 1977; Newhall, 1979; and Mullineaux and Crandell, 1962) of lahar assemblages and the composition of the aprons of large stratovolcanoes suggest that laharic breccias or debris flows can be deposited on slopes up to 5 to 10 degrees. The laharic breccia shown in Figure 12, located stratigraphically high in the Edgar Rock section near Edgar Rock, dips 45 degrees. Based on the above reasoning, at least 35 degrees of steepening has taken place in the section here. On the SE flank of the Edgar Rock dome (NW1/4 section 8, T. 16 N, R. 15 E), a well-sorted and bedded sandstone interbed dips 32 degrees. At least 30 degrees

of steepening is likely here. This location is about 3.7 km from the focal area of the radial dike system.

The best indication of primary dip in the Edgar Rock dome occurs in the Haystack Rock area. In this area the Edgar Rock member dips 45 degrees, whereas the basal contact dips outward about 30 degrees. Assuming that the basal contact was initially flat and that the dip discordance is not a result of tectonic processes, about 15 degrees of primary dip is possible. The estimated steepening in the dome beds , 30 to 35 degrees, corresponds well with the outward dip of the basal contact where it can be reliably determined. Fifteen degrees may represent a maximum value; primary dip of the sedimentary interbeds was certainly much lower, probably less than 5 degrees.

Several stratigraphic and lithologic factors complicate a simple picture of a volcanic cone within the Edgar Rock dome. 1) A simple systematic variation of lithology within the Edgar Rock member indicative of proximal facies (in the flanks of the dome) to more distal facies (north to Bald Mountain) is not obvious. The Edgar Rock member appears superficially similar throughout its lateral extent. 2) The Edgar Rock member is very thick relative to the available space where a higher cone would be present. About 13 km^2 of pre-Edgar Rock member rocks are exposed in the center of the dome, not considering what might be covered by the Nile Creek member. The low dips inferred for the Edgar Rock member restrict the lateral extent of the central cone. 3) The rather restricted size range of the silicic lapilli within tuffs and laharic breccias, though perhaps not prohibiting an origin within the study area, is curious in view of the close proximity of the deposits to the possible volcanic vent and the lack of any coarser grain sizes or flows of similar material.

A possible picture that emerges from the available data is that of a somewhat restricted volcanic cone or central vent located near the focus of the dike system. This cone was comprised mainly of thick flow breccia sequences much like those exposed in the flanks of the dome (section A, Figure 7). A higher cone is required to provide a source for lahars and/or pyroclastic flows deposited at lower elevations. The Edgar Rock member on the flanks of the dome would represent a proximal apron facies of this cone, now mostly removed by erosion. Dikes, which erupted to the surface on the lower flanks of the cone and proximal apron, fed lava flows which flowed to areas beyond the cone. Additional eruptions farther from the cone contributed to abundant lava flows (as at Devils Slide) interbedded with more distal laharic breccias and sediments (Figures 11 and 16) throughout the N-NE part of the study area. One or more episodes of vertical uplift may have partially to completely dismembered the cone structure, resulting in the observed unconformable relationships. The present hollowed-out or bowl-shaped form of the dome could reflect greater erodability of altered(?) near-vent facies rocks, but doming with its resulting extention and fracturing, which facilitated erosion, has probably contributed most to this morphology. Vertical uplift may have been related, in part, to the intrusion of the radial dike system.

PETROGRAPHY OF THE LAVA FLOWS AND DIKES

Classification of the lava flows and dikes of the Fifes Peak Formation has been based primarily on the total alkali silica (TAS) diagram (Fig. 24) of Le Maitre (1984). Flows from the Edgar Rock member span the compositional range from basalt to dacite, but are predominantly basaltic andesite. Dike compositions span a similar range. The Nile Creek member consists of basaltic andesite and andesite. The two members are described separately because of their distinctive petrography, chemical compositions and stratigraphic positions. Modes of chemically analyzed rocks are listed in Tables 2, 3 and 4).

Edgar Rock Member

Basalt and basaltic andesite

The basalt and basaltic andesites of the Edgar Rock member (Figures 25 and 26) are predominantly highly porphyritic rocks with a phenocryst assemblage of plagioclase, olivine, clinopyroxene, minor orthopyroxene and magnetite. Medium- to coarse-grained, gabbroic inclusions are present in some basaltic andesite flows. Descriptions of the pyroxenes and inclusions are reserved for separate sections to follow. On fresh surfaces the lavas are dark gray to bluish black, brown and rarely shades of pink. On weathered surfaces, rusty-brown altered olivine is commonly conspicuous.

Plagioclase is the most abundant phenocryst in all rocks, commonly comprising 85 to 95% of the total phenocryst and microphenocryst volume. Plagioclase phenocryst (greater than 0.5 mm across) content varies between 3 and 32 % by volume in the analyzed samples. Phenocrysts are tabular to equant in form and are generally 1.5 to 3 mm in length, although

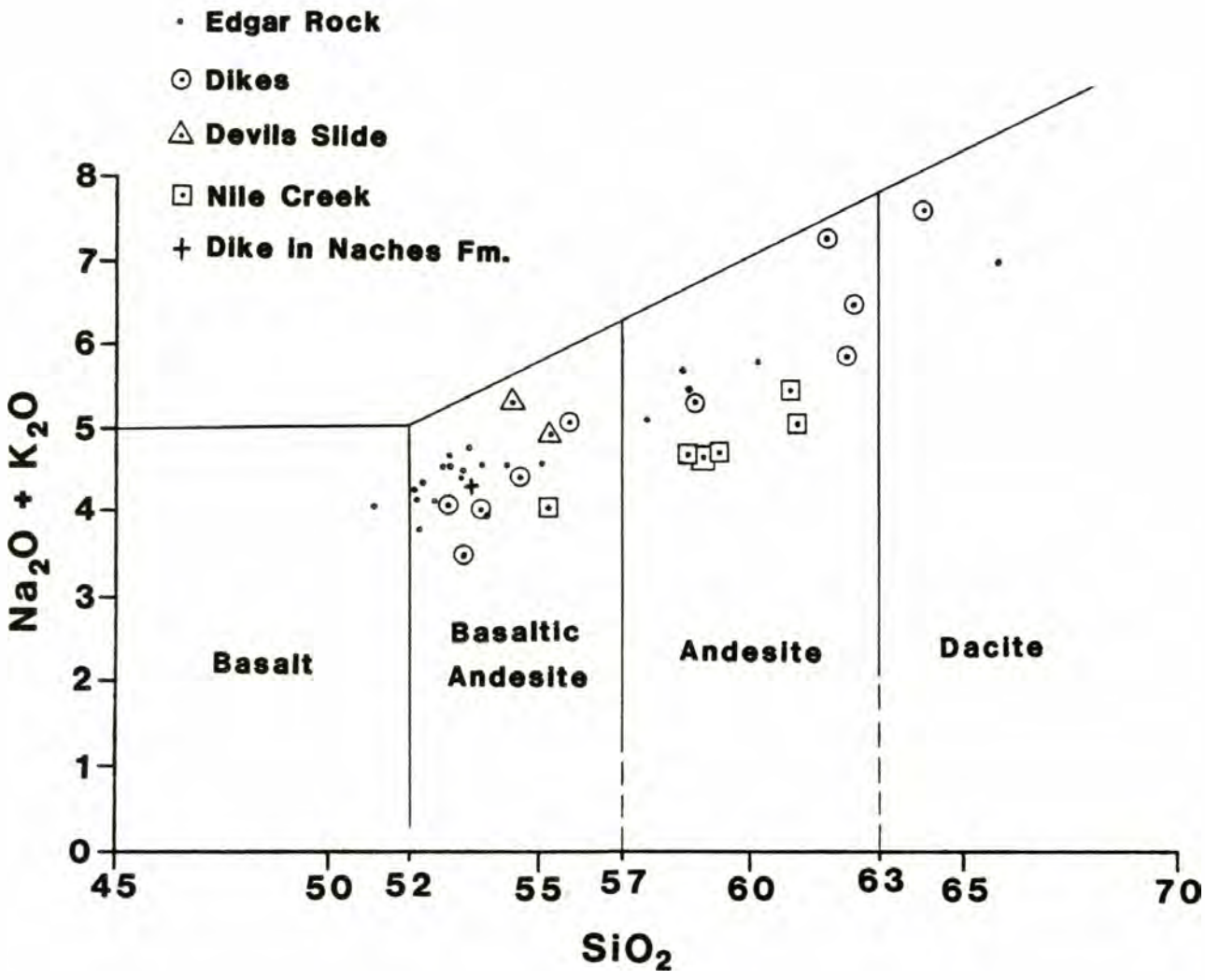

Figure 24. Classification of the lavas and dikes of the Cliffdell area according to the total alkali silica (TAS) diagram of Le Maitre (1984). Only the applicable (quartz normative) portionof the diagram is reproduced here. Symbolism used here is the same for all subsequent diagrams.

Table 2

Modes of Edgar Rock member flows (volume %)

	Basalt and basaltic andesite						
	58	23	40B	98C	80	70	13
Plag. ph.	16.83	21.23	27.45	32.06	19.80	21.09	4.82
Plag. mic.	7.08	5.58	2.85	4.92	3.88	8.59	2.17
Oliv. ph.	0.13	1.03	0.52	1.73	0.18	0.07	0.36
Oliv. mic.	0.33	1.54	0.47	2.77	1.13		1.99
Idd. ph.	0.73	1.73	0.17	2.77	1.85	1.78	0.30
Idd. mic.	0.80	0.38	0.35	0.28	0.12	0.28	0.66
Cpx ph.		tr.	tr.				
Cpx mic.	tr.		tr.				
Opx ph.							
Opx mic.							
Fe-oxide ph.	tr.	tr.	tr.	tr.	0.06	0.21	0.24
Apatite							
Groundmass	74.08	68.51	68.08	55.47	72.98	67.26	88.93
Type	I	I	I	I	I	I	I
	Constituents of point-counted groundmass						
Plagioclase		31.37	38.56	34.49	36.97		52.26
Pyroxene		27.13	17.06	13.09	23.55		25.53
Olivine		0.19	1.11	1.04	0.06		
Fe-oxide		7.18	4.89	5.75	7.16		8.91
Iddingsite		0.64	2.91	0.76	0.83		0.30
Unknown		0.13		0.28	0.06		0.24
Apatite		0.06	0.35	0.07	0.42		0.24
Devit. gl.		1.54	3.09		3.88		1.75
Other sec.		0.26	0.12		0.06	0.64	0.24
Carbonate		tr.					
Total plag.		58.18	68.86	71.47	60.65		59.25
T.P.O.	1.99	4.68	1.51	7.55	3.28	2.13	3.31
Total pyrox.		27.13	17.06	13.09	23.55		25.53
Modal C.I.		39.82	27.54	28.19	34.94		38.29
Inclusions							

Phenocrysts(ph.): > 0.5mm; microphenocrysts(mic.): 0.1mm < mic. < 0.5mm
Fe-oxide phenocrysts: > 0.1mm
Groundmass type: I=predominantly intergranular; H=hyalopilitic
T.P.O.=Total Primary Olivine=Oliv.(ph. + mic.) + Idd.(ph. + mic.)
Modal C.I.=modal color index=total olivine + pyroxenes + Fe-oxide + iddingsite
Unknown=zeolite, K-feldspar or cristobalite; Devit. gl.=devitrified glass; Other sec.=other secondary material

Table 2, continued

	26	20	98B	30	51	35B	40A
Plag. ph.	29.89	6.87	27.13	30.35	31.33	3.31	22.36
Plad. mic.	4.46	21.04	8.31	3.07	1.60		3.37
Oliv. ph.	0.10	0.22	0.78	tr.			
Oliv. mic.	0.67	3.33	0.92				
Idd. ph.	0.05	0.21	0.57	0.05	3.61	0.08	0.81
Idd. mic.	1.87	0.72	0.07	0.52	0.27		1.35
Cpx ph.			0.85		0.14		
Cpx mic.			tr.	0.21			tr.
Opx ph.			tr.		tr.		
Opx mic.		0.07					
Fe-oxide ph.	tr.	0.29	0.36	0.36	0.07	tr.	0.07
Apatite							
Groundmass	62.95	67.24	61.53	65.44	62.98	96.61	72.05
Type	I	I	I	I	I	I	I
	Constituents of point-counted groundmass						
Plagioclase	29.63			31.50		57.84	42.30
Pyroxene	19.93			21.46		28.68	17.31
Olivine	0.05						
Fe-oxide	6.54			5.98		7.41	5.25
Iddingsite	2.23			2.75		1.50	1.55
Unknown	0.21			0.26			0.07
Apatite	0.36			tr.		tr.	tr.
Devit. gl.	3.74			3.27		1.18	4.92
Other sec.	0.26			0.21			0.67
Carbonate							
Total plag.	63.98			64.92		61.15	68.03
T.P.O.	2.69	4.48	2.34	0.57	3.88	0.08	2.16
Total pyrox.	19.93			21.46		28.68	17.31
Modal C.I.	31.44			31.33		37.67	26.34
Inclusions						x	

Table 2, continued

	Devils Slide	Andesite				Dacite
	50	75	66	82	57	71	43
Plag. ph.	20.82	0.18	13.98	0.33	14.43	7.99	3.12
Plag. mic.	5.71	0.82	9.30	9.98	7.55	4.41	1.04
Oliv. ph.				0.07			
Oliv. mic.		0.54					
Idd. ph.	0.89		0.29		tr.	0.21	
Idd. mic.	1.08	0.09	0.87	tr.		0.89	
Cpx ph.	0.21				tr.	0.69	0.06
Cpx mic.				tr.		0.21	0.37
Opx ph.	tr.			0.07		0.48	0.31
Opx mic.				0.07	tr.	0.28	0.24
Fe-oxide ph.	0.51	0.09	0.40	0.13	0.47	1.03	0.67
Apatite						0.07	0.12
Groundmass	70.78	98.27	75.16	89.35	76.69	83.75	93.70
Type	I	I	I	I	H	I	H
Constituents of point-counted groundmass							
Plagioclase	38.24	64.31	40.67				
Pyroxene	26.53	16.44	22.82				
Olivine		1.36					
Fe-oxide	3.64	5.18	4.79				
Iddingsite	0.06	2.63	1.21				
Unknown	0.19		2.60				
Apatite	tr.	2.54	tr.				
Devit. gl.	1.79	5.72	3.00				
Other sec.	0.32	0.09	0.06		0.87		0.37
Carbonate		tr.					
Total plag.	64.77	65.31	63.95				
T.P.O.	1.97	0.63	1.16	0.07	tr.	1.10	
Total pyrox.	26.74	16.44	22.82				
Modal C.I.	32.94	26.33	30.38				
Inclusions							

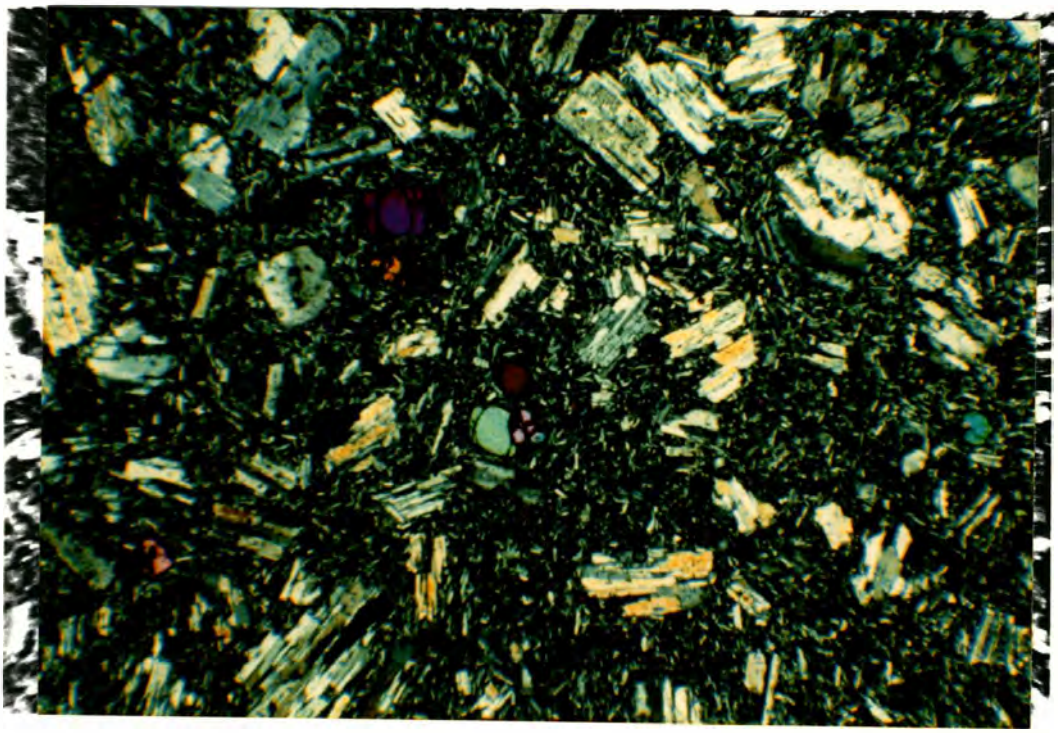

Figure 25. Typical intergranular basaltic andesite flow from the Edgar Rock member. Phenocrysts are plagioclase, olivine and a trace of magnetite. Sample 40B. X-polars. Field of view 10 x 7.6 mm.

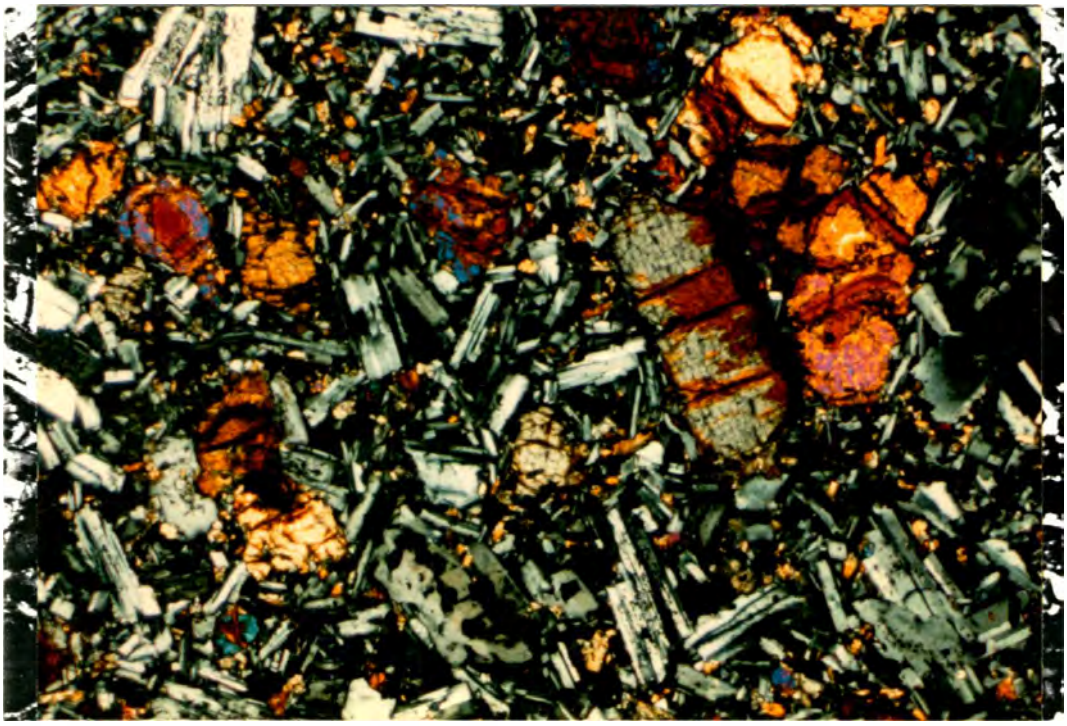

Figure 26. Coarsely crystalline, intergranular basaltic andesite flow from the Edgar Rock member. Olivine phenocrysts are partially replaced by iddingsite. Sample 98C. X-polars. Field of view is 3 x 2 mm.

phenocrysts a centimeter or more across also occur rarely. Seriate texture is common and in such cases no clear distinction can be made between the plagioclase of the microphenocrysts and the groundmass. Plagioclase glomerocrysts consist of tightly interlocking euhedral to anhedral grains.

The most calcic phenocryst cores, determined optically, are about An70. Phenocrysts commonly have large unzoned or weakly normally zoned cores and are surrounded by strongly zoned rims. Oscillatory zoning is not a conspicuous feature of most plagioclase phenocrysts of the basaltic andesites. Large plagioclase phenocrysts (1 to 1.5 cm across) are free of inclusions and are weakly zoned except for a very narrow, strongly zoned rim.

Variations in the abundance, form and zonal pattern of melt inclusions, as well as other small included phases, reveal that many rocks contain more than one population of plagioclase phenocrysts. Distinction among these populations is commonly subtle and the populations are less obvious than those in the flows of the Nile Creek member. Well-developed sieve-textured plagioclase is rare in flows of the Edgar Rock member. Some rocks are relatively homogeneous with relatively clear plagioclase containing few and widely spaced melt inclusions. Where several populations are present, one is generally clear and free of inclusions of any kind. Other populations will consist of plagioclase with phenocryst cores, or an intermediate zone, riddled with melt inclusions containing dusty, semi-opaque material. Within this zone, or in phenocrysts highly riddled throughout, minute opaque or irregular pyroxene granules, or both, are also present.

Inclusions of other phenocryst- or microphenocryst-sized minerals are not common, but olivine and magnetite are rarely found enclosed or

partially enclosed in plagioclase.

Plagioclase phenocrysts show relatively minor alteration. Rarely, carbonate partially replaces some phenocrysts. Light brownish clays are the most common alteration product and often selectively replace zones parallel to the crystal margins. Melt inclusions are usually devitrified or replaced by clays.

Olivine is the principal ferromagnesian phenocryst in all rocks and generally constitutes 1 to 5% by volume. Phenocrysts are typically 0.2 to 1 mm across, but some are as large as 2 to 10 mm. Single grains are euhedral to anhedral and some embayed forms are present. In a few samples olivine is mantled by narrow, granular pyroxene rims. Fe-oxide was not observed on any rims.

Replacement of olivine is variable, both within a single thin section and between different rocks. Highly birefringent, reddish iddingsite commonly forms pseudomorphs after olivine. Other brown to nearly black secondary material also replaces olivine. In the mode tables, all secondary material replacing olivine is referred to as iddingsite. Replacement also occurs along grain boundaries, curved fractures or within the cores of some grains. Two stages of replacement are present in some grains: an initial iddingsite replacement, followed by replacement of the remaining olivine by other secondary materials.

Several types of inclusions occur in olivine. Rounded to faceted melt inclusions containing one or more crystallized phases are common. Larger, irregular melt inclusions can contain quench phases radiating from the interior wall of the inclusion. Small euhedral to rounded opaques are also present; brown spinel (chromite) could not be identified in any olivine. Olivine may also contain small euhedral to rounded plagioclase

grains.

The composition of olivine is known only within a broad range. All appear to be optically negative (less than Fo88) with a 2V that varies from nearly 90 degrees to about 75 degrees. Thus, compositions are probably in the range of Fo80 to Fo60. Fe-rich rims are present in some zoned phenocrysts.

An opaque Fe-oxide, probably Ti-magnetite (referred to as Fe-oxide in the mode tables) is a very minor phenocryst (greater than 0.1 mm across) mineral in most of the basaltic andesites. Phenocryst content varies from a trace up to about 0.5 % by volume. Phenocrysts are up to 0.8 mm across, but are most commonly 0.1 to 0.4 mm. Magnetite phenocrysts occur independently and adhering to or partially included in plagioclase or olivine phenocrysts.

The lavas of basalt to basaltic andesite composition are all nearly holocrystalline with intergranular to slightly intersertal groundmass textures. When the groundmass is sufficiently coarse to permit accurate whole-rock point counts, they reveal a fairly consistent mineralogy. The principal groundmass constituents are, in order of decreasing abundance: plagioclase, pyroxene(s), magnetite, devitrified glass, olivine (or its alteration products) and apatite.

Groundmass plagioclase is lath-like to equant and sometimes shows flow-alignment. Pyroxenes are granular to prismatic; no attempt was made to distinguish pyroxene types. Magnetite in the groundmass makes up 3.6 to 9 % of the rock volume and is always present as discrete euhedral to anhedral grains. Olivine is a groundmass constituent (a trace up to about 4 %) in the basaltic andesite lavas and generally decreases in amount with increasing SiO_2. Most olivine is completely replaced by iddingsite or other secondary material. Acicular apatite occurs in minor amounts

throughout the groundmass.

Greenish, brown or reddish-brown devitrified glass or its alteration products make up from 1 to nearly 6 % of the rocks examined and averages about 3 %. Thus, the lavas are usually at least 95 % crystalline. An unidentified phase, possibly a zeolite, K-feldspar or cristobolite occurs in very minor amounts in the groundmass of some flows.

Another mineral observed in five flows is isotropic, translucent emerald green to opaque and occurs in subhedral cubic, rhombic to triangular and anhedral forms (Fig. 27). The mineral is spinel, perhaps pleonaste or hercynite. The varying opacity suggests a range in composition. The most common occurence is rare isolated grains. One unanalyzed flow, however, contains this mineral more abundantly as isolated grains (one to four grains per thin section), rarely associated with olivine phenocrysts, and as inclusions within or in contact with the margins of large anhedral clinopyroxene grains. One magnetite phenocryst contains a core of green spinel. Spinel grains are 0.1 to 2.2 mm across. All grains, where in contact with the host rock, are surrounded by a double corona of fine-grained opaques (inner) and multigranular plagioclase (outer). Small rounded grains of olivine and plagioclase occur as inclusions in some spinel.

Basaltic andesite flow at Devils Slide

The thick basaltic andesite flow at Devils Slide (Fig. 28) is nearly aphyric and contains very sparse plagioclase phenocrysts and minor microphenocrysts (together totalling about 1.0 vol. %), minor olivine microphenocrysts and a trace of magnetite. The groundmass is rather coarse intergranular and is composed of plagioclase laths, pyroxene granules, variably altered olivine, magnetite, devitrified glass and

Figure 27. Isolated, dark green spinel from an un-analyzed basaltic andesite flow, Edgar Rock member. A: Spinel grain is 0.7 mm across, subhedral and is surrounded by a plagioclase rim. B: Close-up of grain showing deep green color, narrow, multi-granular magnetite rim and small altered olivine inclusion (reddish orange, near bottom). Plane light.

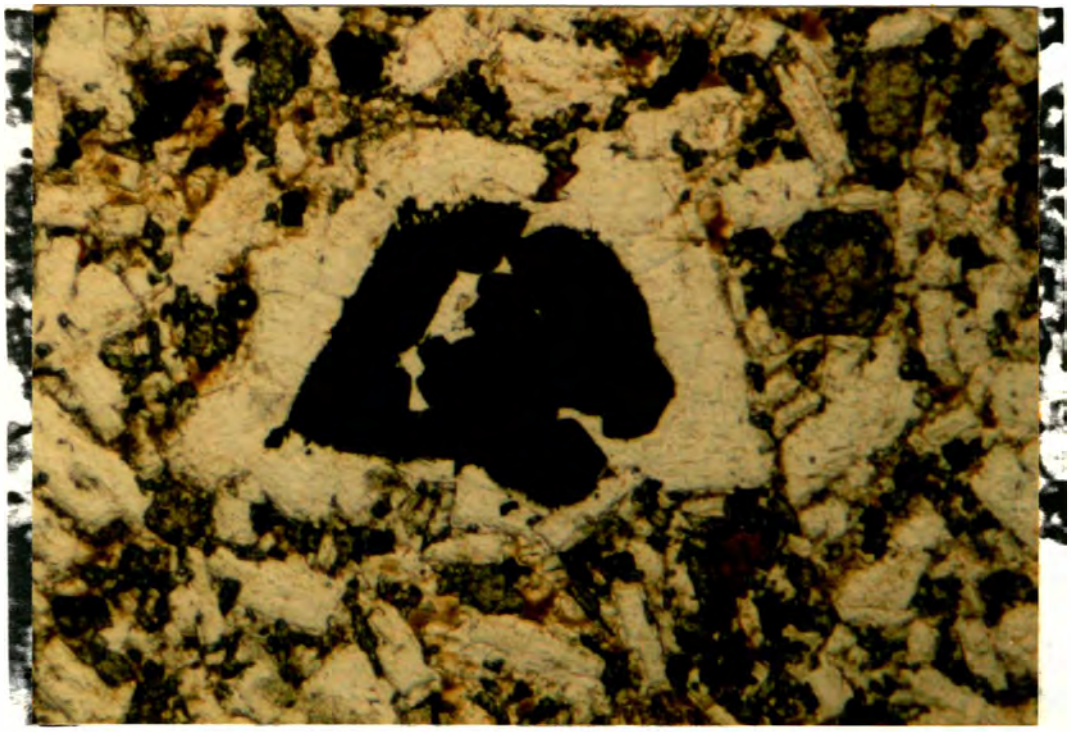

A

B

Figure 28. Intergranular basaltic andesite from the thick flow exposed at Devils Slide. Small birefringent grains are olivine microphenocrysts. X-polars. Field of view 7.6 x 5.2 mm.

apatite needles.

Pyroxene occurrence and morphology

Phenocrystic pyroxene is not abundant in the basaltic andesites of the Edgar Rock member. Three broad groups can be identified on the basis of morphology and composition: 1)-phenocrysts, microphenocrysts and glomeroporphyritic clots or monomineralic cumulate fragments; 2)-clots or single grains containing abundant plagioclase inclusions and; 3)-spinel-bearing clinopyroxene "megacrysts" and other grains without spinel which can be related to this group.

Some basaltic andesite flows seem to lack pyroxene in any of the forms referred to above. Other flows contain phenocrystic pyroxene in only scant amounts. Typically, pyroxene phenocrysts comprise much less than 1 vol.% of a rock. The most common pyroxene , called group 1 (Fig. 29), is a pale yellowish-green, commonly slightly pleochroic and relatively Fe-rich clinopyroxene. Microphenocrysts and phenocrysts (up to 4 mm across) are almost always anhedral or have vague subhedral forms. Deep embayments are present in some phenocrysts. Glomeroporphyritic clots, up to 7 mm across, are generally composed of less than 5 grains. Plagioclase, olivine and magnetite are common minerals included within or associated with pyroxene in the clots.

Group 2 clots are less common, larger (4 mm to 1 cm across) and are composed of a single large subhedral grain to several anhedral and intergrown clinopyroxenes (Fig. 30). The clinopyroxenes are similar to those of group 1 in color and pleochroism, but poikilitically enclose a number of plagioclase grains and clots, with or without olivine, magnetite and, rarely, orthopyroxene. Plagioclase inclusions usually become larger towards the outer margin of the host grain, so that the largest

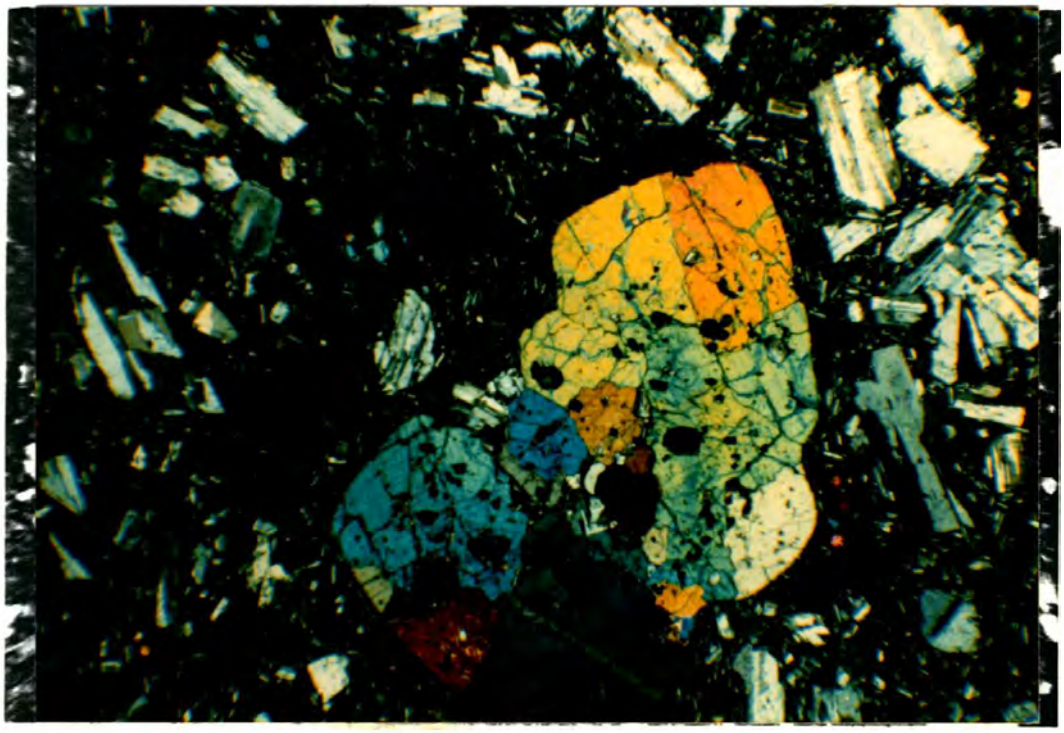

Figure 29. Group 1 clinopyroxene clot from an unanalyzed basaltic andesite flow in the Edgar Rock member. Clinopyroxene encloses tiny plagioclase grains, magnetite and altered olivine. X-polars. Clot is 7 mm long.

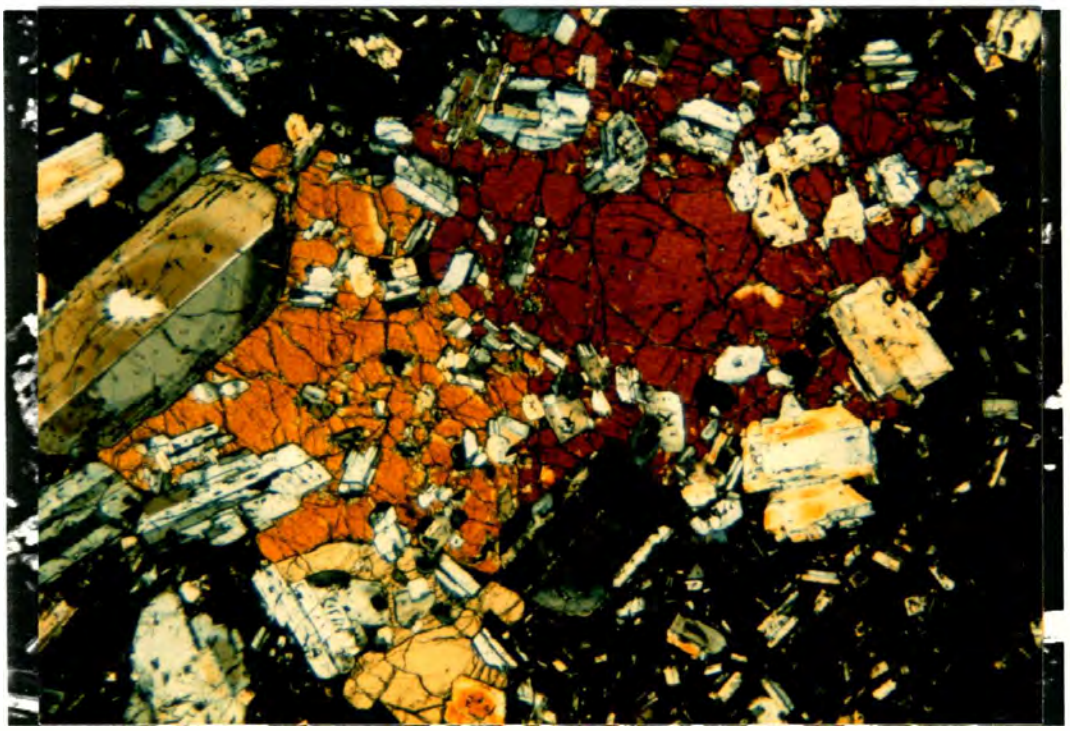

Figure 30. Group 2 clinopyroxene from an unanalyzed basaltic andesite flow (flow 72), Edgar Rock member. These clinopyroxenes are characterized by ophitic texture, with plagioclase as the most abundant enclosed phase. Note that the largest plagioclase inclusions are at or near the margin of the grains. X-polars. Field of view 9 x 6 mm.

plagioclases are partially enclosed or in contact with the clinopyroxene grains. The texture of these clots is similar to that of the pyroxene found in some of the gabbroic inclusions.

Group 3 pyroxenes are distinct from other types and were observed in only one flow (flow 72). This flow also contains groups 1 and 2 pyroxenes, larger feldspathic gabbro inclusions and minor large plagioclase phenocrysts (1 to 1.5 cm across). Group 3 pyroxenes are anhedral, very pale green and nonpleochroic clinoyroxene "megacrysts" and smaller grains ranging from 2 mm to 1 cm across (Fig. 31). Grains may be single or comprised of three to four subgrains, but are usually dominated by one large grain. Internal grain boundaries in clots are anhedral and intergrown. The outer grain or clot margins are rounded, slightly angular or irregular. A narrow (less than 0.1 mm) reaction rim surrounds all or part of a grain or clot. This rim is sharply bounded internally and has a darker-green color and higher birefringence. Euhedral zoning is visible within some grains and is truncated at some grain margins. Inclusion density is low. Anhedral olivine (altered), commonly anhedral plagioclase, magnetite and melt (altered) are minor included minerals. Green spinel is associated with many of these clinopyroxenes as inclusions, partially enclosed or in contact with the grain margins. The largest associated spinels were always observed at the margins of grains or clots. Small green spinel grains were also observed as inclusions in olivine, where the olivine grain was enclosed in a group 3 pyroxene. Where green spinel is not present, other characteristics exhibited by this group serve to distinguish this pyroxene type.

Evidence that the Group 3 pyroxenes crystallized from a melt and are not coarse-grained mantle fragments includes the presence of: 1) melt

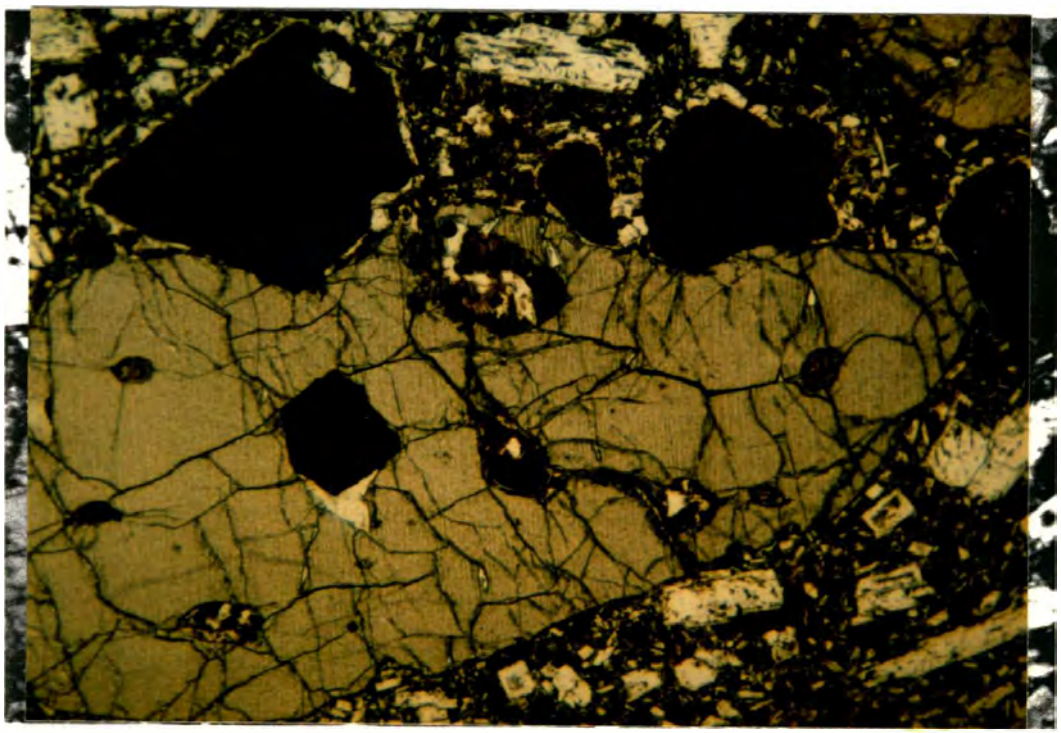

Figure 31. Group 3 clinopyroxene from a basaltic andesite flow (flow 72) in the Edgar Rock member. Dark green spinels (black in this view) are both in contact with and included within the clinopyroxene. Note the subhedral form of the largest spinel (2.2 mm across) and the narrrow plagioclase rims where the spinels are in contact with the groundmass. Other inclusions within the clinopyroxene are altered olivine (near top of Cpx), ellipsoidal melt inclusions and plagioclase (adjacent to included spinel). Plane light. Clinopyroxene grain is 7 mm long.

inclusions, some of which contain plagioclase microlites; 2) included plagioclase with subhedral phenocryst forms; and 3) euhedral zoning within some Group 3 grains.

Orthopyroxene, probably hypersthene, is present in minor amounts in a few flows. Orthopyroxene is most commonly associated with clinopyroxene in clots, with or without plagioclase and olivine. The size range of orthopyroxene is more restricted than that of clinopyroxene. Some orthopyroxene is surrounded by a multigranular corona of altered olivine; the orthopyroxene in flow 72 is characteristically ragged and surrounded by an olivine corona.

Very minor, nearly uniaxial pigeonite was identified in two flows, where it occurs with other clinopyroxene in clots or as an independent grain.

Discussion

Ewart (1976) distinguishes basalt from basaltic andesite by the lack of Ca-poor pyroxene as a phenocryst, microphenocryst or reaction phase (pre-eruptive) on olivine. Using these purely petrographic criteria, many of the basaltic andesites of the Edgar Rock member would be classified as basalts, though their anhydrous silica content is usually more than 52 %.

The phenocryst assemblage of most basaltic andesites (plagioclase - olivine - clinopyroxene - magnetite) is the same as the average western American (western USA, Central America, western South America) basalt of Ewart (1976). The phenocryst assemblage and proportions are also nearly identical to those of the high-alumina basalts of the Aleutians (Marsh, 1982; Meyers et al., 1986).

The inferred crystallization sequence of the basaltic andesites is: plagioclase-olivine-clinopyroxene-orthopyroxene. Magnetite appears after

olivine in many rocks, but appeared with or before olivine in others. Olivine may have followed plagioclase closely in the crystallization sequence based on the following observations. Olivine is present in all of the rocks, even in the least porphyritic sample examined (sample 35B), which contains 3.3% plagioclase phenocrysts. Mutual inclusion relationships between plagioclase and olivine are that plagioclase is included in olivine nearly as commonly as olivine in plagioclase. The plagioclase in gabbroic inclusions is nearly free of any inclusions, as are the largest plagioclase phenocrysts.

The occurrence of olivine relative to plagioclase is in slight contrast to the occurrence of olivine in Aleutian high-alumina basalts. Marsh (1982) states that olivine appears after about 15% crystallization of plagioclase.

Orthopyroxene occurs in the basaltic andesites of the Edgar Rock member only in flows with more than about 53% SiO_2. Magnetite inclusions within olivine are more abundant in flows where orthopyroxene is present, suggesting that magnetite appears earlier in the crystallization sequence with increasing whole-rock SiO_2.

The origin of the group 3 pyroxenes and the associated green spinel is unknown. Based on the color of the spinel, its presence here can be compared with the occurrence of green spinel elsewhere. Green spinel is a common minor mineral present in certain ultramafic and mafic inclusions in highly undersaturated basaltic magmas around the world. The characteristic spinel of Group II xenoliths from San Carlos, Arizona (Frey and Prinz, 1978) is a green, aluminum-rich and chrome-poor spinel (pleonaste). Group II xenoliths encompass abundant clinopyroxenite, websterite, wehrlite and peridotite, which are characterized by Al- and Ti-rich augite. These are distinct from Group I xenoliths containing Mg-

rich olivine, Cr-rich diopside and red-brown chrome spinel. Spinel clinopyroxenites from other locations (Aoki and Kushiro, 1968; Chapman, 1975; Kutolin and Frovlova, 1970) are associated with dark green to black, aluminum-rich (53 to 62% Al_2O_3) and chrome-poor spinel. The Group II xenoliths and the spinel clinopyroxenites are regarded as high pressure (13.5 to 27 kb; Frey and Prinz, 1978) cumulates from alkali basalt magmas.

Green spinel has been less commonly reported associated with subalkaline magmas. Arculus and Wills (1980) report pleonaste (51 to 57% Al_2O_3; less than 0.05% Cr_2O_3) in cumulate xenoliths from St. Kitts, Lesser Antilles, surrounded by a corona of aluminous magnetite and plagioclase, perhaps similar to that observed in the Edgar Rock member flows.

The reaction rims, truncated zoning and rounded or otherwise anhedral forms of the clinopyroxenes are textural features indicating disequilibrium with the host magma. The pyroxene and spinel could therefore be xenocrysts or relict, higher pressure, cognate crystallization products from a similar or more primitive magma.

Inclusions

Medium- to coarse-grained, feldspathic gabbro to gabbro-norite inclusions are present in some basaltic andesite flows of the Edgar Rock member. Inclusions are angular to rounded and, in outcrop, a complete gradation exists between fragments less than 1 cm across to those up to about 5 cm across. Locations where they were observed in abundance are: in the borrow pit in the SE quarter of sec. 13, T. 17N, R. 14E (flow 35B); in a flow along a spur road not depicted on the map (Plate 1) in the NE quarter of sec. 14, T.17N, R. 14E (approx. 0.7 km from the main road; flow 72) and; in a flow along the road in the NE quarter of sec. 18, T. 17N, R. 15E. The following descriptions are based on thin section study of seven

inclusions, one to five cm across, collected at the locations listed above.

The principal constituents of the inclusions are plagioclase, clinopyroxene, orthopyroxene, olivine, magnetite and rare hornblende. Altered, interstitial glass, some with relict scoriaceous texture, occupies angular interstices in some inclusions. Other minor minerals present in one inclusion are apatite and biotite. Textures are ophitic to subophitic, poikilitic and intersertal. All textural varieties can be present in the same inclusion. Typically, variation in the size and morphology of the principal phases gives the inclusions a heterogeneous appearance. This, combined with the small sizes of most inclusions, inhibits determination of representative modes. The inclusions lack layering or fine-scale banding, again, probably because of small size.

Plagioclase is the dominant mineral present in six of the seven inclusions examined, comprising at least 50 % of the inclusions. Grains are tabular to equant, up to 4 mm long, and less commonly are slender laths. Small, plagioclase-rich domains contain tightly interlocking, euhedral to anhedral grains. Plagioclase is calcic labradorite (An 60 to An70) and may be nearly unzoned or zoned outwards to An50 or less rims. Plagioclase does not enclose other minerals, but very small opaque grains are rare inclusions.

Pyroxenes are the second most abundant mineral. Clinopyroxene is more abundant than orthopyroxene where two pyroxenes are present. Clinopyroxene is pale yellowish green, appears unzoned and its habit grades from ophitic to nearly intergranular. The most common habit is ophitic to subophitic with minerals other than plagioclase also included. These clinopyroxene oikocrysts are up to 9 mm across, but are mostly smaller.

Some clinopyroxenes exhibit nearly equant, subhedral forms with altered glass filling surrounding intersticies, hence the intersertal texture (Fig. 32). One inclusion contains poikilitic clinopyroxenes up to 1 cm across with a few euhedral crystal faces against the host rock groundmass, but within the inclusion grain boundaries are anhedral.

Orthopyroxene is pleochroic, probably hypersthene, and is anhedral and subophitic, similar to most clinopyroxene. Clinopyroxene and orthopyroxene can be intergrown to form larger interstitial patches.

Olivine is usually less abundant than the pyroxenes. Olivine occurs as anhedral grains up to 3 mm across or as smaller, anhedral, bleb-like grains enclosed in pyroxene. Where observed, olivine is anhedral against plagioclase. All olivine has been replaced by iddingsite or other secondary material.

Magnetite occurs as subhedral to anhedral grains up to 2 mm across. Some of the larger grains enclose or are interstitial to plagioclase and pyroxene; others are enclosed or partially enclosed in pyroxene. Small magnetite grains 0.1 to 0.3 mm across may be included in some olivine.

Hornblende was present in one of the inclusions examined. It is an anhedral grain about 2 cm across and is entirely replaced by a fine-grained aggregate of black, semi-opaque material. Relict vesicular glass (or groundmass) is present in the inclusion containing the hornblende.

The former presence of interstitial glass in some inclusions indicates that they were incompletely crystalline when incorporated into the host magma and that they are cognate crystallization products. The rare presence of hornblende indicates that sufficiently hydrous conditions for its appearance were attained, at least intermittently, but that hornblende was unstable after incorporation into the host magma.

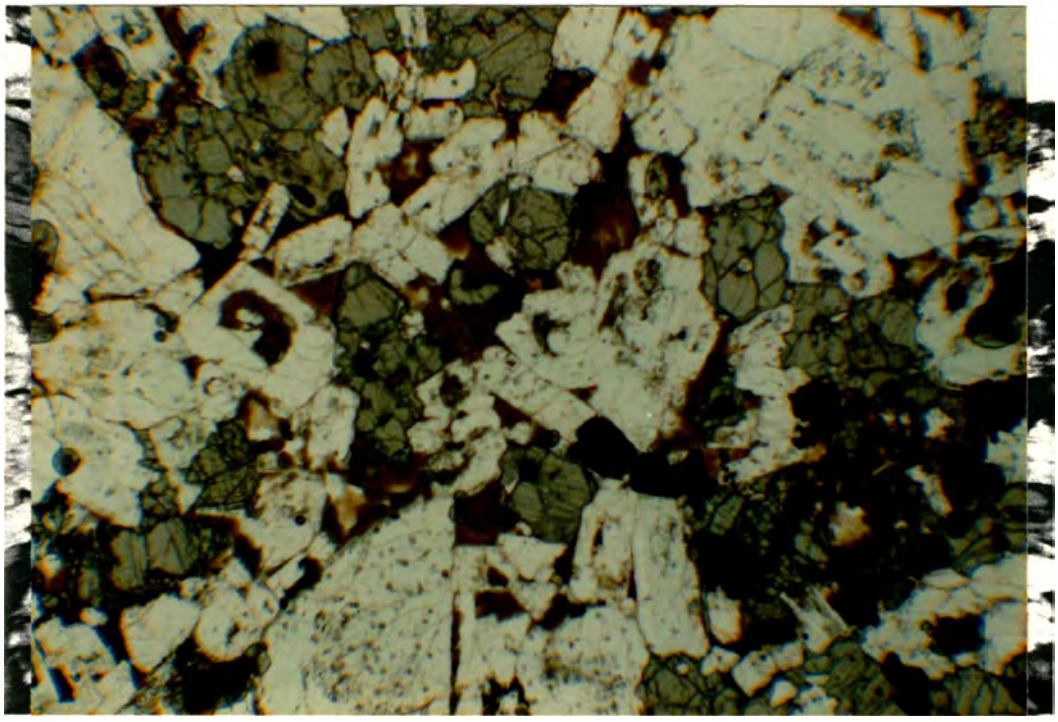

Figure 32. Intersertal texture in a gabbroic inclusion. Brown, altered glass fills interstices between plagioclase, pyroxenes and magnetite. Inclusion from flow 35B. Plane light. Field of view 6.4 x 4.3 mm.

Andesite and dacite

Andesite flows in the Edgar Rock member are far subordinate in abundance to the basaltic andesites. All are petrographically distinct from one another. Textures vary between nearly aphyric and highly porphyritic. On fresh surfaces all andesites are dark gray to black.

Plagioclase is the most abundant phenocryst phase in all andesites, varying from less than 1 up to 14 vol.%. The most calcic composition observed is An66. Clinopyroxene and orthopyroxene abundances are variable and generally low. Phenocrysts are stubby to rounded prisms mainly less than 2 mm in length. Olivine was present, a trace to about 1.1 vol.%, in all andesites, but is mostly replaced by iddingsite or other secondary material. Granular pyroxene rims are present on some olivine phenocrysts.

Apatite is a minor phenocryst (up to 0.7 mm) in one andesite (sample 71). The apatite contains abundant brownish inclusions oriented parallel to the c-axis, similar to apatite described by Mertzmann (1977) in the andesites of the Medicine Lake Volcano, California.

Groundmass textures are intergranular, intersertal and hyalopilitic and are comprised of plagioclase, pyroxene granules, fine-grained magnetite and, in hyalopilitic texture, fresh brownish glass.

Andesite 66 is notable for its lack of pyroxene phenocrysts. Its texture and phenocryst assemblage (plagioclase-olivine-magnetite) are similar to many basaltic andesites of lower SiO_2 content, indicating that this phenocryst assemblage can occur in rocks through a SiO_2 range of 51 to nearly 58 %.

The dacite flow (defined by silica content, greater than 63 %) is nearly black on fresh surfaces and contains phenocrysts of plagioclase, clinopyroxene, orthopyroxene, magnetite and minor apatite. Plagioclase

phenocrysts, up to 3 mm in length, are mostly slender laths with delicate oscillatory zoning, many of which are tied up in glomeroporphyritic clots with other phenocrysts. Pyroxene phenocrysts are stubby to slender prisms up to 1.2 mm in length. The groundmass is flow-aligned hyalopilitic and contains plagioclase microlites, very fine-grained magnetite and fresh brown glass. The dacite is the only flow examined from the Edgar Rock member that does not contain at least a trace of olivine.

Petrography of the dikes

The dikes intruding the Edgar Rock member range from basaltic andesite to dacite in composition and contain a diversity of phenocryst assemblages and textures. The dikes are subdivided into rock types based on silica content (Fig. 24). Petrographic variations serve to further subdivide each rock type. The small basaltic andesite intrusion is also described. Modes are listed in Table 3.

Basaltic andesite dikes and intrusion

The basaltic andesite dikes can be subdivided into two types: porphyritic and nearly aphyric. The porphyritic variety, represented by analyzed samples 54 and 84, is black in color and contains phenocrysts of plagioclase, olivine, clinopyroxene and magnetite.

Plagioclase is the most abundant phenocryst in all of these porphyritic dikes. The largest phenocrysts are tabular to equant, up to 3 to 4 mm across, but are mostly 0.5 to 1.5 mm across. Phenocrysts display variable zoning patterns, but are generally not strongly zoned. The most calcic compositions found are in the range An60 to An65.

Olivine phenocrysts are abundant, comprising 4 to 5 vol. % in two point-counted samples. Phenocrysts are euhedral to subhedral, some are embayed and are up to 2 mm across. Total to partial replacement by iddingsite or other secondary material is common. In two analyzed samples 50 to 60 % of the olivine is replaced. Granular pyroxene rims are present on a few grains. The olivine compositions appear similar to the range found in the basaltic andesite flows (Fo80 to Fo60).

Clinopyroxene is less abundant than olivine in the two analyzed dikes. Subhedral to anhedral phenocrysts and microphenocrysts are present, but most clinopyroxene is clotted. Glomeroporphyritic clots, up to about 3 mm

Table 3

Modes of the dikes (volume %)

	Basaltic andesite				Andesite	
	54	84	85	87	96	68
Plag. ph.	11.72	23.16	0.48	0.24	25.42	2.53
Plag. mic.	13.05	2.97	0.19	0.65	1.06	0.53
Oliv. ph.	0.76	1.22				0.40
Oliv. mic.	1.19	0.87				0.33
Idd. ph.	0.91	1.15				0.27
Idd. mic.	2.02	1.22				0.07
Cpx ph.	0.70	1.47			1.66	0.20
Cpx mic.	0.42	tr.	tr.		0.20	tr.
Opx ph.					1.80	
Opx mic.		tr.			0.13	tr.
Fe-oxide ph.	tr.	0.14		tr.	0.80	0.27
Horn. ph.						
Horn. mic.						
Apatite						0.07
Groundmass	69.16	67.78	95.20	99.11	68.93	95.33
Type	I	I	Is	I	H	H
Other sec.			4.12			
Carbonate						
T.P.O.	4.88	4.46				1.07

Phenocrysts(ph.): >0.5mm; microphenocrysts(mic.): 0.1mm <mic.< 0.5mm
Fe-oxide phenocrysts: >0.1mm
Groundmass type: I=intergranular; Is=intersertal; H=hyalopilitic
Other sec.=other secondary material
T.P.O.=Total Primary Olivine=Oliv.(ph.+mic.)+Idd.(ph.+mic.)

Table 3, continued

			Dacite
	67	53	62
Plag. ph.	18.66	15.98	6.69
Plag. mic.	1.81	0.78	0.97
Oliv. ph.			0.07
Oliv. mic.			0.07
Idd. ph.			tr.
Idd. mic.			tr.
Cpx ph.	1.81	1.21	0.07
Cpx mic.	0.07	0.28	
Opx ph.	0.42	0.28	
Opx mic.	0.63	0.28	0.07
Fe-oxide ph.	1.39	0.57	1.04
Horn. ph.			1.79
Horn mic.			0.34
Apatite		tr.	
Groundmass	75.21	80.26	88.47
Type	H	H	H
Other sec.			0.41
Carbonate		0.28	tr.
T.P.O.			0.14

across, are composed of clinopyroxene and olivine, with lesser amounts of magnetite and plagioclase. Irregular, monomineralic clinopyroxene clots, similar to that in Figures 29 and 33 are small, but contain up to about 20 subgrains. A trace of orthopyroxene is present in dike 84. The clinopyroxene in dike 84 is pale yellowish green and slightly pleochroic; that in dike 54 is more pale and is not pleochroic.

Magnetite phenocrysts are minor, less than 0.2 vol. %, and less than 0.3 mm across.

Groundmass textures are intergranular and intersertal. Groundmasses are comprised of plagioclase microlites, prismatic to granular pyroxene, fine-grained magnetite, altered olivine and, in intersertal textures, fresh brownish glass.

One porphyritic dike (not analyzed) contains green spinel with reaction rims identical to that present in the basaltic andesite flows.

The nearly aphyric basaltic andesite dikes (dikes 85 and 87) are dark gray to black in color and contain less than 1 % phenocrysts and microphenocrysts of plagioclase, magnetite and a trace of anhedral clinopyroxene. Groundmasses are hyalopilitic and very fine-grained intergranular and are composed of plagioclase microlites, pyroxene granules, fine-grained magnetite and brownish glass (dike 85). Dike 85 contains abundant, irregular microvesicles filled with greenish, isotropic secondary material (about 4 vol. %).

The small basaltic andesite intrusion contains abundant, tabular, seriate-textured plagioclase phenocrysts (up to 2 mm, An68), minor, nearly euhedral to anhedral clinopyroxene phenocrysts (0.7 to 3 mm), compact clinopyroxene clots (Fig. 33), a trace of magnetite and abundant altered olivine phenocrysts. The olivine is extensively altered and reduced to

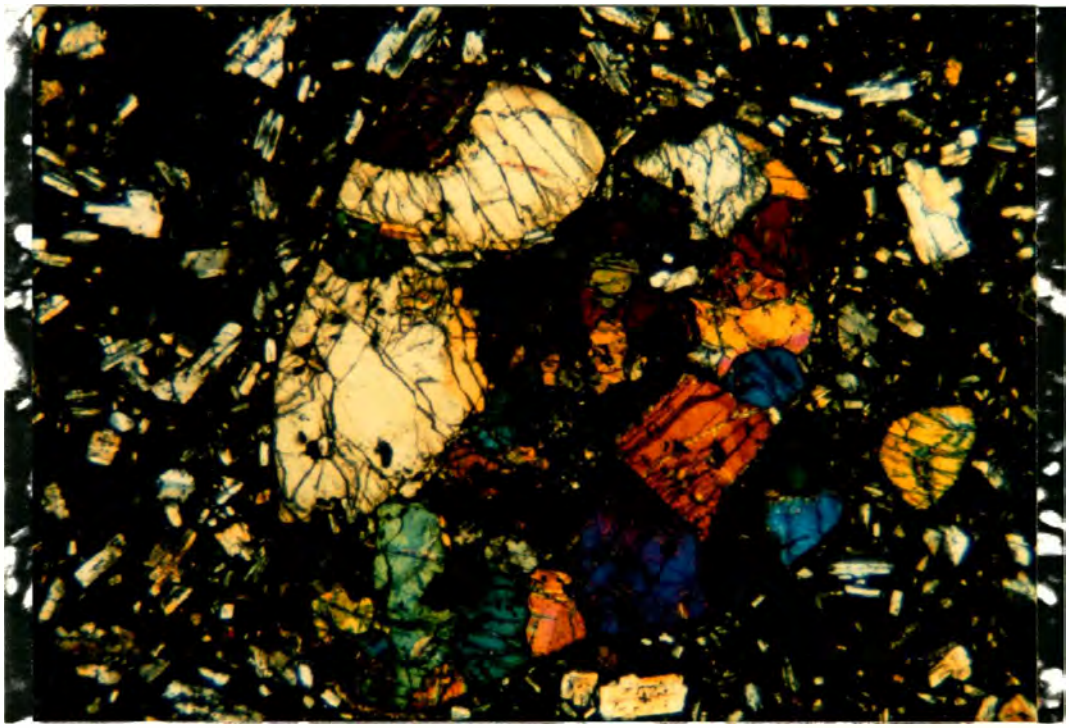

Figure 33. Rounded, multigranular clinopyroxene clot from the small basaltic andesite intrusion. The clot, 4 mm across, consists of 25 to 30 individual grains. The structure of this clot suggests an origin as a fragment of a clinopyroxene cumulate. X-polars.

mere ghosts within an altered groundmass. The sample obtained has an incipient cataclastic (or autoclastic) texture indicated by some shattered plagioclase phenocrysts. No point count was made because of the altered character of the rock, but the intrusion has a phenocryst assemblage similar to other porphyritic basaltic andesite dikes.

Andesite dikes

At least two distinct types of andesite dikes are present. The most common type, represented by analyzed samples 53, 67 and 96, contains a phenocryst assemblage of plagioclase, clinopyroxene, orthopyroxene and magnetite. Olivine and hornblende are rare. These andesite dikes have a distinctive appearance in the field; groundmass colors are pale green to greenish gray. Where these dikes or dike float are present in or near exposures of the pre-Fifes Peak Fm. Tvu_1 unit, the dikes are difficult to distinguish from the Tvu_1 unit in the field.

Plagioclase phenocrysts are abundant (16 to 32 vol. %) and large. Typically, the phenocrysts are tabular to equant and up to 4 to 5 mm across, but some are as large as 7 mm. Seriate texture is usually not present and microphenocrysts are minor in amount, less than 1.5 vol. %. Zoning patterns in plagioclase are complex and varied. The most calcic compositions are in the range An50 to An62. Phenocrysts may be zoned outwards to less than An35. Devitrified glass inclusions are common; small magnetite grains, pyroxene and apatite are less common inclusions.

Clinopyroxene and orthopyroxene are the main ferromagnesian phenocrysts, each generally comprising 1 to 2 vol. %. The clinopyroxene/orthopyroxene phenocryst ratios are variable. Phenocrysts are generally euhedral to subhedral, stubby to elongate prisms up to 4 mm in length. Glomeroporphyritic clots are common and can involve all

phenocryst minerals. Magnetite, plagioclase and apatite are common inclusions in the pyroxenes.

Magnetite phenocrysts (0.5 to 1.4 vol. %) are up to 0.6 mm across, but are mostly 0.1 to 0.3 mm across. Phenocrysts occur floating in the groundmass, with pyroxene phenocrysts or in glomeroporphyritic clots.

Minor brown hornblende was found in one dike (not analyzed) of this type. Phenocrysts are surrounded by opacite rims. Resorbed olivine was observed in one other dike.

Groundmass textures are hyalopilitic, usually flow-aligned, and comprised of slender plagioclase microlites, very fine-grained magnetite and commonly fresh, light brown glass. Groundmass pyroxene is minor and not always present. Vesicles in some dikes may be filled with carbonate.

A different type of andesite dike is represented by one observed dike (dike 68). This dike is black and contains a phenocryst assemblage of plagioclase, olivine, clinopyroxene and magnetite. Olivine is the most abundant ferromagnesian phenocryst.

Dacite dikes

The single dacite (defined by silica content, greater than 63 %) dike analyzed contains phenocrysts of plagioclase, hornblende, Fe-oxide, clinopyroxene, orthopyroxene and olivine (Fig. 34). No quartz was observed. Plagioclase phenocrysts (An 50) occur as laths up to 4 mm in length and exhibit delicate oscillatory zoning. Hornblende (about 2 vol. % ;X=pale yellowish green, Y=brown, Z=brown) occurs as euhedral prisms up to 1 mm wide and 3 to 6 mm long. Opacite rims are absent. Clinopyroxene phenocrysts are stubby and up to 1 mm long; orthopyroxene is resorbed with deep embayments. Olivine is euhedral to anhedral, up to 0.5 mm across, and is partially replaced by iddingsite and carbonate. All ferromagnesian

Figure 34. Phenocrysts in the dacite dike, sample 62. Plagioclase (white) contains magnetite and apatite inclusions. Clinopyroxene (top and in contact with plagioclase) is pale yellowish green. Brown hornblende is at right and olivine is at bottom. Plane light. Field of view 3 x 2 mm.

phenocrysts contain inclusions of magnetite and apatite. Magnetite phenocrysts (about 1 vol. %, 0.2 to 0.4 mm across) are present in the groundmass or adhearing to other phenocrysts. The flow-aligned, hyalopilitic groundmass contains plagioclase microlites, fine-grained magnetite, small apatite prisms and fresh brown glass.

Another type of hornblende-bearing, silicic andesite or dacite dike (not analyzed) is sparsely porphyritic with phenocrysts of plagioclase, brown hornblende, orthopyroxene, minor magnetite and apatite microphenocrysts.

Nile Creek Member

In the TAS diagram (Fig. 24) the lavas of the Nile Creek member are divisible into basaltic andesite (one flow, sample 100) and andesite. The andesites are all highly porphyritic and, in contrast to the andesites of the Edgar Rock member and dike system, form a petrographically coherent group of rocks. The Nile Creek member lavas contain a phenocryst assemblage of plagioclase, orthopyroxene, clinopyroxene, olivine and magnetite. On fresh surfaces the basaltic andesite is black; the andsites are gray to shades of pink. Modes are listed in Table 4.

Plagioclase is the most abundant phenocryst in all rocks and comprises 10 to 27 vol. %. It occurs as euhedral phenocrysts up to 4 to 5 mm in length and may occur in glomeroporphyritic clots with other phenocryst minerals. The most calcic compositions determined are in the range An50 to An60. Complex zoning is present in most phenocrysts.

Two distinct populations of plagioclase are present in all flows (Fig. 35). One population is clear and generally free of inclusions. The other population, perhaps 10 % of the plagioclase phenocrysts, contains a sieve-textured zone beneath a clear rim. This feature is developed best in the basaltic andesite flow and the highest silica andesite (sample 79). The sieve-textured zone is usually at least 0.1 mm wide, but extends throughout some phenocrysts. The clear rim is strongly normally zoned and is euhedral against the groundmass.

Sieve-textured plagioclase, also known as dusty plagioclase, can form in a variety of ways. Resorption, caused by decreasing pressure, increasing pH_2O or mixing with hotter magma, results in sieve-textured zones aligned along twin planes or in sieve-textured zones with diffuse inner boundaries (Morrice and Gill, 1986). Rapid growth of plagioclase

Table 4

Modes of Nile Creek member flows (volume %)

	Basaltic andesite and andesite					
	100	93	89	95B	95A	79
Plag. ph.	10.17	21.76	23.07	18.32	25.25	26.45
Plag. mic.	3.08	3.69	4.06	5.35	3.68	4.16
Cpx ph.	2.28	1.48	1.38	1.34	1.67	1.04
Cpx mic.	1.67	1.75	1.79	2.27	1.61	.76
Opx ph.	1.61	2.08	2.50	2.41	2.70	2.22
Opx mic.	.33	.80	1.93	1.80	2.88	.69
Oliv. ph.	1.81					
Oliv. mic.	.33		.07			
Idd. ph.	.13	.13				
Idd. mic.		.20	1.24	.13		.28
Opaque ph.	.74	1.81	1.24	2.21	1.88	2.63
Horn. ph.						
Horn. mic.						tr.
Quartz ph.					tr.	
Groundmass	77.84	66.15	62.74	66.11	59.61	61.77
Other sec.		.13		.07	.74	
T.P.O.	2.27	.33	1.31	.13		.28
Cpx/Opx	2.04	1.12	.72	.86	.59	.62

Phenocrysts (ph.): > .5mm; microphenocrysts (mic.): .1mm < mic. < .5mm
Other sec. = other secondary material
T.P.O. = Total Primary Olivine = Oliv.(ph.+mic.) + Idd.(ph.+mic.)

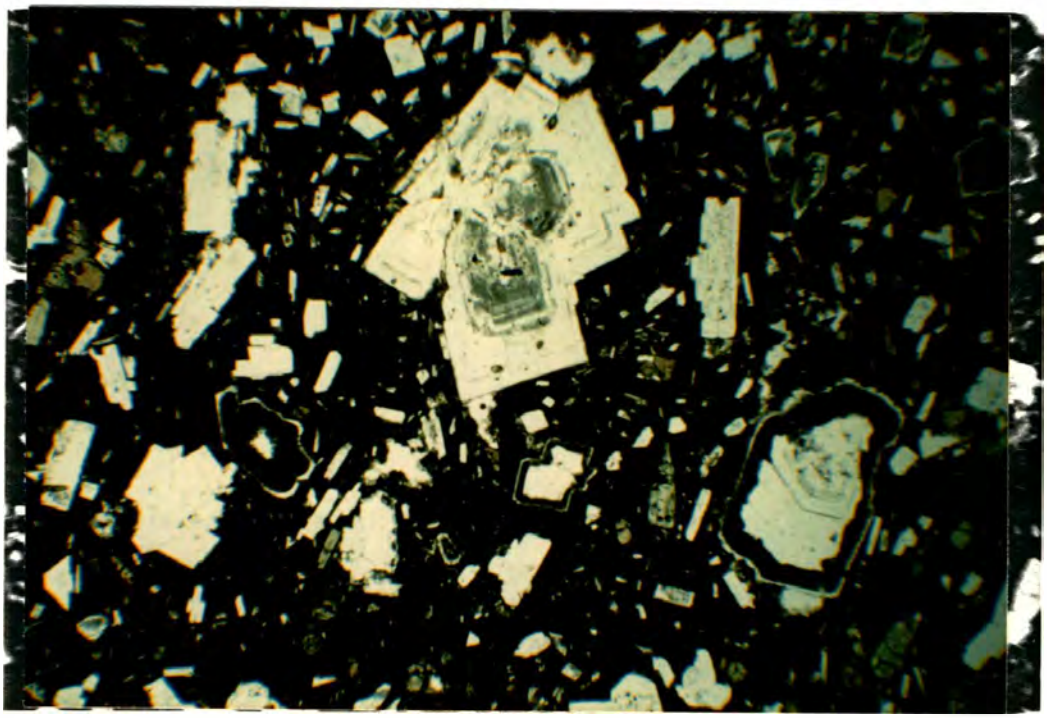

Figure 35. Plagioclase phenocryst populations in a Nile Creek member andesite. The most abundant population is clear and generally free of inclusions, whereas a less common population contains a sieve zone within a clear rim. Sample 79. Plane light. Field of view 18 x 12 mm.

phenocrysts during vapor saturation or mixing with a cooler magma results in sieve zones with sharp inner faces, perhaps confined between oscillatory-zoned regions (Morrice and Gill, 1986). Where resorption is a result of the mixing of two magmas, each carrying a different plagioclase composition, the more sodic plagioclase will possess a sieve zone (Eichelberger, 1978a, b).

A resorption mechanism for the Nile Creek sieve-textured plagioclase is postulated, based on the presence of irregular inner boundaries of the sieve zones. A clear bimodal composition distribution could not be established optically.

A small proportion of both sieve-textured and clear plagioclase phenocrysts are corroded. Primary euhedral margins have been variably lost and sieve zones and oscillatory zoning have been truncated.

Clinopyroxene and orthopyroxene phenocrysts are abundant in all lavas. Phyric clinopyroxene is most abundant in the basaltic andesite flow, where the clinopyroxene/orthopyroxene ratio is about 2:1. The ratio decreases with increasing whole-rock SiO_2 content to less than 1:1 in the most silicic andesite.

Clinopyroxene is pale green and exhibits slight pleochroism. Phenocrysts (1.8 to nearly 4 vol. %) are commonly well-developed, euhedral prisms up to 3.5 mm in length. More Fe-rich rims are present on some phenocrysts and are marked by oscillatory zoning, color change and higher birefringence.

Orthopyroxene phenocrysts (1.9 to 5.6 vol. %) are pleochroic (pink to pale green) and are well-developed, euhedral prisms commonly reaching 2 mm in length and rarely 5 mm. Some orthopyroxenes are mantled by a monocrystalline rim of clinopyroxene. The inner contact of the clino-

pyroxene rim can be both planar or ragged.

Magnetite, plagioclase and apatite are commonly included within the pyroxenes. Small unidentified, brown to yellowish brown inclusions surrounded by radiation halos occur in some pyroxenes, more commonly clinopyroxene.

Olivine is present in all but one of the analyzed samples. Olivine is most abundant (about 2.3 vol. %) in the basaltic andesite flow, where it is commonly very fresh and exhibits a wide variety of delicate skeletal forms (Fig. 36) reaching 4 mm in length. In other flows, olivine is less abundant and is mostly replaced by iddingsite.

Phyric magnetite is abundant in all flows (0.7 to 2.6 vol. %) and its modal abundance increases with increasing whole-rock SiO_2 content. Phenocrysts are subhedral to anhedral and reach 0.5 mm across. Magnetite is commonly included within or associated with pyroxene phenocrysts.

Hornblende and quartz were observed in only trace amounts. Only one grain of each was identified in all thin sections.

The groundmass of the basaltic andesite is flow-aligned intersertal and contains plagioclase laths, pyroxene granules, fine-grained magnetite and fresh brown glass. Groundmass textures of the andesites are intersertal to holocrystalline and are comprised of similar constituents. The groundmass of sample 95B contains a small amount of anhedral biotite; 95A contains "ophimottling" caused by late crystallizing quartz(?) enclosing other groundmass constituents.

Figure 36. Skeletal olivine phenocrysts in the Nile Creek member basaltic andesite flow. Sample 100. X-polars. Field of view is 2.5 x 3.8 mm.

Comparison of Lava Flows and Dikes

Figure 37 displays some significant petrographic and major element variations which are present within and between the members and dikes of the Fifes Peak Formation. The porphyritic basaltic andesite dikes closely resemble the typical, highly porphyritic, basaltic andesite flows in the Edgar Rock member. Overall, these two basaltic andesite groups form the closest petrographic match between the flows and dikes. The phenocryst assemblage of plagioclase-olivine-clinopyroxene-minor magnetite is common to both flows and dikes, as are complex pyroxene morphologies and green spinel, although green spinel was observed in only one dike. The two analyzed porphyritic basaltic andesite dikes, however possess an overall more mafic character than most analyzed flows (Fig. 37A). The appearance of orthopyroxene as a phenocryst phase seems to occur at a similar SiO_2 content as in the flows, about 53 %. Nearly aphyric basaltic andesite occurs more abundantly as dikes than flows.

Andesite dikes are distinct from all observed andesite flows in the Edgar Rock member. The mafic phenocryst content of andesite dikes is commonly greater than that observed in the flows. Plagioclase phenocrysts in the andesite dikes are typically larger and more equant than those in andesite flows.

A major contrast between lava flow and dike mineralogy is the presence of hornblende as a phenocryst in some andesite dikes and in at least one dacite dike. Hornblende was not observed as phenocrysts in any flows in the Edgar Rock member.

Figure 37 shows that, in accord with all other geologic evidence, the dikes bear little resemblance to and appear unrelated to lava flows in the Nile Creek member. As a general statement, petrographic divergence

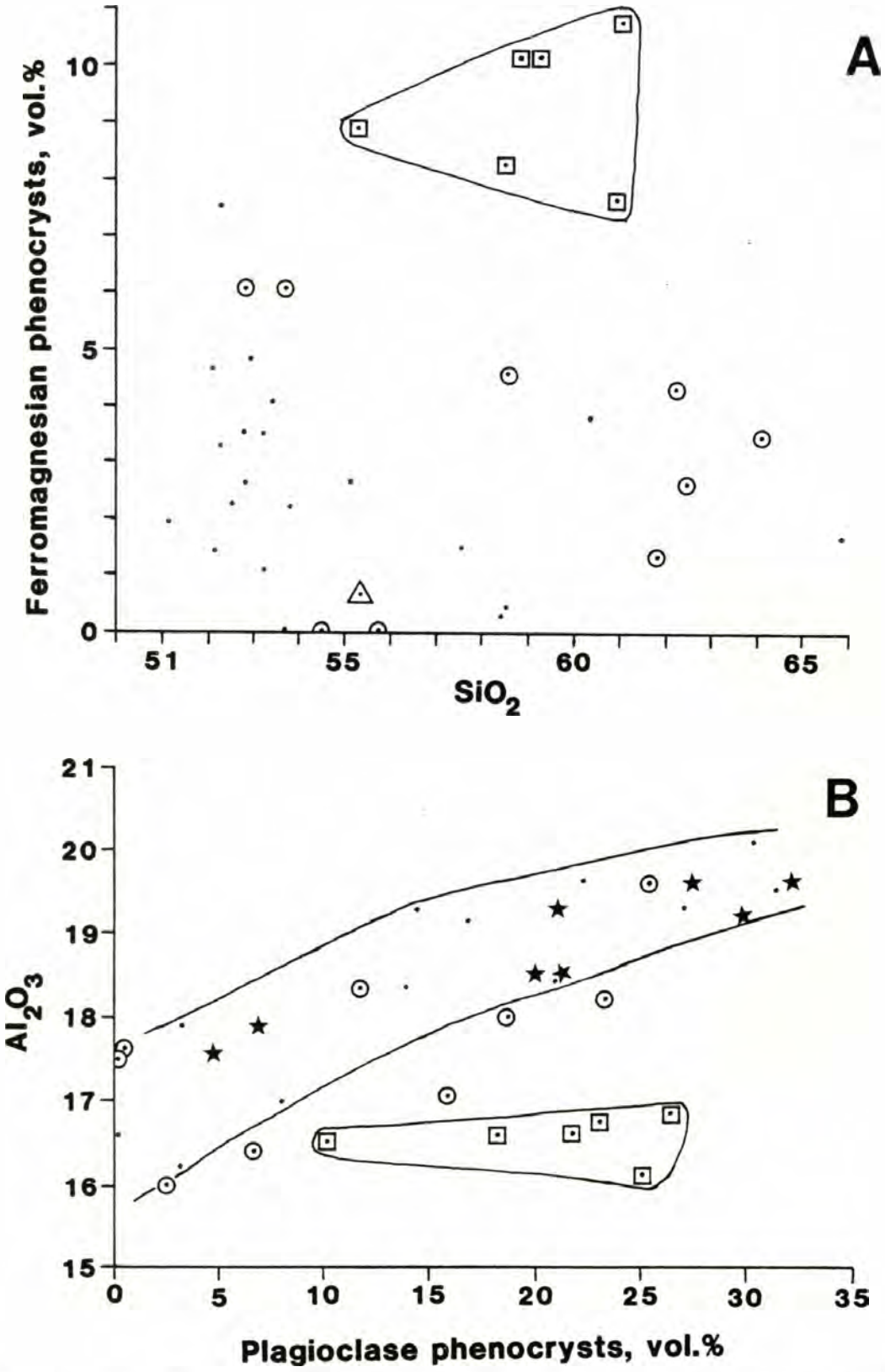

Figure 37. Some significant modal and major-element variations within and between the Edgar Rock member, dikes and the Nile Creek member. In A, ferromagnesian phenocrysts (olivine, pyroxenes, magnetite and iddingsite) total includes microphenocrysts. In B, the star symbols are Edgar Rock basaltic andesites (52 to 53 % SiO_2) that are highlighted to show the variation within a narrow compositional range. Other symbols are those used in Figure 24.

between the lava flows in the Edgar Rock member and the dikes increases with increasing silica content. Hornblende-bearing dikes, being more hydrous, may represent some of the latest intrusive phases in the dike system, and if they ever fed flows in the Edgar Rock member, the flows may have been located higher in the stratigraphic sequence than is now preserved.

GEOCHEMISTRY

Forty major element XRF analyses of lava flows and dikes have been obtained from the Fifes Peak Formation in the Cliffdell area. These analyzed samples span a broad range of chemical and petrographic types and represent much, but probably not all, of the variation present in the Cliffdell area. Major elements are tabulated in Appendices A, B, and C. Trace elements for 22 of these samples are tabulated in Appendices D and E.

Major Elements

The Cliffdell area samples have been previously classified chemically within the TAS diagram (Fig. 24), where they fall within the quartz-normative portion of the diagram. The SiO_2 content of all samples ranges from 51 to 66 wt. %. The Edgar Rock member is a predominantly mafic assemblage with most lavas having less than 55 % SiO_2. Observed whole-rock Fe_2O_3/FeO ratios vary between 0.30 and 2.44 and reflect variable, but not extreme, weathering and oxidation. More realistic unaltered normative compositions were obtained by calculating norms using a Fe_2O_3/FeO ratio of 0.30.

Considered broadly, the Cliffdell samples form a medium-K volcanic suite by the definition of Gill (1981). This potassium range corresponds to the calc-alkaline classifications of other authors (e.g. Peccerillo and Taylor, 1976). The Edgar Rock lavas are calk-alkaline based on the alkali-lime index of Peacock (1931); the Nile Creek lavas form a calcic suite.

High FeO*/MgO (total iron as FeO*) ratios of the lavas and dikes cause these compositions to fall within the tholeiitic field of the FeO*/MgO-

SiO_2 diagram (Fig. 38) of Miyashiro (1974). This ratio of the Nile Creek lavas is consistently lower. On an AMF diagram (Fig. 39), the Cliffdell analyses in part straddle the tholeiitic-calc-alkaline boundary and exhibit moderate Fe-enrichment relative to the Cascade plutonic trend.

Major element vs. SiO_2 Harker variation diagrams are plotted in Figure 40 and display major element variations with increasing SiO_2 content. The Nile Creek suite falls along a trend of higher MgO and CaO, whereas the Edgar Rock suite contains higher Al_2O_3, Na_2O, TiO_2 and P_2O_5. Within the Edgar Rock suite , subtle trends of increasing absolute abundances of FeO*, MnO, P_2O_5 and TiO_2 are present up to about 55 % SiO_2, though scatter is high. This is an iron enrichment trend characteristic of tholeiitic magmas.

Aluminum contents are high and range from about 16 to slightly over 20 wt. %. The most aluminous rocks are the highly porphyritic basaltic andesites which generally have greater than 18 wt. % Al_2O_3. Aphyric or nearly aphyric basaltic andesite lavas and dikes contain between 17 and 18 wt. % Al_2O_3. The Nile Creek lavas contain a more restricted range between 16 and 17 wt. %. High alumina and plagioclase phenocryst contents could be evidence of plagioclase phenocryst accumulation (Ewart, 1976). Within a restricted range of lava composition (52 to 53 % SiO_2), Edgar Rock lavas exhibit a positive correlation between Al_2O_3 and modal plagioclase phenocrysts (Fig. 37B).

MgO content of the basaltic andesites is low, falling between 3 and 5 wt. %. Corresponding Mg-numbers [100 x $Mg/(Mg+Fe^{+2})$, for $Fe_2O_3/FeO = 0.2$] are also low, ranging from 48 to 57 in the most mafic lavas and dikes in the Edgar Rock member. These values indicate either significant fractionation (principally olivine +/- pyroxene and spinel) from a MgO-rich mantle-derived magma or derivation from a source with high FeO*/MgO.

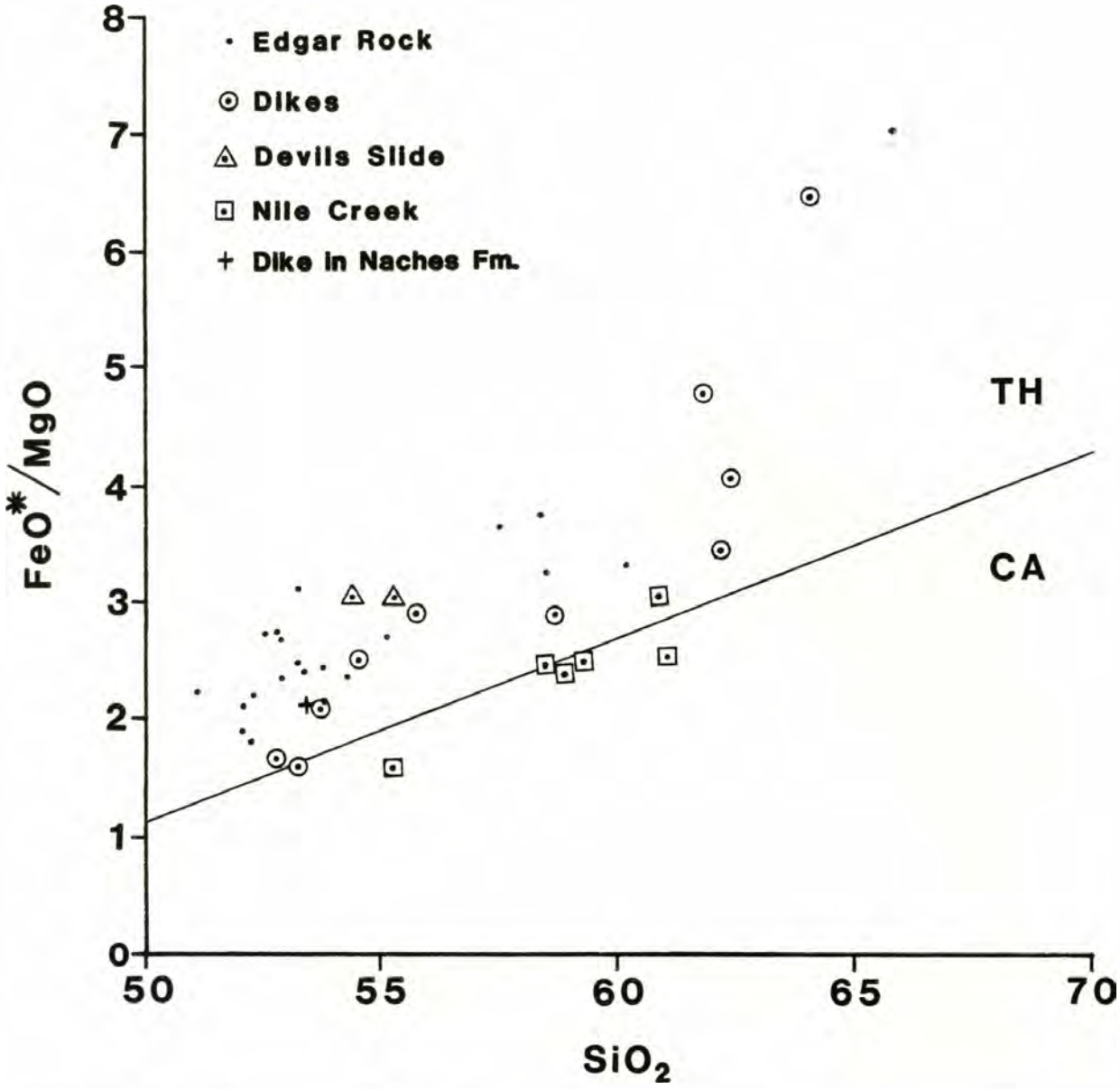

Figure 38. Classification of the Cliffdell area compositions according to the FeO*/MgO - SiO_2 diagram of Miyashiro (1974). TH - tholeiitic field; CA - calc-alkaline field.

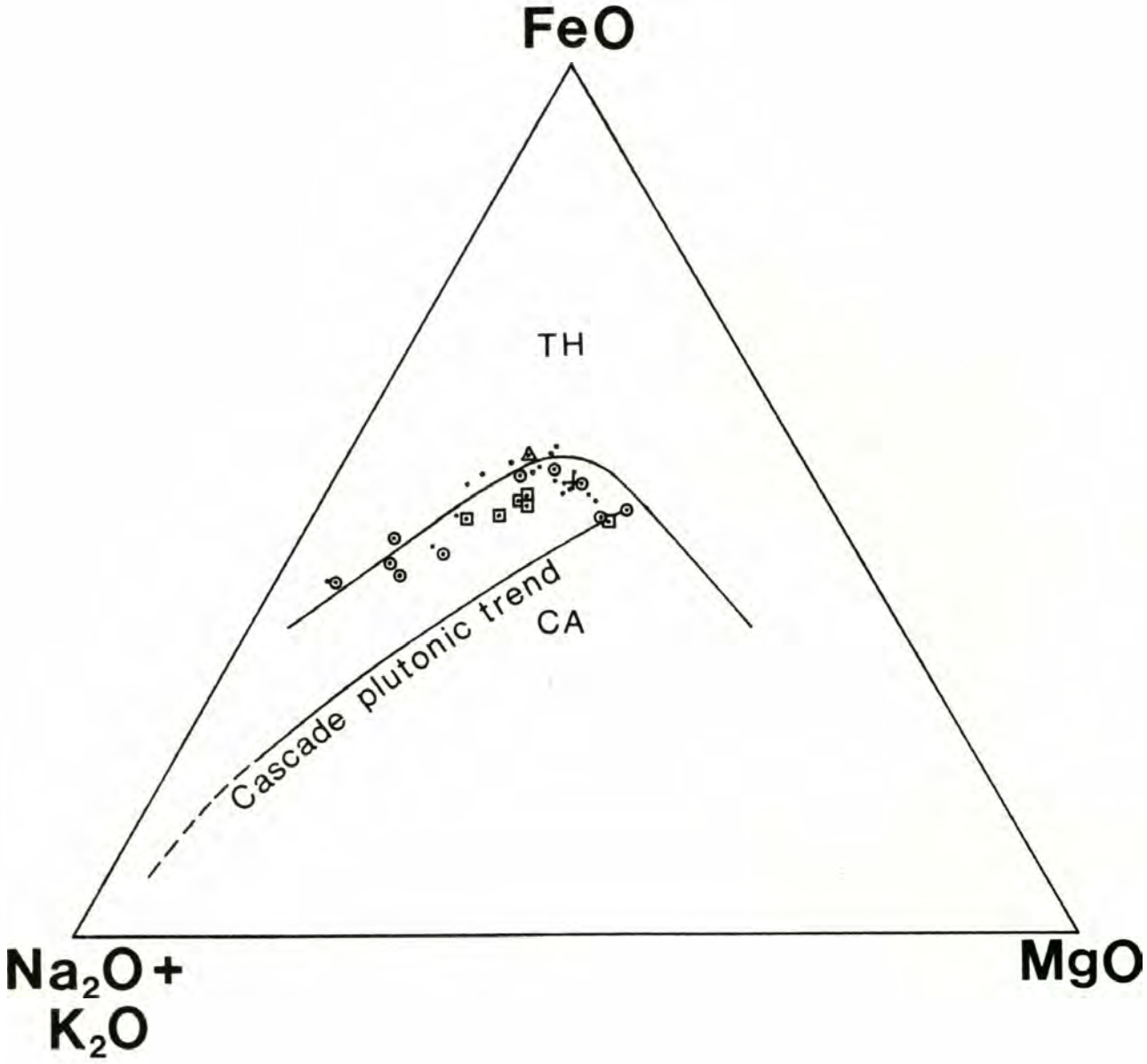

Figure 39. Classification of the Cliffdell area compositions within the AMF diagram. The boundary between the tholeiitic (TH) and calc-alkaline (CA) fields is from Irivine and Baragar (1971). The Cliffdell area compositions are displaced from the Cascade plutonic trend, which is the average trend for the Snoqualmie, Tatoosh, Chilliwack and Mount Barr Batholiths.

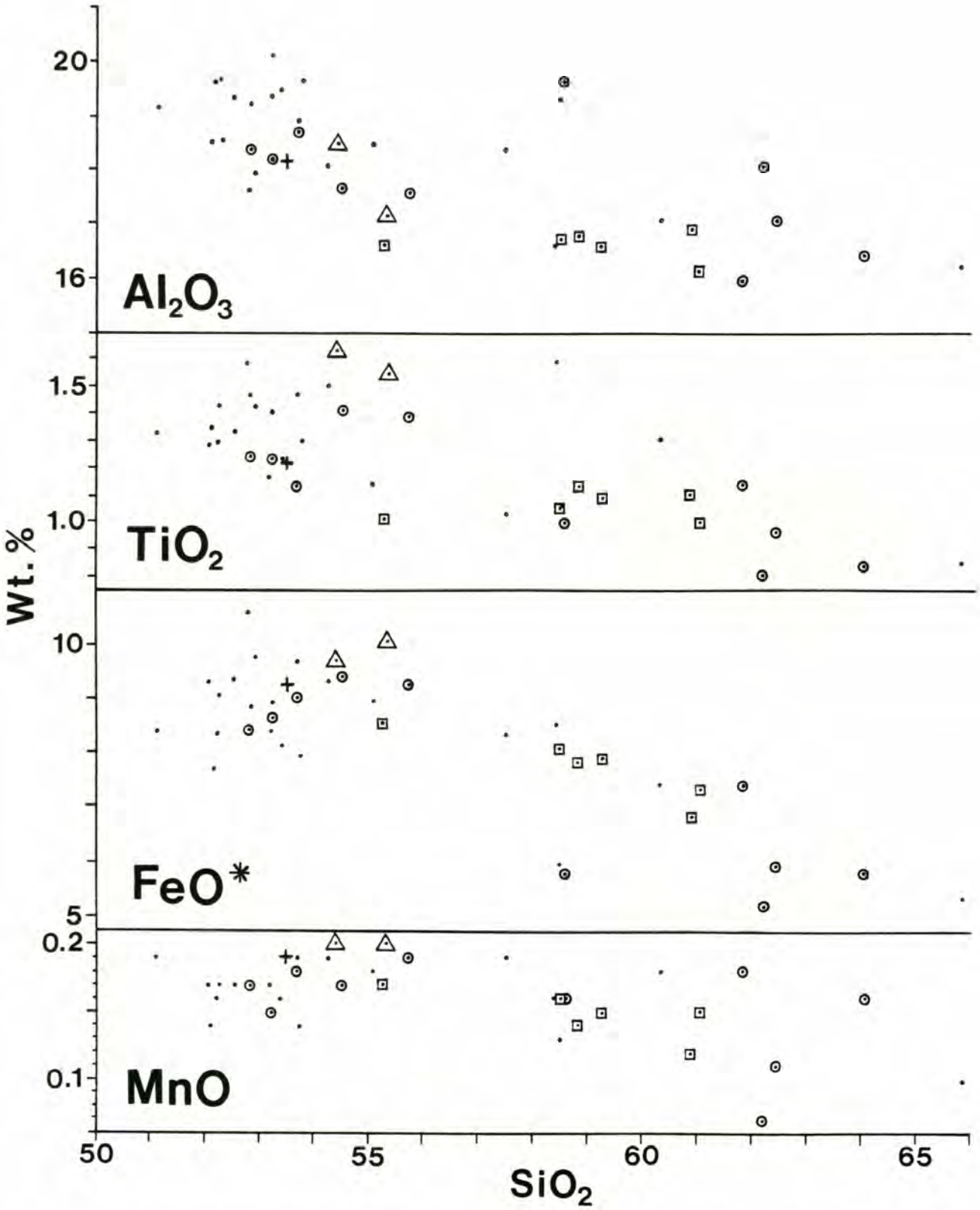

Figure 40. Major-element vs SiO_2 Harker variation diagrams for the Cliffdell area compositions. Symbols are those used in Figure 38.

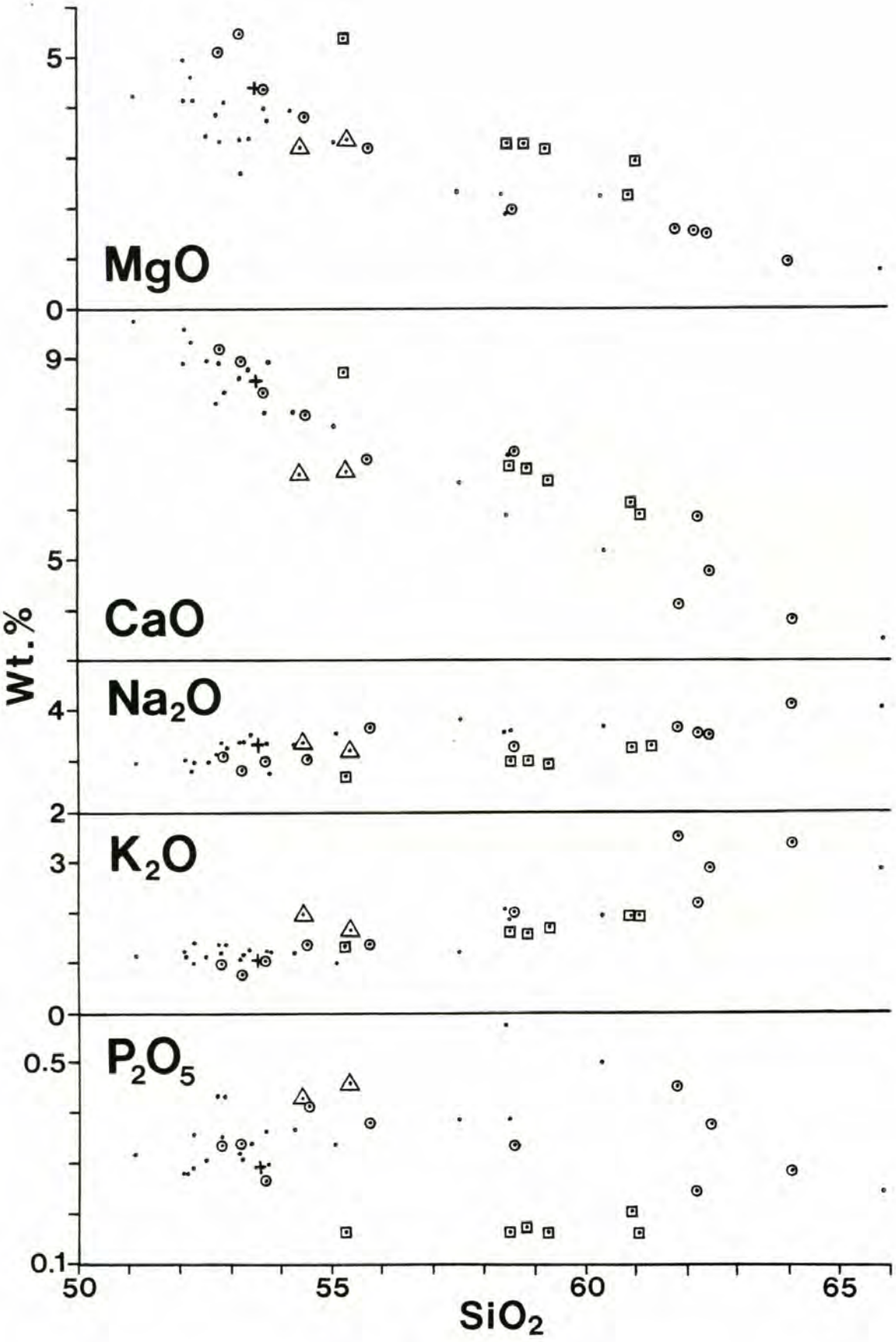

Figure 40, continued

TiO_2 content throughout the Edgar Rock suite is higher than what is regarded as typical for continental margin lavas (Gill, 1981), but is within the range of variation for arc volcanics. Higher TiO_2 contents reflects the Fe-enriched nature of the Edgar Rock suite.

The salient geochemical features of the Edgar Rock member basaltic andesites are high Al_2O_3, low Mg-numbers, moderate TiO_2 and K_2O. These are typical of continental margin basaltic lavas. Although classified in this study as basaltic andesites, the mafic lavas with less than 53 % SiO_2 are mineralogically and chemically nearly indistinguishable from high-alumina basalts (cf. Lopez-Escobar et al., 1977). The andesites of the Nile Creek member are typical orogenic andesites.

Trace Elements

The Cliffdell samples have trace element compositions typical of continental margin lavas. Most important are enrichments in large ion lithophile (LIL) elements (Cs, Rb, Ba, Sr and Th) and light rare-earth elements (REE). Enrichments of high field strentgh (HFS) elements (Zr, Hf and Ta) are variable. Transition elements, especially Ni and Cr, are generally low in abundance.

Log-log correlation diagrams using Th as a differentiation index are plotted in Figure 41. These diagrams illustrate three main points. (1) At a given Th content, the Edgar Rock lavas are enriched in LIL, REE and HFS elements relative to the Nile Creek member. Edgar Rock lavas contain lower levels of transition elements relative to the Nile Creek member, consistent with the major element trends for CaO and MgO. (2) The dike compositions show a consistent affinity with the Edgar Rock lavas. This is in accord with all geologic evidence found in this study. This geochemical similarity is maintained in spite of the significant

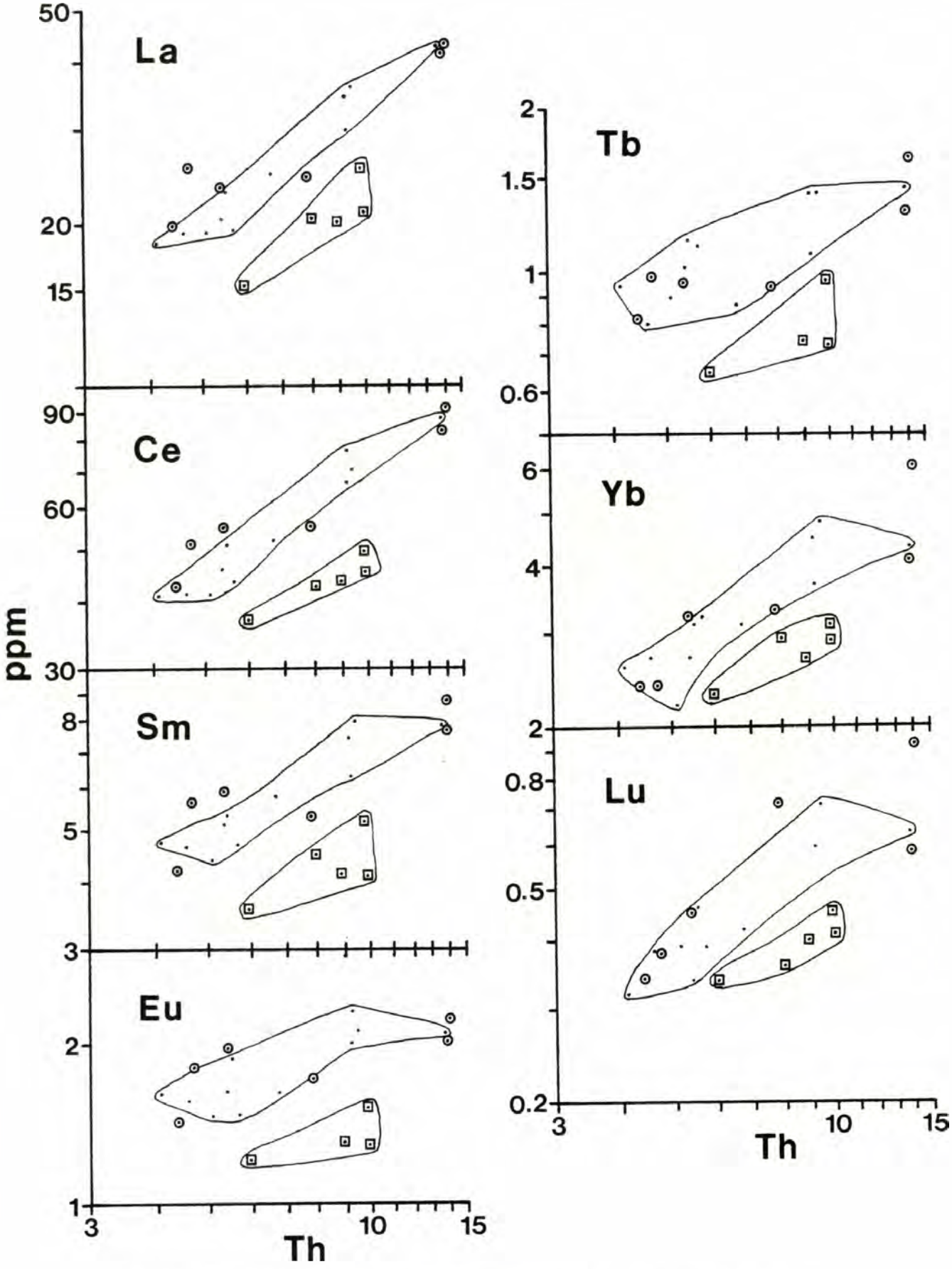

Figure 41. Log-log correlation diagrams using Th as a differentiation index. All quantities in ppm. Symbols are those used in Figure 38.

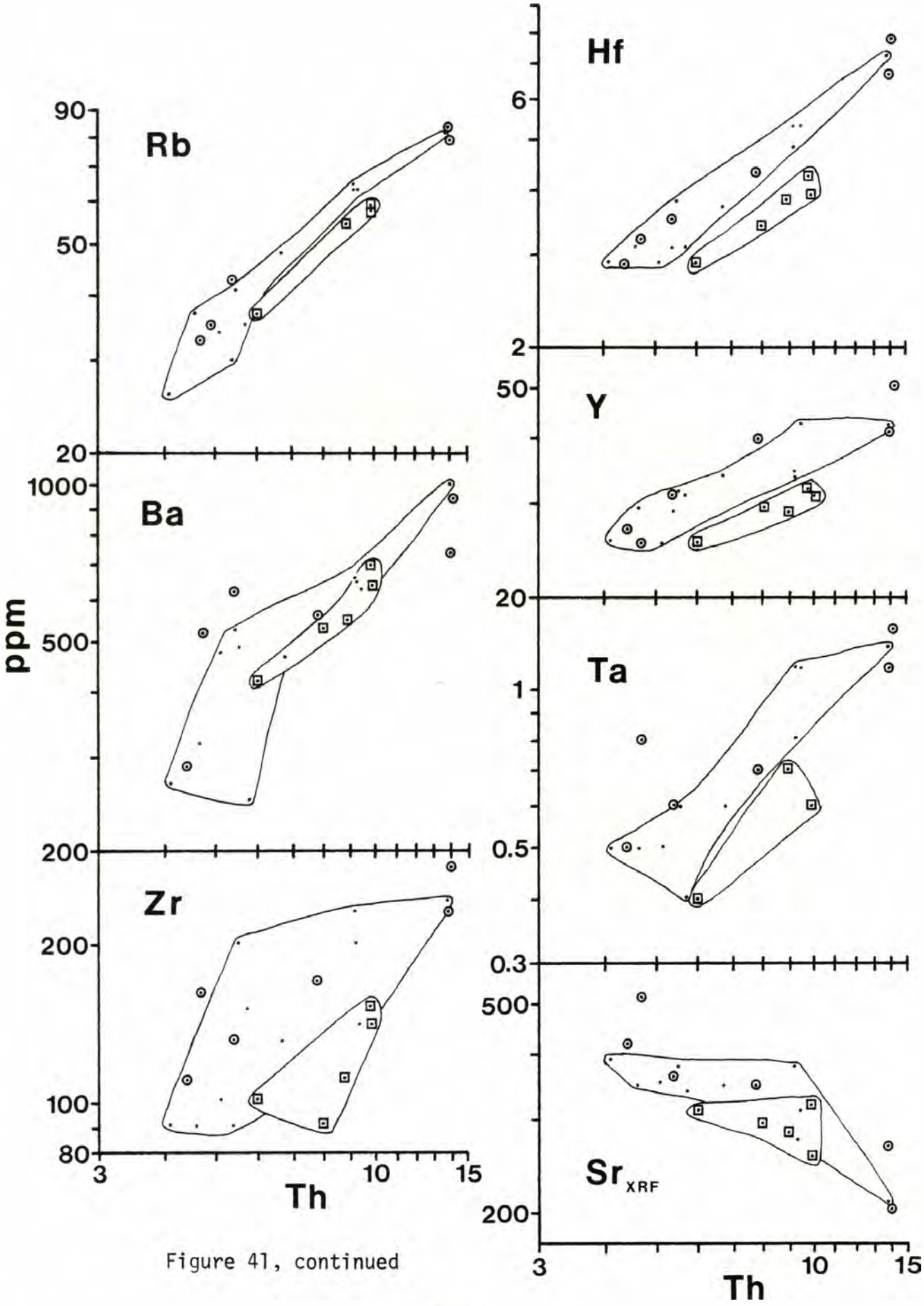

Figure 41, continued

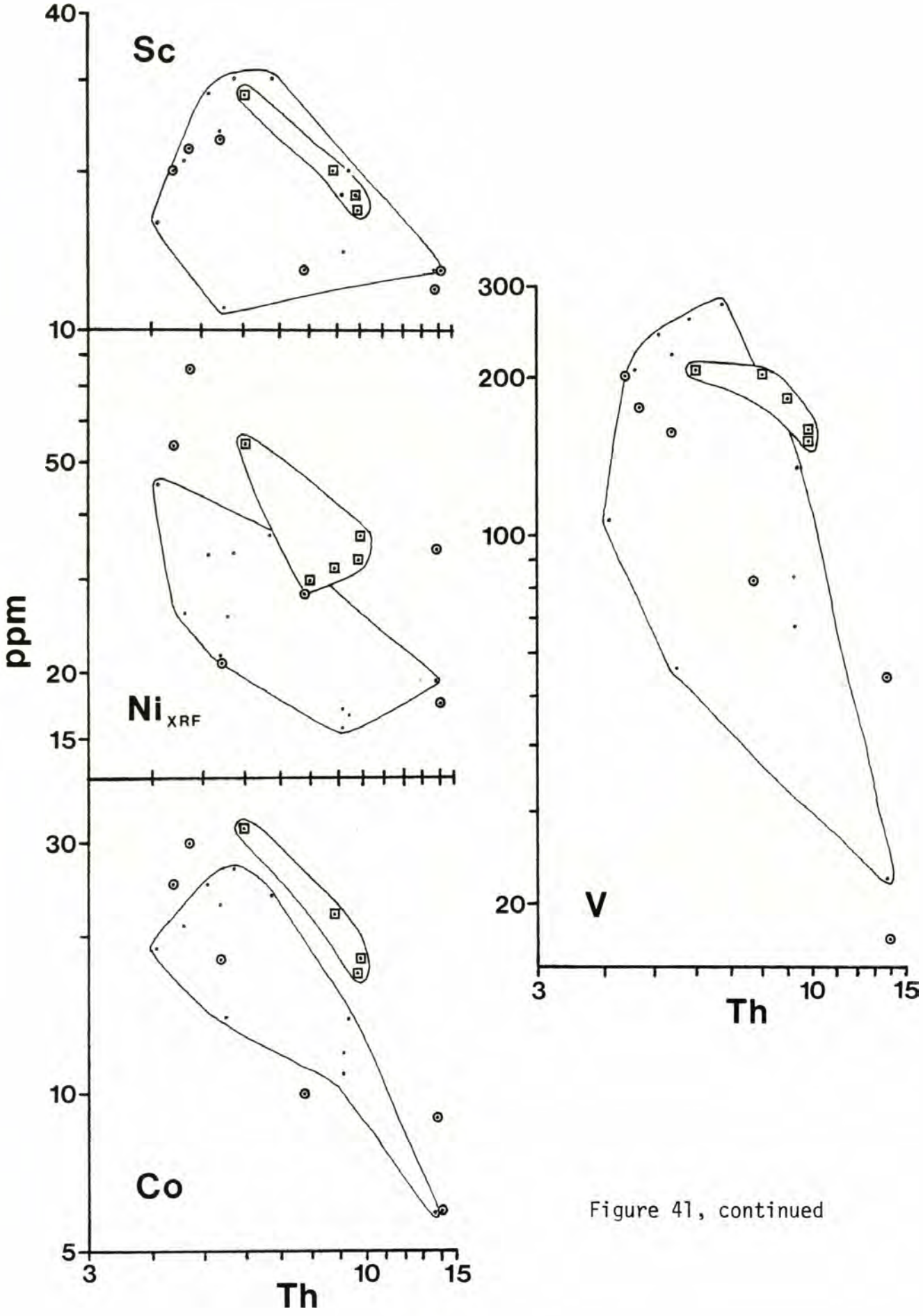

Figure 41, continued

petrographic divergence between the analyzed flows and dikes of andesite and dacite compositions. (3) REE, LIL and HFS elements correlate positively with Th, whereas transition elements correlate negatively. A large amount of scatter, however, is present within the envelopes of most elements.

Chondrite-normalized REE patterns of the Cliffdell area samples are shown in Figures 42, 43 and 44. All patterns are strongly enriched in light-REE. Chondrite-normalized La/Yb ratios for all samples range between 4 and 7. Negative Eu anomalies, indicative of plagioclase fractionation, are present in andesite and dacite samples 53, 62 and 43, and possibly 82 and 79. Heavy-REE of the Nile Creek compositions are flatter and more depleted than corresponding compositions in the Edgar Rock member.

Although Ni and Cr abundances determined by INAA and XRF are in poor agreement, concentrations appear to be low, even in the mafic samples. Exceptions are dikes 54 and 84 and Nile Creek flow 100. Higher Ni and Cr in these samples are compatible with their higher MgO and modal olivine content. Low Ni and Cr values are typical of both island arc and continental margin basaltic lavas.

In contrast to Ni and Cr, V contents are relatively undepleted in the mafic lavas and dikes of the Edgar Rock member. V contents decrease with higher SiO_2 contents. V contents of the three most mafic Edgar Rock flows (23, 98C and 80) are 240 to 271 ppm. This range is similar to typical values observed in high-alumina basaltic suites from both island arc and continental margin settings (Brown et al., 1977; Whitford et al, 1979). V is a highly sensitive indicator of magnetite fractionation and the concentrations observed are consistent with the paucity of magnetite

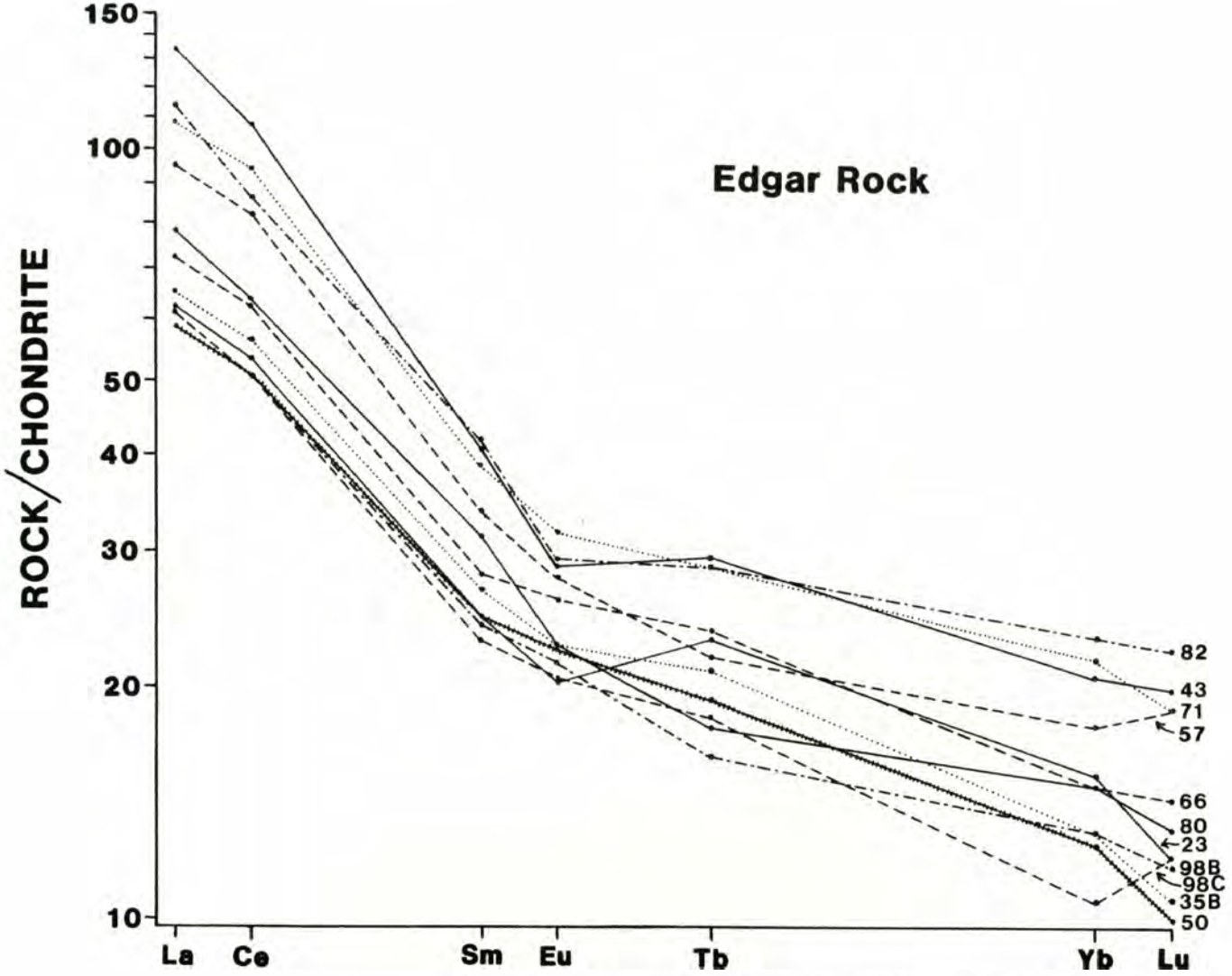

Figure 42. Chondrite-normalized rare earth element patterns of the Edgar Rock member lavas. Normalizing values are those of Taylor and Gorton (1977). Sample numbers are at right.

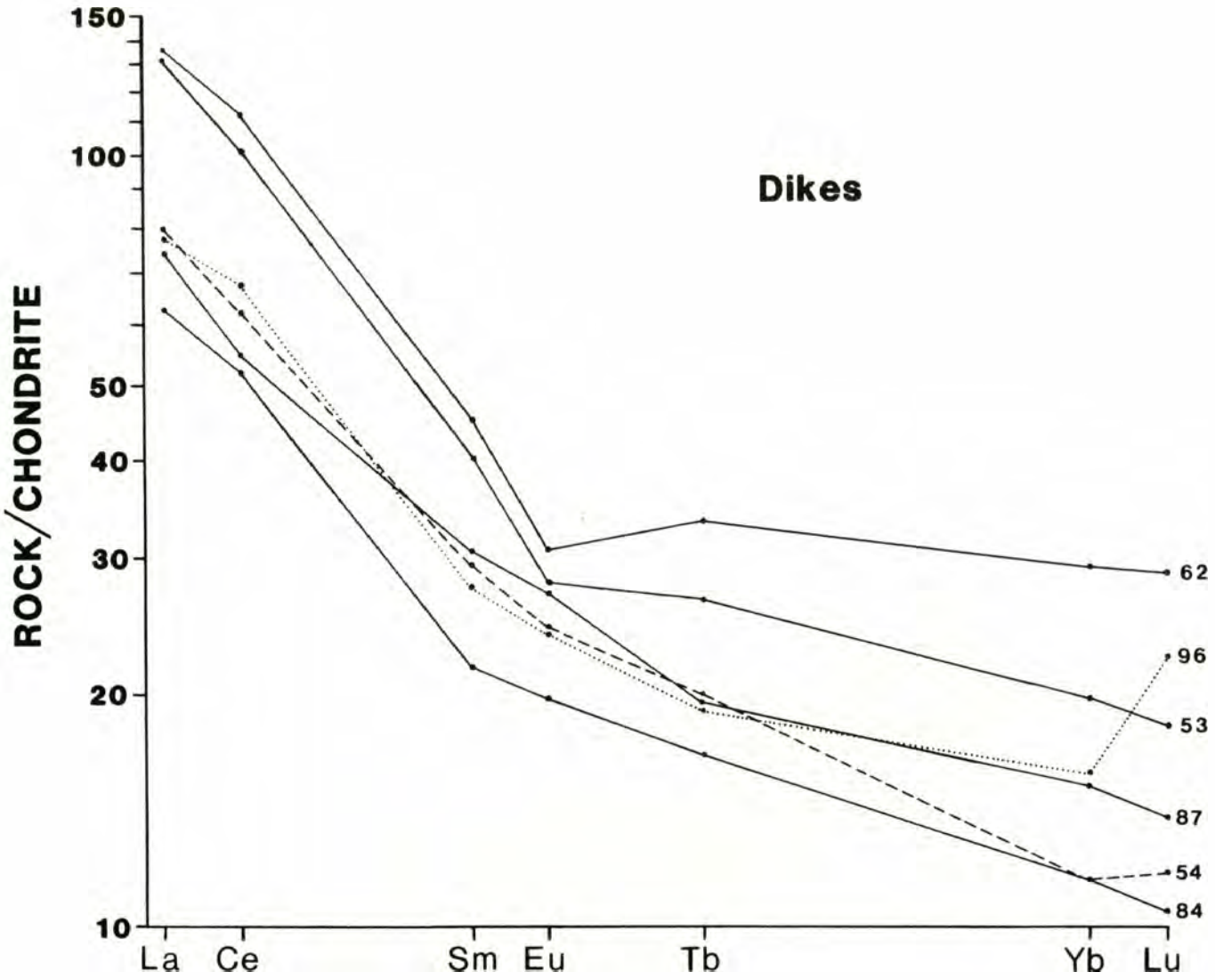

Figure 43. Chondrite-normalized rare earth element patterns of the dikes.

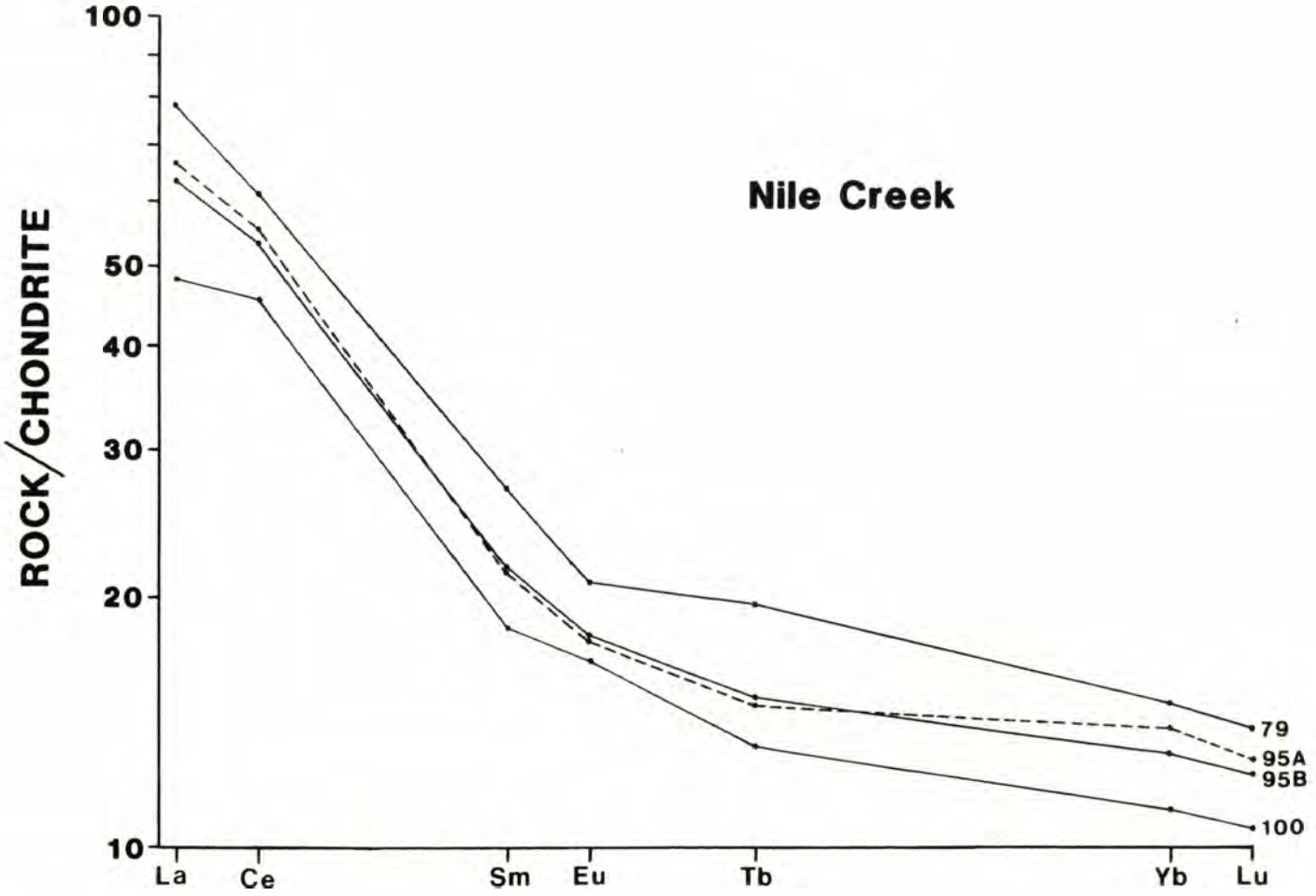

Figure 44. Chondrite-normalized rare earth element patterns of the Nile Creek member lavas.

phenocrysts observed within mafic Edgar Rock flows, indicating that these lavas have undergone little magnetite fractionation. V contents of the Nile Creek lavas are higher relative to the Edgar Rock andesites and exhibit less variation.

Origin and Differentiation of the Cliffdell Area Magmas

Models for the origin of high-alumina basalts (Gust and Perfit, 1987; Luhr and Carmichael, 1985; Lopez-Escobar et al., 1977) are applicable to the origin of the mafic Edgar Rock compositions. Two divergent models are believed to be capable of producing high-alumina basalt magmas of similar composition: (1) an origin largely in the mantle (Gust and Perfit, 1987; Perfit et al., 1980), and (2) through the melting of the basaltic portion (in eclogite mineralogy +/- sediment) of the subducting oceanic slab (Brophy and Marsh, 1986; Brophy, 1986). In the mantle model, high-alumina basalts are derivative magmas produced through the fractionation of MgO-rich olivine tholeiite magma. Fractionation of olivine, clinopyroxene and spinel at uppermost mantle to lower crustal depths produces the characteristic low MgO, Ni and Cr, raises FeO/MgO ratios and enriches liquids in Al_2O_3 and alkalies. In contrast, the slab derived magmas have these characteristics as primary features and are not required to undergo modification before eruption.

Results from this study do not favor one model over the other. The varied pyroxene clots, green spinel and gabbroic inclusions present in basaltic andesites of the Edgar Rock member are indicative of fractionation within the Edgar Rock suite, but links with more primitive compositions are uncertain and require more study. Major and trace element compositions of some Edgar Rock mafic lavas correspond well with the ranges predicted by the Brophy and Marsh (1986) slab melting model. A

major discrepency between the model and the Cliffdell compositions, however, concerns absolute REE abundances and the form of the normalized REE pattern.

Linear trends on log-log correlation diagrams (Fig. 41) are qualitative evidence that fractional crystalization is a dominant process controlling compositions within a volcanic suite (Gill, 1981, p.141). Without being rigorous, the linear covariation, particularly of La, Ce, Rb and Hf with Th is good evidence for a comagmatic relationship amongst some lavas of the Edgar Rock member.

The absence of hydrous phenocrysts throughout the compositional range of the Edgar Rock and Nile Creek lavas is indicative of relatively dry parental magmas. The higher FeO/MgO ratios and the scarcity of magnetite phenocrysts within the Edgar Rock suite are consistent with fractionation under conditions of lower fO_2 compared to the Nile Creek suite. These features are characteristic of Fe-enriched, tholeiitic arc suites elsewhere (Kay and Kay, 1985; Morrice and Gill, 1986). Variation in fO_2 alone, however, is probably not responsible for the compositional divergence of the two Cliffdell suites.

Geochemical Characterization of the Cliffdell Tectonic Environment

The Cascade Range has long been recognized as a magmatic arc (Hammond, 1979), but practically no direct geochemical documentation from the Fifes Peak Formation presently exists in the literature. The data obtained in this study allow the application of geochemical parameters to characterize Fifes Peak volcanism in the study area.

The average Ba/La ratio of the Edgar Rock flows and dikes is close to 20; that of the Nile Creek member is close to 28. These values are

typical of convergent margin volcanic rocks (Gill, 1981, p. 130). Average Ba/Ta and La/Ta ratios for the two members exceed 700 and 30, respectively. These high values are diagnostic of subduction-related magmas and illustrate the lesser enrichment of HFS elements relative to LIL and REE characteristic of arc magmas (Gill, 1981, p. 138).

Suitable Cliffdell analyses plotted within the ternary tectonomagmatic discrimination diagrams of Pearce and Cann (1973) and Wood (1980), not shown, fall within the calc-alkaline and destructive plate margin fields of these diagrams.

An extended means of comparing lava compositions is the mid-ocean ridge basalt (MORB)-normalized geochemical pattern of Pearce (1982). This is shown as Figure 45. In this diagram mafic Edgar Rock compositions are compared with Quaternary, convergent-margin basaltic lavas from southern Chile and from the Sunda arc in Java and Bali. The Edgar Rock compositions display enrichment and depletions, relative to average MORB, nearly identical in form and magnitude to typical calc-alkaline high-alumina basalt and basaltic andesite from these areas. Lesser enrichment of HFS elements (Ta, Nb, Zr, Hf and Ti) is evident in all these suites and are at levels higher than those of the island arc tholeiite association (Pearce, 1982; Dupuy et al., 1982). Ce, P and Sm enrichments are also characteristic of calc-alkaline magmas (Pearce, 1982). Depletion of Cr parallels the low MgO and Ni contents of these suites.

The southern Chile and Sunda arc compositions are situated in relatively simple subduction settings. These comparison suites are also from volcanic centers situated behind the volcanic front in these areas. Across-arc geochemical trends involving increasing K and related LIL elements at a given SiO_2 content with increasing distance from the trench are part of the basis for spatial variation in lava series classification

Figure 45. Mid-ocean ridge basalt (MORB)-normalized geochemical pattern (after Pearce, 1982) of mafic Edgar Rock member lavas. Normalizing values for average MORB composition are given in Pearce (1982). Southern Chile "enriched" high-alumina basalt (HAB) and basaltic andesite pattern is the average of 8 analyses from the Laguna del Maule and Lanin volcanic centers (Frey et al., 1984; Lopez-Escobar et al., 1977). These centers have 49 to 53 % SiO_2, 13 to 22 ppm La (40-70X chondrite) and 0.98 % to 1.14 % K_2O. Less-enriched HAB's have 6 to 11 ppm La (18-34X chondrite) and 0.44 to 0.77 % K_2O.

The Sunda arc range is bounded by the average Quaternary, calc-alkaline basalt (50.8% SiO_2) and basaltic andesite (54.6% SiO_2) compositions from Java and Bali (Whitford et al., 1979).

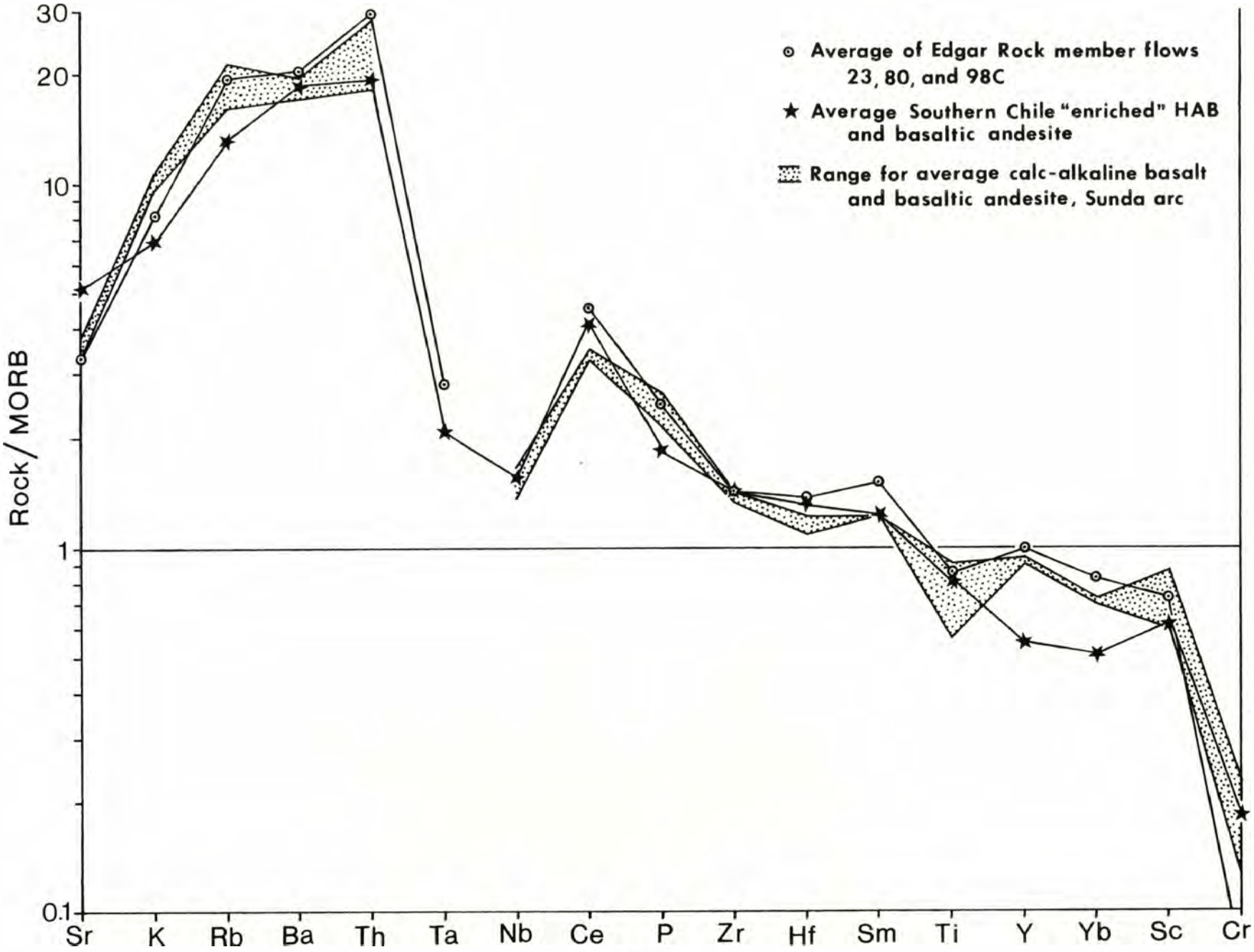
30
20
10
1
0.1
Rock/MORB
Sr
K
Rb
Ba
Th
Ta
Nb
Ce
P
Zr
Hf
Sm
Ti
Y
Yb
Sc
Cr
Average of Edgar Rock member flows 23, 80, and 98C
Average Southern Chile "enriched" HAB and basaltic andesite
Range for average calc-alkaline basalt and basaltic andesite, Sunda arc

Figure 45.

across volcanic arcs (Gill, 1981, ch. 7; Whitford et al., 1979). High-alumina basalts in southern Chile, with overall similar major element compositions, are variably enriched in LIL and light-REE (Lopez-Escobar et al., 1977). The analyses compared in Figure 45 have greater enrichments of these elements and are from volcanoes situated farther from the volcanic front. The Sunda arc calc-alkaline lavas are located over Benioff-zone depths intermediate between those of associated island arc tholeiite and high-K calc-alkaline lavas (Whitford et al., 1979).

In a possibly analogous manner, the Cliffdell area is located along the (present) eastern margin of a volcanic belt that was at least 75 km wide. The Cliffdell area is also located about 50 km east of the axis of batholith emplacement in Miocene time. Mafic lavas of Oligocene to early Miocene age in the Mt. St. Helens area (Evarts et al., 1987) possess lower K_2O contents than mafic lavas in the Cliffdell area, consistent with an eastward, across-arc increase in K_2O levels.

The Fifes Peak Formation Within the Cascade Arc Context

The episode of Fifes Peak volcanism was coeval with the intrusion of the Cascade calc-alkaline batholiths (Hammond, 1979; Frizzell and Vance, 1983) and both were emplaced in close proximity along the Cascade Range. This close association in space and time has suggested a co-magmatic relationship for the intrusive and extrusive assemblages (Erickson, 1969; Hammond, 1979). Most of the major batholiths in Washington (Chilliwack, Cloudy Pass, Snoqualmie, Tatoosh) have vented to the surface during their emplacement resulting in an extrusive volcanic phase (Fuller, 1925; Tabor and Crowder, 1969; Fisk et al., 1963). The chemical evidence from this study, from Swanson (1964) and Phillips et al. (1986) show that lavas of

Fifes Peak Fm. age are not direct extrusive equivalents of the batholithic magmas.

In Figure 46, the iron-enrichment trends of a variety of lava and batholithic suites from the Cascades are compared with the Cliffdell area compositions. Compositional variation amongst the Cascade batholiths defines a classic calc-alkaline variation trend characterized by suppression of Fe-enrichment and a low and nearly constant Fe-ratio through much of their compositional range. Deviation of the Cliffdell area compositions, in particular the Edgar Rock suite, to higher Fe-ratios suggests two simplified possibilities. One, the parental Fifes Peak magmas are derived from a source or sources distinct from the batholiths, or two, the the batholiths and Fifes Peak lavas originated from the same or similar parental magmas, but during an early stage of evolution diverged along different fractionation paths. The Tieton Volcano is intermediate between the two Cliffdell members in its degree of Fe-enrichment.

Individual volcanic arcs typically contain a gradational spectrum of differention trends resulting in variable Fe-enrichment (Miyashiro, 1974; Gill, 1981; Morrice and Gill, 1986). Within the framework of similar parental magma compositions, the divergence in Fe-enrichment trends between the Cascade batholiths and the Edgar Rock lavas reflects variable operation of magmatic processes, including fractional crystallization, magma mixing and crustal interaction.

Petrographic and geochemical evidence from the Edgar Rock member are consistent with a view that this suite reflects a drier magmatic system and has probably undergone less crustal interaction relative to the Cascade batholiths. Fe-enriched lavas of the Fifes Peak Formation may have resulted from localized extentional environments that tapped lower

Explanation for Figure 46

Comparative FeO*/(FeO*+MgO)-SiO_2 diagram for some selected volcanic and plutonic rocks from the Cascades Range of Washington, Oregon and California.

Quaternary volcanoes

R Rainier
⊕ late basaltic andesite (1)
S Shasta

SH St. Helens
★ St. Helens basalt, SH 14 (2)

White Pass area

HMM Hogback Mtn. mafic magma
⊕ Devils Washbasin basalt
▲ Pyroxene andesites of Goat Rocks volcano (3)
▽ Hornblende andesites
SB Spiral Butte

Cliffdell area

·ER Edgar Rock member
⊙ Dikes
△ Devils Slide (4)
⊡NC Nile Creek member
+ Dike in Naches Fm.

Tieton River area

● Tieton Volcano
✳ Westfall Rocks (5)

Oregon Cascades

HCB High Cascade basalts
☆ Mt. Washington-type basaltic andesites (6)
⚙ North Sister-type basaltic andesites

Cascades Batholiths

TP Tatoosh Pluton (7)
◆ Snoqualmie Batholith (averages) (8)
CH Chilliwack Batholith
MB Mount Barr Batholith (9)

Sources of data: (1) Condie and Swenson, 1973; (2) Halliday et al., 1983; (3) Clayton, 1983; (4) This study; (5) Swanson, 1964; (6) Hughes and Taylor, 1986; (7) Thompson, 1983; (8) Erickson, 1969; (9) Richards and McTaggart, 1976.

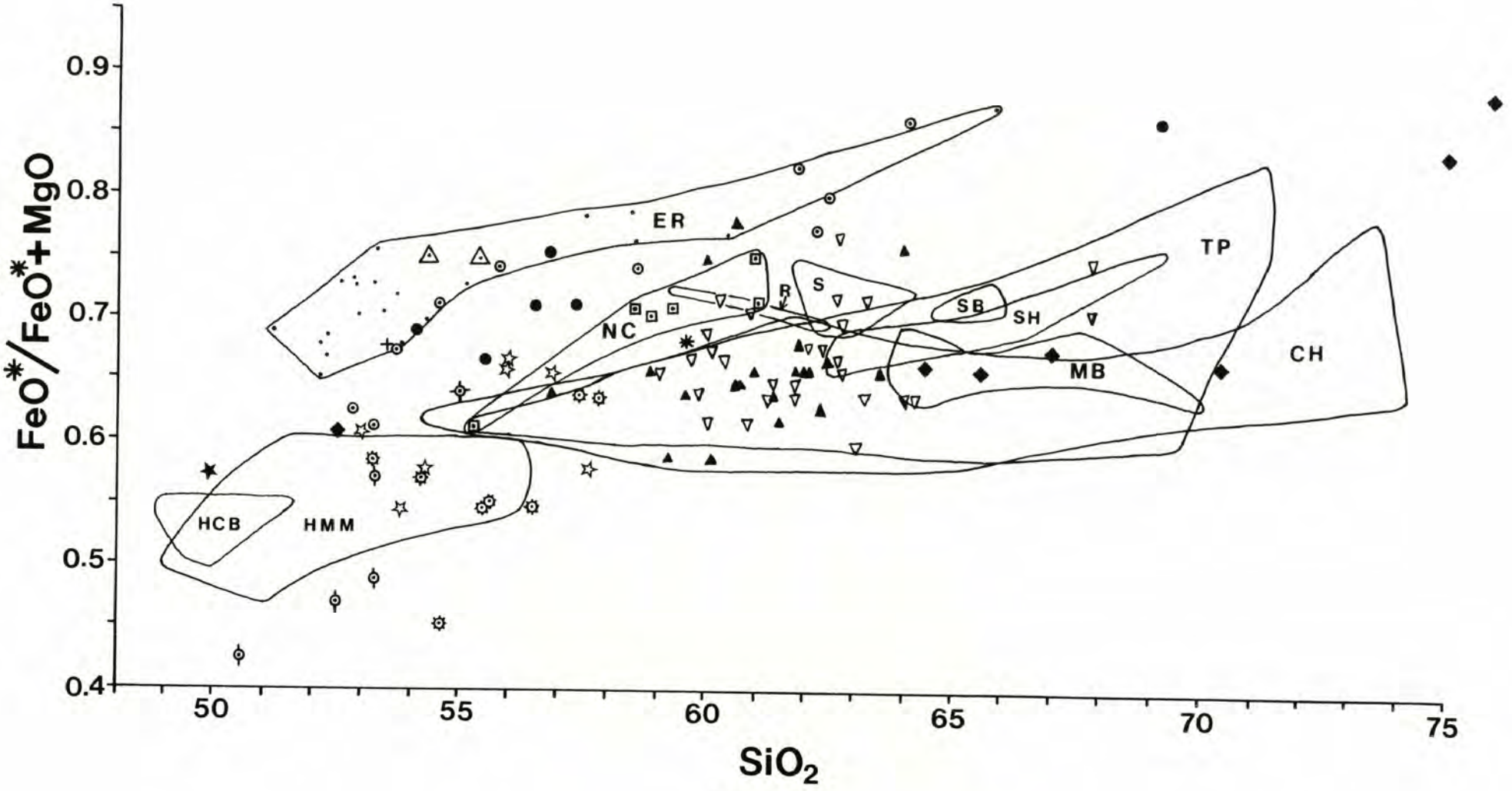
0.9
0.8
0.7
0.6
0.5
0.4
FeO*/FeO*+MgO
50
55
60
65
70
75
SiO2
ER
NC
R
S
SB
SH
TP
CH
MB
HCB
HMM

Figure 46.

crustal magma chambers allowing more rapid ascent of the parental magma to the surface. This would reduce crustal interaction and allow shallower fractionation, both promoting Fe-enrichment.

Mafic lavas in the Cliffdell area broadly resemble mafic lavas of similar or slightly older age near Mt. St. Helens (Evarts et al., 1987) in their mode of occurrence and high-alumina, Fe-enriched character. Temporal compositional evolution of volcanic suites in the Cliffdell area is shown by a greater proportion of andesitic lavas in the younger Nile Creek member. This evolution is similar to that observed in the Oligocene to early Miocene strata of the Mt. St. Helens area (Evarts et al., 1987).

SUMMARY AND CONCLUSIONS

1) The Fifes Peak Formation in the Cliffdell area has been divided into two structurally, lithologically and geochemically distinct members separated by a pronounced unconformity. The older member, informally referred to as the Edgar Rock member, is comprised of generally highly brecciated lava flows, laharic breccia and lesser volcaniclastic sediments and tuffs. A thickness of at least 1,800 meters is exposed near Edgar Rock. K-Ar ages indicate a latest Oligocene age of about 24 to 27 Ma.

2) Lavas in the Edgar Rock member range in composition from basalt to dacite, but are mostly basaltic andesite. All compositions are typically highly porphyritic and contain an anhydrous phenocryst assemblage of plagioclase, olivine, minor clinopyroxene and magnetite. Orthopyroxene is present in some flows with more than 53 % SiO_2. Some basaltic andesite flows contain diverse assemblages of gabbroic inclusions and pyroxene clots. One group of clinopyroxene clots is compositionally distinct from typical phenocryst clinopyroxenes and is associated with green spinel. Green spinel occurring by itself is also a rare constituent of some other basaltic andesite flows.

3) Two distinct types of laharic or lahar-like breccias are present in the Edgar Rock member. The most common type contains porphyritic clasts and matrix constituents petrographically similar to the to the most abundant lavas of the Edgar Rock member. Abundant vesicular matrix components and vertical color changes within some units may indicate deposition at high temperature. A less common type of lahar-like breccia contains abundant silicic lapilli (averaging 1 cm across) and variable admixture of basaltic andesite material. Clasts of non-Fifes Peak Fm. lithologies, including gabbroic plutonic rocks, sandstone and altered

volcanic rocks, are most commonly associated with these units.

4) Beds in the Edgar Rock member define a circular dome , the Edgar Rock dome. Dips in the dome are typically 30 to 50 degrees. An extensive system of radial dikes has a focal area near the structural center of the dome. Dikes are present out to at least 5 km from the focal area. Dike compositions range from basaltic andesite to dacite and are petrographically diverse, indicating a history of multiple magma intrusions. One probable feeder dike for a flow was located. Mafic dikes broadly resemble the basaltic andesite flows in the Edgar Rock member, but observed andesite and dacite dikes are petrographically distinct from flows of similar composition. Neither intrusive bodies nor a volcanic neck were were indentified at the focus of the dike system. The radial dike system is truncated at the unconformity between the two members.

5) The Edgar Rock dome is probably the site of a volcanic center in the Fifes Peak Formation. Present steep dips are a combination of primary depositional attitudes and syn- and post-depositional uplift, perhaps related in part to the intrusion of the radial dike system. Volcaniclastic interbeds and laharic breccias restrict primary dip in the dome, here inferred to have ranged from nearly horizontal up to no more than about 15 degrees. The Edgar Rock member on the flanks of the dome represents the proximal apron facies of a cone, now mostly removed by erosion, located at or near the focus of the radial dike system.

6) The younger member of the Fifes Peak Fm., informally referred to as the Nile Creek member, unconformably overlies the Edgar Rock member, which had undergone considerable erosion before Nile Creek deposition. The Nile Creek member is comprised mostly of andesite flows and coarse laharic breccias and is up to 550 meters thick. K-Ar ages indicate an early Miocene age of about 24 to 19.5 Ma. Lavas are petrographically rather

uniform, highly porphyritic and contain phenocrysts of plagioclase, clinopyroxene, orthopyroxene, magnetite and olivine. An ash-flow tuff has a fission-track age of 23.3 Ma. The source of the Nile Creek materials was not identified in this study.

7) The Cliffdell area is located along the SW margin of the Cle Elum-Wallula lineament, the central third of the Olympic-Wallowa lineament and contains structures which pre-date and formed with adjacent Columbia River Basalt (CRB) structures. The principal structure of the study area, the Edgar Rock dome, formed during Fifes Peak time (pre-24 Ma) as its truncated beds are overlain by the Nile Creek member and gently-dipping CRB. The NW part of the study area has been the most clearly affected by post-CRB deformation. The Edgar Rock member there has been offset by a NW-trending monocline that formed with the adjacent Little Naches Syncline.

8) The Cliffdell area lavas and dikes possess geochemical features common to continental margin, subduction-related lavas. Enrichments in K and related LIL and light-REE are characteristic of calc-alkaline magmas, but high FeO/MgO ratios, especially of the Edgar Rock member, are typical of tholeiitic magmas. High Al_2O_3 and low MgO, Ni and Cr of Edgar Rock basaltic andesites ally these compositions with orogenic high-alumina basalts. The Edgar Rock lavas and dikes are enriched in LIL, REE and HFS elements relative to the Nile Creek compositions. The Cliffdell suites, especially the Edgar Rock member, are markedly Fe-enriched relative to the coeval Cascade batholiths. Separate magma sources or magmatic differentiation processes, or both, are implied.

REFERENCES CITED

Abbott, A.T., 1953, The geology of the northwest portion of the Mount Aix quadrangle, Washington [Ph.D. Dissertation]: Seattle, Washington, University of Washington, 256 p.

Aoki, K., and Kushiro, I., 1968, Some Clinopyroxenes from Ultramafic Inclusions in Dreiser Weiher, Eifel: Contributions to Mineralogy and Petrology, 18, 326-337.

Arculus, R.J., and Wills, K.J.A., 1980, The Petrology of Plutonic Blocks and Inclusions from the Lesser Antilles Island Arc: Journal of Petrology, 21, part 4, 743-799.

Bentley, R.D., 1977, Western Columbia Plateau margin studies, Tieton River to Yakima River: Shannon and Wilson, Inc., in Washington Public Power Supply System PSAR for WPPSS Nuclear Project 1 and 4, Amendment 23, Subappendix 2R D, Chapter 6, D.6.1-D.6.34, Nuclear Regulatory System, Docket Nos. 50-460, 50-513.

Bentley, R.D., and Campbell, N.P., 1983, Geologic map of the Ellensburg Quadrangle: Washington Division of Geology and Earth Resources Geologic Map GM-28.

Bloomfield, K., and Valastro, S., 1977, Late Quaternary tephrochronology of Nevado de Toluca volcano, central Mexico: Overseas Geology and Mineral Resources, No. 46, 15 p.

Brophy, J.G., 1986, The Cold Bay Volcanic Center, Aleutian Volcanic Arc I. Implications for the origin of Hi-Alumina Arc Basalt: Contributions to Mineralogy and Petrology, 93, 368-380.

Brophy, J.G., and Marsh, B.D., 1986, On the Origin of High-Alumina Arc Basalt and the Mechanics of Melt Extraction: Journal of Petrology, 27, pt. 4, 763-789.

Brown, G.M., Holland, J.G., Sigurdsson, H., Tomblin, J.F., and Arculus, R.J., 1977, Geochemistry of the Lesser Antilles volcanic island arc: Geochimica et Cosmochimica Acta, 41, 785-801.

Campbell, N.P., 1975, A geologic roadlog over Chinook, White Pass, and Ellensburg to Yakima Highways: State of Washington, Department of Natural Resources, Division of Geology and Earth Resources, Information Circular 54, 82 p.

Chapman, N.A., 1975, An Experimental Study of Spinel Clinopyroxenite Xenoliths from the Duncansby Ness Vent, Caithness, Scotland: Contributions to Mineralogy and Petrology, 51, 223-230.

Clayton, G.A., 1983, Geology of the White Pass Area, South-Central Cascade Range, Washington [M.S. Thesis]: Seattle, Washington, University of Washington, 212 p.

Condie, K.C., and Swenson,, D.H., 1973, Compositional Variation in Three

Cascade Stratovolcanoes: Jefferson, Rainier, and Shasta: Bulletin of Volcanology, 37, 205-230.

Crandell, D.R., and Mullineaux, D.R., 1973, Pine Creek Volcanic Assemblage at Mount St. Helens, Washington: U.S. Geological Survey Bulletin 1383-A, 23 p.

Curtis, G.H., 1954, Mode of origin of pyroclastic debris in the Mehrten Formation of the Sierra Nevada: University of California Publications in Geological Sciences, 29, No. 9, 453-502.

Dupuy, C., Dostal, J., Marcelot, G., Bougault, H., Joron, J.L., and Treuil, M., 1982, Geochemistry of basalts from central and southern New Hebrides arc: implications for their source rock compositions: Earth and Planetary Science Letters, 60, 207-225.

Eichelberger, J.C., 1978a, Andesitic volcanism and crustal evolution: Nature, 275, 21-27.

Eichelberger, J.C., 1978b, Andesites in Island Arcs and Continental Margins: Relationship to Crustal Evolution: Bulletin of Volcanology, 41, No.4, 480-500.

Erickson, E.H., 1969, Petrology of the Composite Snoqualmie Batholith, Central Cascade Mountains, Washington: Geological Society of America Bulletin, 80, 2213-2236.

Evarts, R.C., Ashley, R.P., and Smith, J.G., 1987, Geology of the Mt. St. Helens Area: Record of Discontinuous Volcanic and Plutonic Activity in the Cascade Arc of Southern Washington: Journal of Geophysical Research, 92, No. B10, 10,155-10,169.

Ewart, A., 1976, Mineralogy and chemistry of modern orogenic lavas-some statistics and implications: Earth and Planetary Science Letters, 31, 417-432.

Fisher, R.V., 1960, Classification of volcanic breccias: Geological Society of America Bulletin, 71, 973-982.

Fisher, R.V., and Schmincke, H.-U., 1984, Pyroclastic Rocks: Berlin, Heidelburg, Springer-Verlag, 472 p.

Fiske, R.S., Hopson, C.A., and Waters, A.C., 1963, Geology of Mount Rainier National Park, Washington: U.S. Geological Survey Professional Paper 444, 93 p.

Frey, F.A., and Prinz, M., 1978, Ultramafic inclusions from San Carlos, Arizona: Petrologic and geochemical data bearing on their petrogenesis: Earth and Planetary Science Letters, 38, 129-176.

Frey, F.A., Gerlach, D.C., Hickey, R.L., Lopez-Escobar, L., and Munizaga-Villavicencio, F., 1984, Petrogenesis of the Laguna del Maule volcanic complex, Chile (36 S): Contributions to Mineralogy and Petrology, 88, 133-149.

Frizzell, V.A., Jr., Tabor, R.W., Booth, D.B., and Ort, K.M., 1984, Preliminary geologic map of the Snoqualmie Pass 1:100,000 quadrangle, Washington: U.S. Geological Survey Open-File Map OF-84-693.

Frizzell, V.A., and Vance, J.A., 1983, Cenozoic volcanism of the Cascades Washington: EOS, v. 64, No. 45, p. 886.

Fuller, R.E., 1925, The geology of the northeast part of the Cedar Lake quadrangle, with special reference to the deroofed Snoqualmie batholith [M.S. Thesis]: Seattle, Washington, University of Washington, 96 p.

Furlong, P.O., 1982, Paleomagnetism of the Mount Rainier area, western Washington [M.S. Thesis]: Bellingham, Washington, Western Washington University, 76 p.

Gill, J.B., 1981, Orogenic Andesites and Plate Tectonics: New York, Springer-Verlag, 390 p.

Gust, D.A., and Perfit, M.R., 1987, Phase relations of a high-Mg basalt from the Aleutian Island Arc: Implications for primary island arc basalts and high-Al basalts: Contributions to Mineralogy and Petrology, 97, 7-18.

Halliday, A.N., Fallick, A.E., Dickin, A.P., Mackenzie, A.B., Stephens, W.E., and Hildreth, W., 1983, The isotopic and chemical evolution of Mount St. Helens: Earth and Planetary Science Letters, 63, 241-256.

Hartman, D.A., 1973, Geology and low-grade metamorphism of the Greenwater River area, central Cascades, Washington [Ph.D. Thesis]: Seattle, Washington, University of Washington, 99 p.

Hammond, P.E., 1979, A tectonic model for evolution of the Cascade Range, in Armentrout, J.M., Cole, M.R., and Terbest, H., Jr., eds., Cenozoic paleogeography of the western United States: Pacific Section, Society of Economic Paleontologists and Mineralogists, Los Angeles, California, 219-237.

Hammond, P.E., 1980, Reconnaissance geologic map of southern Washington Cascade Range: Publications of the Department of Earth Sciences, Portland State University, Portland, Oregon.

Hoblitt, R.P., and Kellogg, K.S., 1979, Emplacement temperatures of unsorted and unstratified deposits of volcanic rock debris as determined by paleomagnetic techniques: Geological Society of America Bulletin, 90, part 1, 633-642.

Hughes, S.S., and Taylor, E.M., 1986, Geochemistry, petrogenesis, and tectonic implications of central High Cascade mafic platform lavas: Geological Society of America Bulletin, 97, 1024-1036.

Hyde, J.H., 1975, Upper Pleistocene Pyroclastic-Flow Deposits and Lahars South of Mount St. Helens, Washington: U.S. Geological Survey Bulletin 1383-B, 20 p.

Irvine, T.N., and Baragar, W.R.A., 1971, A Guide to the Chemical Classification of the Common Volcanic Rocks: Canadian Journal of Earth Science, 8, 523-548.

Kay, S.M., and Kay, R.W., 1985, Aleutian tholeiitic and calc-alkaline magmas I: The mafic phenocrysts: Contributions to Mineralogy and Petrology, 90, 276-290.

Kienle, C.F., Jr., Bentley, R.D., and Anderson, J.L., 1977, Geologic reconnaissance of the Cle Elum-Wallula lineament and related structures: Shannon and Wilson, Inc., in Washington Public Power Supply System PSAR for WPPSS Nuclear Project 1 and 4 , Amendment 23, 33 p.

Kutolin, V.A., and Frolova, V.M., 1970, Petrology of Ultrabasic Inclusions from Basalts of Minusa and Transbaikalain Regions (Siberia, USSR): Contributions to Mineralogy and Petrology, 29, 163-179.

Le Maitre, R.W., 1984, A proposal by the IUGS Subcommision on the systematics of Igneous Rocks for a chemical classification of volcanic rocks based on the total alkali silica (TAS) diagram: Australian Journal of Earth Sciences, 31, no. 2, 243-255.

Lopez-Escobar, L., Frey, F.A., and Vergara, M., 1977, Andesites and High-Alumina Basalts from the Central-South Chile High Andes: Geochemical Evidence Bearing on Their Petrogenesis: Contributions to Mineralogy and Petrology, 63, 199-228.

Luhr, J.F., and Carmichael, I.S.E., 1985, Jorullo Volcano, Michoacan, Mexico (1759-1774): The earliest stages of fractionation in calc-alkaline magmas: Contributions to Mineralogy and Petrology, 90, 142-161.

Luker, J.A., 1985, Sedimentology of the Ellensburg Formation northwest of Yakima, Washington [M.S. Thesis]: Cheney, Washington, Eastern Washington University, 184 p.

Macdonald, G.A., 1953, Pahoehoe, aa, and block lava: American Journal of Science, 251, No. 3, 169-191.

Marsh, B.D., 1982, The Aleutians, in Thorpe, R.S., ed., Andesites: Orogenic Andesites and Related Rocks: New York, John Wiley and Sons Ltd., 99-114.

Mertzman, S.A., Jr., 1977, The Petrology and Geochemistry of the Medicine Lake Volcano, California: Contributions to Mineralogy and Petrology, 62, 221-247.

Meyers, J.D., Marsh, B.D., and Sinha, A.K., 1986, Geochemical and strontium isotopic characteristics of parental Aleutian Arc magmas: evidence from the basaltic lavas of Atka: Contributions to Mineralogy and Petrology, 94, 1-11.

Miyashiro, A., 1974, Volcanic rock series in island arc and active continental margins: American Journal of Science, 274, 321-355.

Morrice, M.G., and Gill, J.B., 1986, Spatial patterns in the mineralogy of island arc magma series: Sangihe arc, Indonesia: Journal of Volcanology and Geothermal Research, 29, 311-353.

Mullineaux, D.R., and Crandell, D.R., 1962, Recent lahars from Mount St. Helens, Washington: Geological Society of America Bulletin, 73, 855-870.

Newhall, C.G., 1979, Temporal variation in the lavas of Mayon Volcano, Philippines: Journal of Volcanology and Geothermal Research, 6, 61-83.

Parsons, W.H., 1939, Volcanic centers of the Sunlight area, Park County, Wyoming: Journal of Geology, 47, No. 1, 1-26.

Parsons, W.H., 1969, Criteria for Recognition of Volcanic Breccia: Review, in Larsen, L.H., ed., Prinz, M. and Manson, V., co-eds., Igneous and Metamorphic Geology: Geological Society of America Memoir 115, 263-304.

Peacock, M.A., 1931, Classification of Igneous Rock Series: Journal of Geology, 39, 54-67.

Pearce, J.A., 1982, Trace element characteristics of lavas from destructive plate boundaries, in Thorpe, R.S., ed., Andesites: Orogenic Andesites and Related Rocks: New York, John Wiley and Sons Ltd., 525-548.

Pearce, J.A., and Cann, J.R., 1973, Tectonic setting of basic volcanic rocks determined using trace element analyses: Earth and Planetary Science Letters, 19, 290-300.

Peccarillo, A., and Taylor, S.R., 1976, Geochemistry of Eocene calc-alkaline volcanic igneous rocks from the Kastamonu area, northern Turkey: Contributions to Mineralogy and Petrology, 58, 63-81.

Perfit, M.R., Gust, D.A., Bence, A.E., Arculus, R.J., and Taylor, S.R., 1980, Chemical characteristics of island arc basalts: implications for mantle sources: Chemical Geology, 30, 227-256.

Peters, Von Arnd, 1968, Ein neues Verfahren zur Bestimmung von Eisen (11) oxid in Mineralen und Gesteinen: Neues Jahrbuch fur Mineralogie, v. 3-4, 119-125.

Phillips, W.M., Korosec, M.A., Schasse, H.W., Anderson, J.L., Hagen, R.A., 1986, K-Ar ages of volcanic rocks in southwest Washington: Isochron West, no. 47, December, 18-24.

Raisz, E., 1945, The Olympic-Wallowa lineament: American Journal of Science, 243-A, 479-485.

Reidel, S.P., Tolan, T.L., Anderson, M.H., Fecht, K.R., and Hooper, P.R., in press, The Grande Ronde Basalt from Washington, Oregon, and Idaho: regional stratigraphic relationships, in Reidel, S.P., and Hooper, P.R., eds., Volcanism and Tectonism on the Columbia Plateau-The

Proceedings of the 4th Columbia River Basalt Symposium: Geological Society of America Special Paper.

Richards, T.A., and McTaggart, K.C., 1976, Granitic rocks of the southern Coast Plutonic Complex and Northern Cascades of British Columbia: Geological Society of America Bulletin, 87, 935-953.

Schreiber, S.A., 1981, Geology of the Nelson Butte Area, south-central Cascade Range, Washington [M.S. Thesis]: Seattle, Washington, University of Washington, 81 p.

Shultz, J.M., 1988, Mid-Tertiary Volcanic Rocks of the Timberwolf Mtn. Area, South-Central Cascades, Washington [M.S. Thesis]: Bellingham, Washington, Western Washington University, in press.

Smedes, H.W., and Prostka, H.J., 1972, Stratigraphic Framework of the Absaroka Volcanic Supergroup in the Yellowstone National Park Region: U.S. Geological Survey Professional Paper 729-C, 33 p.

Smith, G.A., 1986, Coarse-grained nonmarine volcaniclastic sediment: Terminology and depositional process: Geological Society of America Bulletin, 97, 1-10.

Smith, G.O., 1903, Description of the Ellensburg quadrangle [Washington]: U.S. Geological Survey Geology Atlas, Folio 86, 7 p.

Smith, G.O., and Calkins, F.C., 1906, Description of the Snoqualmie quadrangle [Washington]: U.S. Geological Survey Geology Atlas, Folio 139, 14 p.

Stout, M.L., 1964, Geology of a part of the south-central Cascade Mountains, Washington: Geological Society of America Bulletin, 75, 317-334.

Swanson, D.A., 1964, The middle and late Cenozoic volcanic rocks of the Tieton River area, south-central Washington [Ph.D. Dissertation]: Baltimore, Maryland, The Johns Hopkins University, 329 p.

Swanson, D.A., 1966, Tieton Volcano, a Miocene Eruptive Center in the Southern Cascade Mountains, Washington: Geological Society of America Bulletin, 77, 1293-1314.

Tabor, R.W., Frizzell, V.A., Jr., Vance, J.A., and Naeser, C.W., 1984, Ages and stratigraphy of lower and middle Tertiary sedimentary and volcanic rocks of the central Cascades, Washington: Application to the tectonic history of the Straight Creek fault: Geological Society of America Bulletin, 95, 26-44.

Tabor, R.W., and Crowder, D.F., 1969, On batholiths and volcanoes - Intrusion and eruption of late Cenozoic magmas in the Glacier Peak area, North Cascades, Washington: U.S. Geological Survey Prefessional Paper 604, 67 p.

Taylor, S.R., and Gorton, M.P., 1977, Geochemical applications of spark source mass spectrography-III. Element sensitivity, precesion and

accuracy: Geochimica et Cosmochimica Acta, 41, 1375-1380.

Thompson, M.E., 1983, Solidification in magmas. Part one: The magmatic history of the Tatoosh volcanic-plutonic complex, Mount Rainier National Park. Part two: Numerical simulation of heat and mass transfer in solidifying magmas [M.S. Thesis]: Eugene, Oregon, University of Oregon, 190 p.

Vance, J.A., Clayton, G.A., Mattinson, J.M., and Naeser, C.W., 1987, Early and Middle Cenozoic Stratigraphy of the Mt. Rainier-Tieton River Area, Southern Washington Cascades, in Schuster, J.E., ed., Selected papers on the geology of Washington: Washington Division of Geology and Earth Resources Bulletin 77, 395 p.

Vance, J.A., 1985, Early Tertiary Faulting in the North Cascades: Geological Society of America Abstracts with Programs, v. 17, no. 6, p. 415.

Vance, J.A., and Miller, R.B., 1981, Movement History of the Straight Creek Fault: Geological Society of America Abstracts with Programs, v. 13, no. 2, p. 87.

Walsh, T.J., Koresec, M.A., Phillips, W.M., Logan, R.L., and Schasse, H.W., 1987, Geologic Map of Washington-southwest quadrant: Washington Division of Geology and Earth Resources Geologic Map 34, scale 1:250,000.

Warren, W.C., 1941, Relation of the Yakima basalt to the Keechelus andesitic series: Journal of Geology, 49, 795-814.

Waters, A.C., 1961, Keechelus problem, Cascade Mountains, Washington: Northwest Science, 35, 39-57.

Whitford, D.J., Nicholls, I.A., and Taylor, S.R., 1979, Spatial Variations in the Geochemistry of Quaternary Lavas Across the Sunda Arc in Java and Bali: Contributions to Mineralogy and Petrology, 70, 341-356.

Wood, D.A., 1980, The application of a Th-Hf-Ta diagram to problems of tectonomagmatic classification and to establish the nature of crustal contamination of basaltic lavas of the British Tertiary Volcanic Province: Earth and Planetary Science Letters, 50, 11-30.

Appendix A

Major element XRF analyses and CIPW norms of Edgar Rock member flows

	Basalt and basaltic andesite						
	58	23	40B	98C	80	70	13
SiO_2	51.15	52.11	52.17	52.25	52.29	52.56	52.77
TiO_2	1.23	1.18	1.25	1.20	1.36	1.27	1.49
Al_2O_3	19.14	18.50	19.60	19.64	18.52	19.29	17.59
Fe_2O_3	5.39	3.60		3.91	3.91	4.77	4.87
FeO	4.58	6.07	8.71	4.86	5.58	5.06	6.20
MnO	.19	.17	.14	.16	.17	.17	.17
MgO	4.22	4.91	4.12	4.59	4.14	3.44	3.86
CaO	9.72	8.92	9.56	9.31	9.31	8.99	8.09
Na_2O	2.96	3.02	3.04	2.78	2.96	3.01	3.17
K_2O	1.11	1.23	1.13	1.01	1.40	1.12	1.35
P_2O_5	.32	.28	.28	.29	.36	.31	.43
$Mg/Mg+\Sigma Fe$	.44	.48	.46	.49	.45	.40	.39
Fe_2O_3/FeO	1.18	.59		.80	.70	.94	.79
FeO*/MgO	2.23	1.90	2.11	1.82	2.20	2.72	2.74
CIPW norms: calculated with $Fe_2O_3/FeO = 0.3$							
Q	1.14	1.63	2.17	3.59	2.63	4.21	3.89
C							
OR	6.56	7.27	6.68	5.97	8.27	6.62	7.98
AB	25.04	25.55	25.72	23.52	25.04	25.47	26.82
AN	35.66	33.29	36.50	38.13	33.11	35.81	29.78
DI	8.66	7.50	7.49	5.05	8.86	5.61	6.26
HY	16.32	18.52	15.63	17.71	15.36	15.67	17.56
MT	3.22	3.18	2.97	2.87	3.12	3.19	3.61
IL	2.34	2.24	2.37	2.28	2.58	2.41	2.83
AP	.76	.66	.66	.69	.85	.73	1.02
D.I.	32.74	34.45	34.57	33.08	35.95	36.29	38.69
N.P.	58.7	56.6	58.7	61.8	56.9	58.4	52.6

D.I. = Differentiation Index; N.P. = Normative Plagioclase

Appendix A, continued

	26	20	98B	30	51	35B	35
SiO_2	52.82	52.91	53.23	53.25	53.40	53.71	54.27
TiO_2	1.37	1.33	1.21	1.30	1.13	1.37	1.40
Al_2O_3	19.23	17.89	19.32	20.09	19.48	17.88	18.01
Fe_2O_3	4.51	5.00	4.28	3.83	4.22	3.73	
FeO	4.78	5.25	5.11	4.95	4.36	6.34	9.33
MnO	.17	.17	.17	.15	.16	.19	.19
MgO	3.31	4.09	3.31	2.68	3.37	3.96	3.95
CaO	8.92	8.32	8.61	8.93	8.77	7.91	7.93
Na_2O	3.32	3.24	3.36	3.37	3.50	3.34	3.31
K_2O	1.21	1.37	1.07	1.13	1.26	1.22	1.24
P_2O_5	.35	.43	.32	.31	.34	.34	.37
Mg/Mg+ΣFe	.40	.43	.40	.36	.42	.42	.43
Fe_2O_3/FeO	.94	.95	.84	.77	.97	.59	
FeO*/MgO	2.67	2.38	2.48	3.13	2.42	2.45	2.36
CIPW norms							
Q	3.40	3.21	4.11	4.43	3.08	4.56	5.39
C							
OR	7.15	8.10	6.32	6.68	7.45	7.21	7.33
AB	28.09	27.41	28.43	28.51	29.61	28.26	28.01
AN	33.99	30.22	34.47	36.35	33.72	30.19	30.62
DI	6.62	6.80	5.12	4.94	6.25	5.65	5.20
HY	14.05	17.10	15.20	12.82	13.91	17.25	16.95
MT	3.02	3.33	3.06	2.87	2.78	3.32	3.19
IL	2.60	2.53	2.30	2.47	2.15	2.60	2.66
AP	.83	1.02	.76	.73	.81	.81	.88
D.I.	38.64	38.72	38.87	39.62	40.14	40.03	40.73
N.P.	54.8	52.4	54.8	56.0	53.2	51.7	52.2

35 and 35B are separate samples from a single flow.

Appendix A, continued

	Devils Slide				Andesite		
	40A	50	75	88211	66	82	57
SiO_2	53.77	55.11	55.37	54.42	57.54	58.44	58.51
TiO_2	1.20	1.04	1.45	1.53	.93	1.49	.95
Al_2O_3	19.66	18.44	17.16	18.42	18.33	16.58	19.28
Fe_2O_3	3.81	4.13	3.70		3.78	4.16	4.18
FeO	4.50	5.23	6.71	9.72	4.92	4.77	2.21
MnO	.14	.18	.20	.20	.19	.16	.13
MgO	3.72	3.31	3.32	3.21	2.28	2.27	1.83
CaO	8.94	7.64	6.76	6.71	6.53	5.89	7.04
Na_2O	2.77	3.56	3.20	3.34	3.84	3.60	3.61
K_2O	1.21	1.01	1.67	1.97	1.25	2.05	1.88
P_2O_5	.30	.34	.46	.43	.39	.58	.39
$Mg/Mg+\Sigma Fe$	.46	.40	.37	.37	.33	.32	.35
Fe_2O_3/FeO	.85	.79	.55		.77	.87	1.89
FeO*/MgO	2.13	2.70	3.02	3.03	3.65	3.75	3.26
CIPW norms							
Q	6.48	6.68	8.10	5.20	10.11	11.95	11.15
C							
OR	7.15	5.97	9.87	11.64	7.39	12.11	11.11
AB	23.44	30.12	27.08	28.26	32.49	30.46	30.54
AN	37.64	31.35	27.53	29.45	29.09	23.03	30.85
DI	3.92	3.59	2.49	.84	.65	2.03	1.29
HY	15.51	16.24	17.53	17.54	14.54	13.09	10.03
MT	2.71	3.06	3.44	3.32	2.84	2.91	2.04
IL	2.28	1.98	2.75	2.91	1.77	2.83	1.80
AP	.71	.81	1.09	1.02	.92	1.37	.92
D.I.	37.07	42.77	45.05	45.10	49.99	54.53	52.80
N.P.	61.6	51.0	50.4	51.0	47.2	43.1	50.2

Analysis 88211 provided by R. D. Bentley. Analysis at WSU by Peter Hooper.

Appendix A, continued

	Dacite	
	71	43
SiO_2	60.34	65.84
TiO_2	1.20	.75
Al_2O_3	17.00	16.23
Fe_2O_3	2.67	3.65
FeO	5.04	2.03
MnO	.18	.10
MgO	2.21	.76
CaO	5.18	3.45
Na_2O	3.71	4.04
K_2O	1.97	2.90
P_2O_5	.51	.25
Mg/Mg+ΣFe	.35	.20
Fe_2O_3/FeO	.53	1.80
FeO*/MgO	3.37	7.00
CIPW norms		
Q	14.79	20.88
C	.57	.77
OR	11.64	17.14
AB	31.39	34.18
AN	22.37	15.48
DI		
HY	13.14	7.48
MT	2.55	1.81
IL	2.28	1.42
AP	1.21	.59
D.I.	57.82	72.20
N.P.	41.6	31.2

Appendix B

Major element XRF analyses and CIPW norms of dikes and small intrusion

	Basaltic andesite						Andesite
	54	55	76	84	85	87	96
SiO_2	52.83	53.25	53.49	53.71	54.53	55.75	58.60
TiO_2	1.14	1.13	1.21	1.04	1.31	1.29	.90
Al_2O_3	18.35	18.20	18.13	18.67	17.62	17.52	19.57
Fe_2O_3	3.14	2.55	4.39	3.88	4.38	3.53	2.49
FeO	5.66	6.36	5.23	5.53	5.49	6.07	3.52
MnO	.17	.15	.19	.18	.17	.19	.14
MgO	5.08	5.45	4.33	4.31	3.79	3.21	1.98
CaO	9.19	8.96	8.50	8.36	7.86	7.00	7.14
Na_2O	3.09	2.81	3.22	3.02	3.07	3.68	3.30
K_2O	1.00	.79	1.02	1.03	1.35	1.38	2.02
P_2O_5	.34	.34	.28	.27	.42	.38	.34
$Mg/Mg+\Sigma Fe$	.52	.53	.46	.46	.42	.38	.38
Fe_2O_3/FeO	.55	.40	.84	.70	.80	.58	.71
FeO*/MgO	1.67	1.59	2.12	2.09	2.49	2.88	2.91
CIPW norms: calculated with $Fe_2O_3/FeO = 0.3$							
Q	2.81	4.95	4.32	5.29	6.96	6.99	11.79
C							
OR	5.91	4.67	6.03	6.09	7.98	8.15	11.94
AB	26.14	23.78	27.24	25.55	25.98	31.14	27.92
AN	33.25	34.71	32.00	34.34	30.31	27.21	32.62
DI	8.27	6.13	6.87	4.41	4.93	4.19	.49
HY	17.63	19.79	17.20	18.43	16.92	15.67	10.66
MT	2.90	2.96	3.13	3.09	3.22	3.16	1.97
IL	2.17	2.15	2.30	1.98	2.49	2.45	1.71
AP	.81	.81	.66	.64	.99	.70	.81
D.I.	34.86	33.40	37.59	36.93	40.92	46.28	51.65
N.P.	56.0	59.4	54.0	57.3	53.9	46.6	53.9

Analysis 76 is of dike intruding the Naches Fm. Analysis 55 is of small basaltic andesite intrusion.

Appendix B, continued

				Dacite
	68	67	53	62
SiO_2	61.82	62.24	62.48	64.09
TiO_2	1.04	.71	.86	.74
Al_2O_3	15.97	18.02	17.07	16.42
Fe_2O_3	2.02	3.52	4.54	1.97
FeO	5.59	2.03	1.86	4.04
MnO	.18	.07	.11	.16
MgO	1.55	1.51	1.47	.90
CaO	4.12	5.84	4.76	3.82
Na_2O	3.70	3.59	3.53	4.16
K_2O	3.55	2.23	2.94	3.40
P_2O_5	.46	.25	.38	.29
$Mg/Mg+\Sigma Fe$	.27	.34	.31	.22
Fe_2O_3/FeO	.36	1.73	2.44	.49
FeO*/MgO	4.78	3.44	4.05	6.45
CIPW norms				
Q	13.51	16.47	16.56	15.65
C			.34	
OR	20.98	13.18	17.37	20.09
AB	31.31	30.38	29.87	35.20
AN	16.48	26.47	21.13	16.09
DI	.79	.73		.28
HY	11.32	8.85	9.86	8.41
MT	2.54	1.78	2.03	1.99
IL	1.98	1.35	1.63	1.41
AP	1.09	.59	.90	.67
D.I.	65.79	60.03	63.80	70.93
N.P.	34.5	46.6	41.4	31.4

Appendix C

Major element XRF analyses and CIPW norms of Nile Creek member flows

	Basaltic andesite and andesite					
	100	93	89	95B	95A	79
SiO_2	55.27	58.51	58.86	59.26	61.07	60.91
TiO_2	.91	.96	1.03	.99	.90	1.00
Al_2O_3	16.54	16.64	16.75	16.60	16.11	16.84
Fe_2O_3	2.02	4.00	4.68	4.02	3.80	4.82
FeO	6.74	4.49	3.60	4.30	3.94	2.50
MnO	.17	.16	.14	.15	.15	.12
MgO	5.37	3.27	3.25	3.20	2.88	2.24
CaO	8.74	7.09	6.83	6.58	5.93	6.16
Na_2O	2.72	3.02	3.04	2.99	3.08	3.27
K_2O	1.35	1.69	1.64	1.73	1.97	1.93
P_2O_5	.17	.17	.18	.17	.17	.21
Mg/Mg+ΣFe	.53	.42	.43	.42	.41	.37
Fe_2O_3/FeO	.30	.89	1.30	.93	.96	1.93
FeO*/MgO	1.59	2.47	2.40	2.48	2.56	3.05
CIPW norms: calculated with Fe_2O_3/FeO = 0.3						
Q	6.57	12.43	13.34	13.77	16.32	16.11
OR	7.98	9.99	9.69	10.22	11.64	11.40
AB	23.01	25.55	25.72	25.30	26.06	27.67
AN	28.93	26.86	27.21	26.76	24.31	25.57
DI	10.91	5.99	4.54	3.98	3.33	3.00
HY	17.55	13.98	14.16	15.02	13.49	11.18
MT	2.93	2.77	2.67	1.81	2.51	3.33
IL	1.73	1.82	1.96	1.88	1.71	1.90
AP	.40	.40	.43	.40	.40	.50
D.I.	37.56	47.97	48.75	49.29	54.03	55.18
N.P.	55.7	51.2	51.4	51.4	48.3	48.0

95A and 95B are separate samples from a single flow.

Appendix D

Trace element compositions of Edgar Rock member flows

	23	98C	80	98B	35B	50	66	82	57	71	43
Cs	0.56	0.46	0.40	0.38	0.30	0.33	0.21	1.03	1.83	0.38	1.44
Rb	35	34	48	37	30	26	41	63	63	65	82
Sr	390 (344)	410 (358)	400 (352)	380 (349)	410 (365)	450 (391)	390 (381)	210 (318)	380 (380)	180 (276)	250 (212)
Ba	250	480	470	320	530	270	490	630	660	650	1000
Sc	30	28	30	21	24	16	11	20	14	18	13
V	257	240	271	209	221	107	57	135	83	67	22
Cr	16	20	21	5	5	13	<2	<2	<2	<2	<1
Co	27	25	24	21	23	19	14	14	11	12	6
Ni	14 (34)	<27 (33)	<27 (36)	<24 (26)	<25 (23)	<21 (46)	<19 (25)	<23 (17)	<20 (16)	<21 (17)	4 (19)
Y	31	25	34	29	29	26	32	43	34	35	42
Zr	150	100	130	90	90	90	200	140	200	230	240
Hf	3.1	2.9	3.7	3.1	3.1	2.9	3.8	5.3	4.8	5.3	7.2
Th	5.7	5.1	6.7	4.6	5.4	4.1	5.5	9.4	9.2	9.2	13.7
Ta	0.4	0.5	0.6	0.5	0.6	0.5	0.6	1.1	0.8	1.1	1.2
La	19.6	19.3	24.7	19.3	20.6	18.5	22.9	36.0	29.9	34.3	42.3
Ce	43.6	41.2	51.8	41.2	46.0	41.0	51.0	70.4	66.7	76.4	87.2
Sm	4.76	4.44	5.79	4.64	5.14	4.74	5.37	7.98	6.37	7.45	7.81
Eu	1.47	1.48	1.64	1.56	1.64	1.63	1.87	2.11	2.01	2.30	2.08
Tb	1.13	0.90	0.87	0.80	1.03	0.95	1.15	1.40	1.07	1.41	1.44
Yb	3.2	2.2	3.1	2.7	2.7	2.6	3.1	4.8	3.7	4.5	4.3
Lu	0.39	0.39	0.42	0.38	0.34	0.32	0.46	0.72	0.60	0.60	0.64

All values in ppm. V and Y determined by XRF. Values in parenthesis for Sr and Ni are by XRF. All others by INAA.

Appendix E

Trace element compositions of the dikes and Nile Creek member flows

	Dikes						Nile Creek member				
	54	84	87	96	53	62	100	93*	95B	95A	79
Cs	0.63	0.68	0.35	1.52	0.72	3.30	1.69	0.38	1.06	1.33	2.04
Rb	33	35	43	58	83	79	37	21	55	58	59
Sr	630 (516)	470 (418)	400 (365)	360 (353)	280 (268)	240 (205)	290 (312)	210 (296)	340 (284)	240 (255)	390 (320)
Ba	520	290	620	560	740	940	420	530	550	640	700
Sc	22	20	23	13	12	13	28	9	20	17	18
V	175	202	157	82	54	17	207	202	182	152	159
Cr	100	28	3	3	<2	<2	73	8	8	7	<2
Co	30	25	18	10	9	6	32	9	22	18	17
Ni	57 (76)	<23 (54)	<25 (21)	<9 (28)	<18 (34)	<17 (17)	<26 (54)	<46 (30)	<23 (31)	<21 (36)	<21 (32)
Y	25	27	31	31	41	50	25	29	29	32	32
Zr	160	110	130	170	230	280	100	90	110	140	150
Hf	3.2	2.9	3.5	4.3	6.6	7.7	2.9	3.4	3.8	3.9	4.2
Th	4.7	4.4	5.4	7.8	13.8	14.0	6.0	8.0	8.9	9.9	9.8
Ta	0.8	0.5	0.6	0.7	1.1	1.3	0.4	0.2	0.7	0.6	0.6
La	25.4	19.9	23.4	24.5	41.8	42.9	15.3	20.4	20.1	21.0	24.8
Ce	51.0	42.6	52.8	55.1	82.7	91.7	37.1	42.9	43.5	45.2	49.7
Sm	5.67	4.20	5.86	5.33	7.73	8.69	3.54	4.47	4.16	4.12	5.20
Eu	1.77	1.43	1.95	1.74	2.02	2.22	1.21		1.30	1.28	1.51
Tb	0.98	0.82	0.96	0.94	1.30	1.64	0.65		0.74	0.73	0.96
Yb	2.4	2.4	3.2	3.3	4.1	6.1	2.3	2.9	2.7	2.9	3.1
Lu	0.38	0.34	0.45	0.72	0.59	0.93	0.34	0.36	0.40	0.41	0.45

Elemental determinations as for the Edgar Rock member flows.
* See Analytical Methods section.

Appendix F

Analytical Precision of Oregon State University INAA Results

	BHVO	BHVO*	CRB2	BCR*	Est. error %
Cs			0.89	0.96	
Rb			47	46.8	
Sr	440	443	460	330	20-50
Ba	150	149	670	678	20-50
Sc	31	31.4	32	32.8	1-3
V					
Cr	272	272	9	16	20-50
Co	44	44	35	36.3	1-4
Ni	130	129		13	20-50
Y					
Zr	190	189	200	191	20-50
Hf	4.5	4.47	4.7	4.9	4-8
Th	1.1	1.10	6.0	6.04	4-8
Ta	1.3	1.31	0.9	0.79	10-15
La	15.3	15.2	24.9	25.0	1-3
Ce	39.5	38	51.7	53.7	4-8
Sm	6.01	6.38	6.41	6.58	2-4
Eu	2.16	2.05	2.01	1.96	2-4
Tb	1.10	0.92	0.93	1.05	10-15
Yb		1.97	3.3	3.39	2-4
Lu	0.32	0.29	0.47	0.51	4-8

* Published values and values assumed for OSU standards.

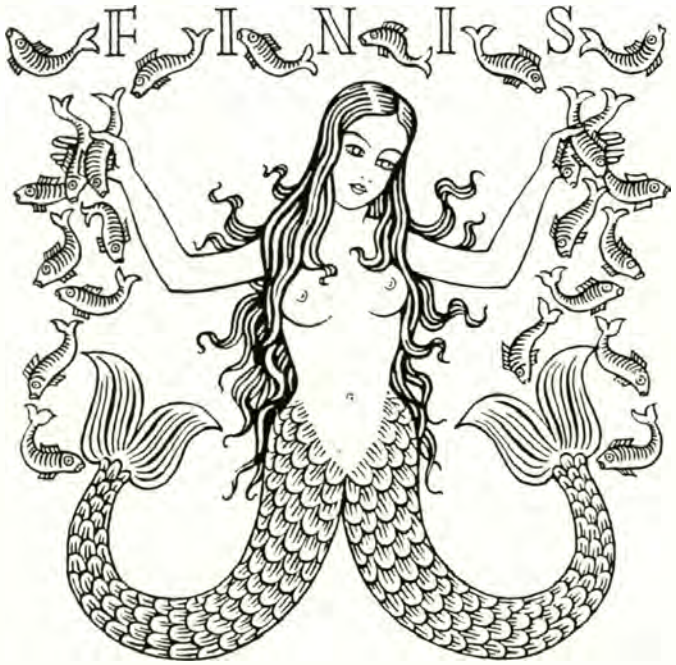

From a publication of the
Innwerk AG München 1950